Massive Spinor Helicity Amplitudes, Cross Sections, and Coalescence

Camille Gómez-Laberge

Physics Department, Northeastern University, Boston, Massachusetts 02115, USA

Manuscript v.04 (first arXiv posting)

We examine recent advancements of the spinor helicity formalism of massive particles. Technical aspects about the formulation of massive helicity spinors are presented in detail to analyze the projective-geometry kinematics of helicity spinors as well as the diagrammatical and analytical structure of their interactions. Two new methods for calculating massive cross sections are derived and tested on Bhabha and Compton processes: a quasi-high-energy limit and an assembly of partial cross sections. The acquisition of mass, where ultrarelativistic amplitudes coalesce at low energy, is given a physical interpretation as the localization of particle worldlines in twistor theory. By subsuming the spinor helicity formalism in this way, both spacetime and particle content can emerge from null, lightlike, and timelike twistors.

Contents

1. Introduction

Theoretical particle physics is undergoing a remarkable period of growth due to recent developments of the on-shell formulation of scattering amplitudes, now capable of describing the interaction of particles of any mass and spin within a generalized spinor helicity formalism. This alternative approach to scattering theory distinguishes itself from quantum field theory (QFT) already at the kinematical level by representing particles using helicity spinors, objects that quantify momentum as a complex bi-spinor and explicitly transform under the little group with the correct spin degrees of freedom. Centering the *particle* as the primary object of the theory, rather than as a subordinate embedding within the Lorentz 4-vector *field*, has proven beneficial for allowing us to cut through much of the computational complexity of QFT and, more importantly, to glean the analytical structure of scattering amplitudes in a broader and more primordial setting bereft of a spacetime backdrop.

One century ago, Dirac's first calculations of a relativistic quantum theory [1] set us in search of the fundamental laws of nature to eventually construct the Standard Model of elementary particles. Yielding the sharpest experimental predictions ever made, each inward bound to probe shorter distances demanded a staggering increase in computational complexity. If history is any guide, an increase in complexity for more fundamental processes was an early clue that QFT is a framework for an effective theory that is now beginning to exceed its energy scale. It was the landmark discovery

reported by Parke and Taylor forty years ago [2], showing that gluonic amplitudes are in fact much simpler at higher energies than QFT suggests, that raised the possibility that we have yet to find the theory that poses the right questions, to which the Parke–Taylor formula and other amplitudes like it are the answer.[1] And so, something new was afoot. Though initially limited to massless particles, the development of the spinor helicity formalism revolutionized scattering theory with its new kinematical and diagrammatical prescription for reconstructing a given amplitude recursively, from the ground up, using three-particle interactions [3, 4, 5].

The last decade or so saw the first efforts to represent massive particles as helicity spinors [6, 7, 8]. Many applications have since been reported, for example, in the Standard Model [9, 10], black hole physics [11], supersymmetry [12], supergravity [13], and twistor space [14]. Progress also continues in advancing our understanding the formalism itself and its utility, which is our focus here.

With the explosion of research into this subject, we see a pedagogical opportunity to examine the recent description of massive particles in terms of helicity spinors and to further see how we can interpret these objects within the projective geometry of twistor theory. It will be both insightful and practical to compare our calculations of scattering amplitudes and their cross sections to those obtained from the standard quantum field treatment. In doing so, we shall come to see—as others also recently have—that each massive spinor helicity amplitude is the unique object that is consistent with all helicity configurations of a corresponding ultrarelativistic scattering process. If only as a concise metaphor, we shall refer to this merging of all high-energy configurations into a single massive amplitude as *coalescence*. This analytical property seems to be of central importance to the extending the spectrum of particles represented by the spinor helicity formalism, and we shall see its manifestations through this paper, which is organized as follows.

We begin in section 2 by setting notation and examining the basic properties of the massive

[1] The simplest amplitude $gg \to gg$ expands to 48 terms using QFT before collapsing to two terms, both given by the Parke–Taylor formula. Its cross section reaches 2 304 terms before reducing to four. This gets much worse even for one extra gluon: $gg \to ggg$ has of order 10 000 terms yet collapses down to four terms after the dust clears!

helicity spinor. Scattering amplitudes and their on-shell diagrams are constructed in section 3, highlighting their distinctive transformation properties, the singularity structure of their couplings, and their crossing symmetry relations. New methodology based on the above for calculating cross sections are presented in section 4, and direct comparisons with QFT are made for Bhabha and Compton cross sections. We pause whenever appropriate throughout these foundational sections to explore features and methods that sharply contrast with the field theory canon. In section 5, given its importance and currency for calculating massive amplitudes and cross sections, we explore the physics of mass acquisition in terms of coalescence and worldline parametrization. Before concluding, the simplicity of doing spinor helicity calculations for massless and, now, massive scattering amplitudes motivates us to search for a deeper understanding of what's going on. Thus the final section pursues a more fundamental picture by subsuming the spinor helicity formalism within twistor theory, whose program also aims to derive representations for particles of any mass and spin—as well as the spacetime they occupy—from a more primitive object.

2. Massive helicity spinors

We begin by reviewing recent advancements on how massive particles are represented by spinor helicity variables. The reader is referred to the literature for the full treatment for massless particles. An introduction to the spinor helicity formalism appears in the quantum field theory textbook by Schwartz [15] and in a TASI conference proceedings paper by Dixon [16]. A comprehensive study of on-shell scattering theory is the subject of the textbook by Elvang & Huang [17]. We generically follow the notation and conventions of these works (see appendix A) and adopt the groundbreaking approach for massive helicity spinors by Arkani-Hamed, Huang, and Huang [6].

2.1. Bi-spinor representations with positive energy

The on-shell program aims to construct amplitudes exclusively from the asymptotic state of each external particle $|p, \sigma\rangle$ with 4-momentum p^μ and spin state labeled by σ. The spinor helicity

formalism distinguishes itself by leveraging the fact that 4-momenta transform according to the Lorentz group $\mathrm{SO}(1,3)$, whose algebra can be decomposed into two subalgebras representing the commuting generators J^+ and J^- of 3D rotations. Therefore, $\mathfrak{so}(1,3) = \mathfrak{su}(2) \oplus \mathfrak{su}(2)$, and p^μ naturally has a bi-spinor representation of the Lorentz group $\left(\frac{1}{2},0\right) \oplus \left(0,\frac{1}{2}\right)$, given by the direct sum of left- and right-handed helicity spinors λ and $\tilde{\lambda}$, respectively. The spinors both transform under the particle's little group and must do so inversely with respect to the other so to ensure the overall invariance of p^μ. Hence, the Lorentz index μ is replaced by a pair of spinorial indices α and $\dot{\alpha}$, which identify the elements of the 2×2 Pauli matrices $\sigma_\mu \equiv (\mathbb{1} \;\; \vec{\sigma})$ that provide passage between representations: $p^{\alpha\dot{\alpha}} = \sigma_\mu^{\alpha\dot{\alpha}} p^\mu$ or alternatively $p_{\dot{\alpha}\alpha} = \bar{\sigma}^\mu_{\dot{\alpha}\alpha} p_\mu$ with $\bar{\sigma}^\mu_{\dot{\alpha}\alpha} \equiv (\mathbb{1}, \; -\vec{\sigma})$.

To see energy positivity between representations, first consider the equivalence between $\lambda\tilde{\lambda}$ and $\sigma_\mu p^\mu$. Following Schwartz [15], massless particles with little group U(1) are simply represented by Weyl spinors λ^α and $\tilde{\lambda}^{\dot{\alpha}}$ with complex-valued weight z

$$\lambda^\alpha \equiv \frac{z}{\sqrt{p_0 - p_3}} \begin{pmatrix} p_0 - p_3 \\ -p_1 - \mathrm{i}p_2 \end{pmatrix} \qquad \tilde{\lambda}^{\dot{\alpha}} = \frac{z^{-1}}{\sqrt{p_0 - p_3}} \begin{pmatrix} p_0 - p_3 & -p_1 + \mathrm{i}p_2 \end{pmatrix}. \tag{2.1}$$

Note the spinorial outer product $\lambda^\alpha \tilde{\lambda}^{\dot{\alpha}}$ and the Lorentz contraction $\sigma_\mu^{\alpha\dot{\alpha}} p^\mu$ both yield

$$p^{\alpha\dot{\alpha}} = \begin{pmatrix} p_0 - p_3 & -p_1 + \mathrm{i}p_2 \\ -p_1 - \mathrm{i}p_2 & p_0 + p_3 \end{pmatrix}. \tag{2.2}$$

Writing our spinors in column form with conventions $\lambda\rangle \equiv \lambda^\alpha \equiv \left(\begin{smallmatrix} a \\ b \end{smallmatrix}\right)$ and $\lambda] \equiv \tilde{\lambda}_{\dot{\alpha}} \equiv \left(\begin{smallmatrix} \tilde{a} \\ \tilde{b} \end{smallmatrix}\right)$, we move from $p^{\alpha\dot{\alpha}} \equiv \lambda^\alpha \tilde{\lambda}^{\dot{\alpha}} = \lambda\rangle[\lambda$ to $p_{\dot{\alpha}\alpha} \equiv \tilde{\lambda}_{\dot{\alpha}} \lambda_\alpha = \lambda]\langle\lambda$ by raising/lowering indices via contraction with the Levi–Civita symbol $\varepsilon_{\alpha\beta} = \varepsilon_{\dot{\alpha}\dot{\beta}} \equiv \left(\begin{smallmatrix} 0 & -1 \\ 1 & 0 \end{smallmatrix}\right)$. In eq. (2.1), for example, we computed $\varepsilon^{\dot{\alpha}\dot{\beta}} \tilde{\lambda}_{\dot{\beta}} = \tilde{\lambda}^{\dot{\alpha}} \equiv [\lambda$. A full description of conventions are given in appendix A. In fact, all invariants are obtained by the Levi–Civita symbol contractions, since all SU(2) irreducible representations can be constructed from symmetric tensors with all lower indices [18]. Proceeding accordingly, we find the representation $p_{\dot{\alpha}\alpha} \equiv \lambda]\langle\lambda$ by outer product $\tilde{\lambda}_{\dot{\alpha}} \lambda_\alpha$ or by Lorentz contraction $\bar{\sigma}^\mu_{\dot{\alpha}\alpha} p_\mu$ to be

$$p_{\dot{\alpha}\alpha} = \begin{pmatrix} p_0 + p_3 & p_1 - \mathrm{i}p_2 \\ p_1 + \mathrm{i}p_2 & p_0 - p_3 \end{pmatrix}. \tag{2.3}$$

But this calculation seems to contradict the results from the usual index gymnastics for spinors

$$p_{\dot{\alpha}\alpha} = \left(-\mathbb{1}\cdot\varepsilon^2\right) p_{\dot{\beta}\beta} = -\varepsilon^{\alpha\beta}\varepsilon^{\dot{\alpha}\dot{\beta}} p_{\dot{\beta}\beta} = -p^{\alpha\dot{\alpha}} \tag{2.4}$$

and Lorentz tensors

$$p_{\dot{\alpha}\alpha} = p_\mu \bar{\sigma}^\mu_{\dot{\alpha}\alpha} = p_\mu (g^{\mu\nu}\bar{\sigma}_{\nu\dot{\alpha}\alpha}) = p_\mu(-g^{\mu\nu}\sigma_\nu^{\alpha\dot{\alpha}}) = -\sigma_\nu^{\alpha\dot{\alpha}} p^\nu = -p^{\alpha\dot{\alpha}}, \tag{2.5}$$

since p_0 appears in eq. (2.3) *without* a minus sign. We can avoid the situation where particles take on negative energy after a change in spinor basis $\alpha\dot{\alpha} \to \dot{\alpha}\alpha$ by adopting the remapping of energy $E \equiv p_0 \mapsto -p_0$ to always ensure its positivity. This convention seems to be widely observed without explicit mention [19, 17]. One final point is that massless particles require $p^2 = m^2 = 0$, which is guaranteed by the singular matrices in eqs. (2.2) and (2.3) both with $\det p^{\alpha\dot{\alpha}} = \det p_{\dot{\alpha}\alpha} = 0$.

2.2. Little group bases

Let us turn our attention to on-shell massive particles of spin s with energy $E^2 = p^2 + m^2$ in natural units ($c \equiv 1$). The little group is now SU(2), and a $(2s+1)$-dimensional irreducible representation as a tensor with $2s$ symmetric little group indices $(I_1 \cdots I_{2s})$ is mathematically guaranteed [18].

The simplest non-trivial case is massive spin $\frac{1}{2}$, which requires only one SU(2) index. Following Arkani-Hamed *et al.* [6], the massive helicity spinors can be written as

$$|\boldsymbol{\lambda}\rangle \equiv \lambda_I^\alpha \equiv \lambda^\alpha \zeta_I^- + \eta^\alpha \zeta_I^+ \quad \text{and} \quad |\boldsymbol{\lambda}] \equiv \tilde{\lambda}_{\dot{\alpha}I} \equiv \tilde{\lambda}_{\dot{\alpha}} \zeta_I^+ + \tilde{\eta}_{\dot{\alpha}} \zeta_I^- \tag{2.6}$$

by factorizing the energy–momentum relation as $m = \sqrt{E+p_z}\sqrt{E-p_z}$ so that both the mass/energy and the spin in the arbitrary frame p^μ, say, pointing along the z-axis relative to reference k^μ, are encoded as Weyl spinors

$$\lambda^\alpha \equiv \frac{1}{\sqrt[4]{2}}\sqrt{E+p_z}\,\zeta^{+\alpha}, \qquad \eta^\alpha \equiv \frac{1}{\sqrt[4]{2}}\sqrt{E-p_z}\,\zeta^{-\alpha}, \tag{2.7}$$

$$\tilde{\lambda}_{\dot{\alpha}} \equiv \frac{1}{\sqrt[4]{2}}\sqrt{E+p_z}\,\tilde{\zeta}^-_{\dot{\alpha}}, \qquad \tilde{\eta}_{\dot{\alpha}} \equiv \frac{1}{\sqrt[4]{2}}\sqrt{E-p_z}\,\tilde{\zeta}^+_{\dot{\alpha}}. \tag{2.8}$$

In the high-energy limit, when $p_z \to E$, we see that λ and $\tilde{\lambda}$ scale up as $\sqrt{2E}$ into the ultraviolet while η and $\tilde{\eta}$ vanish into the infrared. This factorization will feature prominently in this paper and is crucial for flowing between representations of massive variables at low energies to massless ones at high energies.

In addition to the usual left- and right-handed spinor bases $\{\zeta^{+\alpha}, \zeta^{-\alpha}\}$ and $\{\tilde{\zeta}^{-}_{\dot{\alpha}}, \tilde{\zeta}^{+}_{\dot{\alpha}}\}$, we now also require a *little group basis* $\{\zeta^{-}_{I}, \zeta^{+}_{I}\}$ so that λ^{α}_{I} and $\tilde{\lambda}_{\dot{\alpha}I}$ inherit the properties of λ^{α} and $\tilde{\lambda}_{\dot{\alpha}}$ but with non-zero mass. In frame p^{μ}, recall that $\zeta^{+\alpha} = \left(\begin{smallmatrix} c \\ s \end{smallmatrix}\right)$ and $\zeta^{-\alpha} = \left(\begin{smallmatrix} -s^* \\ c \end{smallmatrix}\right)$ have been rotated by $c \equiv \cos\frac{\theta}{2}$ and $s \equiv e^{\mathrm{i}\phi}\sin\frac{\theta}{2}$, and the right basis is identified with the conjugate of the left basis $\tilde{\zeta}^{-}_{\dot{\alpha}} \equiv (\zeta^{+\alpha})^* = \left(\begin{smallmatrix} c \\ s^* \end{smallmatrix}\right)$ and $\tilde{\zeta}^{+}_{\dot{\alpha}} \equiv (\zeta^{-\alpha})^* = \left(\begin{smallmatrix} -s \\ c \end{smallmatrix}\right)$. A third independent basis for the little group can be defined without loss of generality as co-spinors of $\{\zeta^{+\alpha}, \zeta^{-\alpha}\}$ in the reference frame[2] where $\theta = \phi = 0$:

$$\zeta^{+}_{\alpha} = \varepsilon_{\alpha\beta}\zeta^{+\beta} = \begin{pmatrix} -s & c \end{pmatrix} \longrightarrow \zeta^{+}_{I} \equiv \begin{pmatrix} 0 & 1 \end{pmatrix}, \tag{2.9}$$

$$\zeta^{-}_{\alpha} = \varepsilon_{\alpha\beta}\zeta^{-\beta} = \begin{pmatrix} -c & -s^* \end{pmatrix} \longrightarrow \zeta^{-}_{I} \equiv \begin{pmatrix} -1 & 0 \end{pmatrix}. \tag{2.10}$$

All three bases describe their respective spinorial spaces on the same footing. They all have the same orthonormality conditions $\langle \zeta^{\pm}\zeta^{\mp} \rangle = \pm 1$ and $\langle \zeta^{\pm}\zeta^{\pm} \rangle = 0$. For example, $\zeta^{+}_{\alpha}\zeta^{-\alpha} = \zeta^{+}_{I}\zeta^{-I} = \langle \zeta^{+}\zeta^{-} \rangle = 1$ and $\tilde{\zeta}^{+}_{\dot{\alpha}}\tilde{\zeta}^{-\dot{\alpha}} = \left\langle \tilde{\zeta}^{+}\tilde{\zeta}^{-} \right\rangle = 1$. Basis representations in matrix form are tabulated in appendix A.

Massive particles of higher spin s are represented as a $[\begin{smallmatrix} 2s \\ 2s \end{smallmatrix}]$-tensor, constructed as the product of $2s$ copies of λ^{α}_{I} and $\tilde{\lambda}^{\dot{\alpha}}_{I}$ in total. We could express this as

$$\boldsymbol{\lambda}^{2s} \equiv \lambda^{\alpha_1 \cdots}_{(I_1 \cdots} \tilde{\lambda}^{\cdots \dot{\alpha}_{2s}}_{\cdots I_{2s})}, \tag{2.11}$$

where symmetrized indices (in round brackets) run through all copies of λ and $\tilde{\lambda}$. Thankfully, the heavily indexed notation on the right hand side is unnecessary in practice because the constraints on each term of the amplitude leave no ambiguity and provide a simple validity check: each massive

[2]The Pauli matrices do not change under rotations and neither should our little group basis.

spin s particle must appear in each term of the amplitude exactly $2s$ times. How these spinors are contracted will depend on the asymptotic state of the external particles. We shall focus almost entirely on the spin $\frac{1}{2}$ processes, but many higher spin amplitudes appear in the literature.

The bi-spinor momentum of the massive particle is given by

$$\boldsymbol{p}^{\alpha\dot{\alpha}} \equiv \boldsymbol{\lambda}\rangle[\boldsymbol{\lambda} = \lambda_I^{\alpha}\tilde{\lambda}^{\dot{\alpha}I} \quad \text{and} \quad \boldsymbol{p}_{\dot{\alpha}\alpha} \equiv \boldsymbol{\lambda}]\langle\boldsymbol{\lambda} = \tilde{\lambda}_{\dot{\alpha}I}\lambda_{\alpha}^{I} \quad \text{for any } I \in \{I_1, \ldots, I_{2s}\}. \tag{2.12}$$

Like α and $\dot{\alpha}$, the little group indices are raised/lowered by the Levi–Civita symbol $\varepsilon_{IJ} \equiv \left(\begin{smallmatrix} 0 & -1 \\ 1 & 0 \end{smallmatrix}\right)$, and the bi-spinor momentum must now be full-rank to span the entire symmetry group $\mathrm{SU}(2) \otimes \mathrm{SU}(2) = \mathrm{SL}(2,\mathbb{C})$, the universal cover of the proper Lorentz group $\mathrm{SO}(1,3)$, such that $p^2 = \boldsymbol{p}_\mu \boldsymbol{p}^\mu = -\frac{1}{2}\boldsymbol{p}^{\alpha\dot{\alpha}}\boldsymbol{p}_{\dot{\alpha}\alpha} = m^2$. Very soon we shall generalize the kinematics to complex-valued momentum, where the little group weight $z \in \mathbb{C}$ is no longer restricted to be a pure phase $e^{\mathrm{i}\phi}$ and where the universal cover becomes the product group $\mathrm{SL}(2,\mathbb{C})_{\mathcal{L}} \otimes \mathrm{SL}(2,\mathbb{C})_{\mathcal{R}}$. Formulating helicity spinors for complex momenta has remarkable consequences for our work ahead: i) scattering amplitudes become analytic (holomorphic) functions whose structure can be studied using the powerful results of residue theory, ii) the three-point scattering amplitude no longer vanishes and can thus serve as the fundamental building block for all amplitudes, and iii) the bi-spinor representation of particles, their interactions, and even spacetime itself can all be encoded onto the projective geometry of twistor theory. Going forward, the momentum and spinor helicity variables corresponding to massive particles will always appear in boldface to distinguish them from massless particles and clarify manipulations involving their transformation and contraction as well as the taking of their high-energy limit.

Finally, let us check that $p^2 = -\frac{1}{2}\boldsymbol{p}^{\alpha\dot{\alpha}}\boldsymbol{p}_{\dot{\alpha}\alpha} = m^2$. Since $\boldsymbol{p}^{\alpha\dot{\alpha}}\boldsymbol{p}_{\dot{\alpha}\alpha} = \boldsymbol{\lambda}\rangle[\boldsymbol{\lambda}\cdot\boldsymbol{\lambda}]\langle\boldsymbol{\lambda} = \langle\boldsymbol{\lambda}\boldsymbol{\lambda}\rangle[\boldsymbol{\lambda}\boldsymbol{\lambda}]$, we

begin by expanding the angle brackets using the little group basis to find

$$\begin{aligned}\langle \boldsymbol{\lambda\lambda}\rangle &= \Big(\langle\lambda\,\zeta^{-I} + \langle\eta\,\zeta^{+I}\Big)\cdot\Big(\,\lambda\rangle\,\zeta_I^- + \eta\rangle\,\zeta_I^+\Big)\\ &= \langle\lambda\lambda\rangle\,\zeta_I^-\zeta^{-I} + \langle\eta\eta\rangle\,\zeta_I^+\zeta^{+I} + \langle\lambda\eta\rangle\,\zeta_I^+\zeta^{-I} + \langle\eta\lambda\rangle\,\zeta_I^-\zeta^{+I}\\ &= \langle\lambda\lambda\rangle\langle\zeta^-\zeta^-\rangle + \langle\eta\eta\rangle\langle\zeta^+\zeta^+\rangle + \langle\lambda\eta\rangle\langle\zeta^+\zeta^-\rangle + \langle\eta\lambda\rangle\langle\zeta^-\zeta^+\rangle\\ &= \langle\lambda\eta\rangle - \langle\eta\lambda\rangle\\ &= 2\,\langle\lambda\eta\rangle\,,\end{aligned}$$

where the anticommutativity property $\langle\eta\lambda\rangle = -\langle\lambda\eta\rangle$ was used in the last step. This expression can now be evaluated using the definitions in eqs. (2.7) and (2.8)

$$\begin{aligned}2\,\langle\lambda\eta\rangle &= 2\left(\frac{1}{\sqrt[4]{2}}\sqrt{E+p_z}\zeta_\alpha^+\right)\cdot\left(\frac{1}{\sqrt[4]{2}}\sqrt{E-p_z}\zeta^{-\alpha}\right)\\ &= \frac{2}{\sqrt{2}}\sqrt{E^2-p_z^2}\,\langle\zeta^+\zeta^-\rangle\\ &= \sqrt{2}m.\end{aligned}\tag{2.13}$$

Similarly, for the square brackets, we obtain

$$\begin{aligned}[\boldsymbol{\lambda\lambda}] &= \Big([\lambda\,\zeta^{+I} + [\eta\,\zeta^{-I}\Big)\cdot\Big(\,\lambda]\,\zeta_I^+ + \eta]\,\zeta_I^-\Big)\\ &= \frac{2}{\sqrt{2}}\sqrt{E^2-p_z^2}\left\langle\tilde\zeta^-\tilde\zeta^+\right\rangle\\ &= -\sqrt{2}m,\end{aligned}\tag{2.14}$$

which taken together with the above shows that $\boldsymbol{p}^{\alpha\dot\alpha}\boldsymbol{p}_{\dot\alpha\alpha} = -2m^2$, as required.

2.3. Projective geometry of massive helicity spinors

Originally considered merely as a convenient tool, the spinor helicity formalism now deserves a closer look within the context of our growing understanding of the fundamental physics. Thus, before moving on to dynamics, let us first see how helicity spinors encode mass and spin, and then

let us try to see why their distinct properties might confer a simpler reformulation of scattering theory.

From the get-go, helicity spinors transform correctly under the little group and, thus, possess the right structure and degrees of freedom to represent particles. Indeed, the complex number z, introduced in eq. (2.1), encodes little group transformations and appropriately cancels itself out in the bi-spinor representation of momentum in eqs. (2.2) and (2.3). Thus, when constructed from helicity spinors, scattering amplitudes are Lorentz invariant objects upon arrival, as they should be. This is, of course, not the case in QFT, since amplitudes written in terms of 4-momenta require the so-called polarization "vectors" (though they are not Lorentz covariant) to introduce redundancies between vector components in order to eliminate the superfluous degrees of freedom of the vector and tensor fields. Unavoidable in field theory, this artifice is responsible for the familiar complications when calculating a scattering amplitude by having to sum terms obtained from Feynman diagrams, which are not individually gauge invariant. Cross sections lead to further overhead when expanding the square of the magnitude of this sum.

The spinor helicity story applies equally well to particles of any mass and spin. Mass acquisition categorically changes particle kinematics by providing additional spin degrees of freedom and by peeling the worldline off of the lightcone surface and into its timelike interior. In the case of massive spin $\frac{1}{2}$, both changes can be understood as consequences of eq. (2.6), which shows how a massive spinor can be represented as a linear combination of massless ones. There is no fundamental difference for general spin s. The massive spinor will appear in each term of the amplitude $2s$ times so represent a completely symmetric SU(2) tensor with $2s$ little group indices, as in eq. (2.11).

Perhaps the most important insight that is now coming into view is that helicity spinors describe particle interactions and even spacetime itself from a certain projective geometry. The rationale for this interest stems from the requirement, according to the optical theorem, to formulate the scattering amplitude as an analytic (complex) function of the momenta in order to describe the causal evolution of processes. Generalizing this formulation to include complex-momentum kine-

matics leads to the on-shell program, namely, a re-formulation of scattering without virtual particles. With complex momentum having a $SO(2,2)$ signature and its bi-spinor representation transforming under $SL(2,\mathbb{C})_{\mathcal{L}} \otimes SL(2,\mathbb{C})_{\mathcal{R}}$ rather than the Lorentzian group $SO(1,3)$, the conformal structure of Minkowski spacetime and its Poincaré subgroup become clear. Particles and their interactions can be reformulated in terms of helicity spinors, objects that can be thought of as a "square root" of a 4-vector and, thus, belonging to the boundary of spacetime. Finally, it may be possible to subsume helicity spinors within the broader theory of twistors [20], where spacetime and particle content can emerge from null, lightlike, and timelike twistors in an abstract projective geometry. The last section of the paper takes a first step in this direction. Meanwhile, we keep the above perspective in mind as we now re-examine the analytical structure of scattering amplitudes and cross sections from this perspective.

3. Scattering amplitudes

With the kinematic structure of the spinor helicity variables in place, we now turn to dynamics. Powerful constraints coming from unitarity and Poincaré symmetry will lead us to a concise diagrammatic depiction of scattering processes that is manifestly Lorentz invariant. We shall see that a single on-shell diagram can encode the scattering amplitude by embedding each factorization channel as a subdiagram. The simplest subdiagrams, representing the fundamental three-particle interactions, will be the focus of this section. We shall examine their transformation properties, singularity structure, and symmetries in order to develop the analytical tools needed for our work ahead. To demonstrate the formalism, we end by deriving scattering amplitudes for Bhabha annihilation and Compton scattering, as both are primordial in nature and ubiquitous in the literature.

3.1. On-shell diagrams are multi-channel amplitudes

Formulating scattering amplitudes using helicity spinors in a complexified spacetime eliminates the need for virtual particles, since the fundamental three-particle interactions underlying all scattering

processes do not generically vanish for complex momenta. The benefits that follow from this first change are remarkable. The three-particle interaction, or *coupling* used here for brevity, is fully constrained by Poincaré symmetry; it is the non-perturbative object containing everything we need to know about the particles and how they interact. And so, constructing an on-shell diagram by gluing together couplings, first, implies that all internal lines are on-shell and, second, that the resulting amplitude is guaranteed to be a unitary and well-defined analytic function of the asymptotic particle states—it is free of the infamous infinities encountered in quantum field theory. This constructive process, by now a celebrated result known as BCFW recursion, named after Britto, Cachazo, Feng, and Witten, can be used to compute scattering amplitudes at all loop orders in quantum field theories of massless particles [3].

For a unitary theory, the spectral decomposition of quantum fields guarantees that each pole of the S-matrix corresponds to a particular internal line going on-shell. All internal lines in the spinor helicity formalism are on-shell; therefore, a tree-like on-shell diagram must automatically be singular and thus fully constrained by momentum- and energy-conservation. In other words, a tree-like on-shell diagram represents a factorization channel, not an amplitude. The on-shell diagram corresponding to a scattering amplitude, i.e., to the analytic function of *generic* asymptotic particle states, requires at least one degree of freedom, which can be conferred by adding an internal BCFW bridge to any of the tree-like factorization channel diagrams. In this way, the Feynman diagrams for the usual s, t, and u channels are simultaneously embedded into a *single* on-shell diagram representing the entire scattering process [21]. To illustrate this, consider Compton scattering $e^-\gamma \to \gamma e^-$.

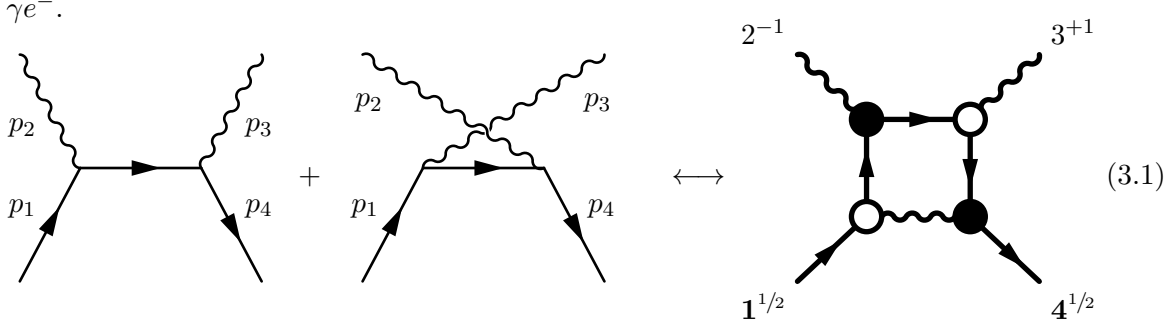

(3.1)

The left-hand side shows the two Feynman diagrams, representing the s and u channels, that together prescribe how to formulate the amplitude in QFT. On the right-hand side is the equivalent on-shell diagram drawn with thicker lines and colored vertices to distinguish it from Feynman diagrams. Perhaps the most important difference between these formalisms is a moral one. This single on-shell diagram represents the entirety of the scattering process at leading order or "tree level," a phrase referring to the dentritic structure of the Feynman diagrams used in the calculation. We shall see in the following pages that the amplitude derived from the on-shell diagram is a monolithic and physical object possessing only the correct transformation properties. In contrast, while the terms coming from individual Feynman diagrams do yield the correct amplitude *as a sum*, they are unfortunately meaningless *on their own* due to their lack of gauge invariance. A secondary difference is that the on-shell diagram looks more loop-like than tree-like, a consequence of the BCFW bridge that forms the internal square in the diagram. The bridge introduces a little-group variable $\xi \in \mathbb{C}$ to ingeniously shift the helicity spinors representing the external particles such that the internal momenta become variables, but the asymptotic-state momenta remain fixed, thus adhering to momentum conservation. More to follow on this point in section 3.2. In order to strike this delicate balance, the couplings of the amplitude must have opposing helicity. This information is provided by the diagram's colored vertices. We shall see in section 3.3 that white corresponds to a mostly positive helicity coupling where all λ variables are parallel, and black corresponds to a mostly negative helicity one with parallel $\tilde{\lambda}$ variables. Cursory inspection of the diagram reveals the embedded factorization channels. For example, we obtain the s channel diagram by letting the internal momentum through the bottom edge of the box vanish, thus also eliminating two lower vertices. The left and right edges of the box become lines **1** and **4**, respectively. The u channel diagram is a bit harder to see. Let the right edge of the box vanish and thus also the two right-side vertices. The bottom (massless) edge of the box takes up the role of line 3, while the top (massive) edge of the box becomes line **4**.[3] An equivalent u channel can be obtained by instead

[3]To recover the typical u channel diagram shape, imagine dragging the remaining black vertex downward to be

deleting the left edge of the box. There are no other valid factorizations. If we try to delete the top edge of the box, then we cannot recover the two external photons. Such a factorization would be inconsistent with the external particle data and must therefore vanish. Regarding this last point on external particle data, finally note that the external particles of the on-shell diagram are not labeled by their momentum but rather by their mass and spin. Massive particles appear in boldface with a superscript indicating their spin, while massless ones appear in regular type with a helicity superscript. For example, $\mathbf{1}^{1/2}$ is a massive spin $\frac{1}{2}$ particle, and 2^{-1} is a massless spin 1 particle with negative helicity.

Taken together, we learn that the on-shell-ness of internal lines guarantees that the analytic function for a scattering amplitude must factorize into all possible channels. Note that the above arguments make no distinction about mass and thus apply to all particles. However, the analytic structure of the amplitude, especially its residues, will depend on the particle spectrum in interesting ways, as we shall see mathematically in the following section.

3.2. Amplitude transformation and factorization

Scattering amplitudes $\mathcal{M} \equiv \langle f|\mathcal{M}|i\rangle$ are Lorentz invariant objects that transform under the little group. With Feynman rules $\mathcal{M} = \epsilon^\mu A_\mu$, this transformation property is hidden behind the contraction of each quantum field and its polarization vector. In contrast, when constructing amplitudes with helicity spinors, the little group is made manifest by the presence of little group indices I for massive particles and helicity indices h for massless ones.

In the massless case, the little group is GL(1) and is represented by the complex weight z in eq. (2.1), since rescalings $\lambda^\alpha \to z\lambda^\alpha$ and $\tilde{\lambda}^{\dot{\alpha}} \to z^{-1}\tilde{\lambda}^{\dot{\alpha}}$ leave the momentum $\lambda^\alpha\tilde{\lambda}^{\dot{\alpha}}$ unchanged.[4] As

horizontal with the remaining white vertex and adjust the new external legs.

[4]For real null momenta, the little group is reduced to the familiar U(1) as represented by the pure phase $z = e^{i\phi/2}$ that guarantees the Hermiticity of $p^{\alpha\dot{\alpha}}$.

mentioned above, Poincaré symmetry fully determines the massless coupling, and thus any massless scattering amplitude can be constructed by gluing together couplings. Whatever the amplitude, it must scale by $W^h = z^{-2h}$ under a little group transformation of each external particle with helicity h [17]. Famously, the Parke–Taylor formula

$$\mathcal{M}(1^+2^+\cdots j^-\cdots k^-\cdots n^+) = \frac{\langle jk\rangle^4}{\langle 12\rangle\langle 23\rangle\cdots\langle n1\rangle} \tag{3.2}$$

owes its elegance to this fact, which is clearly seen by counting the powers of any of the n gluons.[5] The negative helicity momenta j and k each have power 2, while the remaining postivity helicity momenta each have power -2. Therefore, any scattering amplitude involving a massless external particle with momentum $\lambda^\alpha\tilde{\lambda}^{\dot{\alpha}}$ and helicity h transforms under that particle's little group as

$$\mathcal{M}(\lambda^\alpha, \tilde{\lambda}^{\dot{\alpha}}) \longrightarrow z^{-2h}\mathcal{M}(\lambda^\alpha, \tilde{\lambda}^{\dot{\alpha}}). \tag{3.3}$$

In the massive case, the little group is SU(2), and an irreducible representation for spin s can always be constructed as a tensor $W^{(I_1\cdots I_{2s})}$ with totally symmetric indices [18]. Therefore, any amplitude involving a massive external particle of momentum $\lambda^\alpha\tilde{\lambda}^{\dot{\alpha}}$ and spin s transforms under that particle's little group as

$$\mathcal{M}(\lambda^\alpha, \tilde{\lambda}^{\dot{\alpha}}) \longrightarrow W^{(I_1\cdots I_{2s})}\mathcal{M}(\lambda^\alpha, \tilde{\lambda}^{\dot{\alpha}}). \tag{3.4}$$

We pause to note the simplicity that $W^{(I_1\cdots I_{2s})}$ offers compared to the standard notation in quantum mechanics. The above suggests that there is no need to choose an arbitrary axis z and diagonalize the spin angular momentum S_z to form the complete set of commuting observables $S^2\,|s,m\rangle = s(s+1)\,|s,m\rangle$ and $S_z\,|s,m\rangle = m\,|s,m\rangle$, which is the standard notation [22]. Instead, the electron's spin state can be simply described by a tensor W^I without indicating a privileged direction.

Taken together, we can unambiguously express a scattering amplitude as an object carrying little group indices for its external particles. For example, the coupling in fig. (3.1) represents one

[5] Correct little-group scaling requires that positive helicity photons have a total power of -2 when adding λ exponents and subtracting $\tilde{\lambda}$ exponents, while a negative helicity photon requires a total power of $+2$. See [15] for details.

photon and two electrons and can be expressed as $\mathcal{M}^h_{IJ}$, where the symmetrization brackets have been dropped to avoid clutter. This coupling is manifestly Lorentz-invariant and transforms most generally under the little group as $\mathcal{M}(p_1,p_2,p_3) \longrightarrow z^{-2h} W_I W_J \mathcal{M}(p_1,p_2,p_3)$.

With this notation in place, we can see how unitarity and BCFW recursion guarantees that a four-particle amplitude must factorize into two couplings, usually denoted by left $\mathcal{L}$ and right $\mathcal{R}$, along a massive internal line by Levi–Civita contraction

$$\mathcal{M} \longrightarrow \frac{\mathcal{L}^h_{IJ}\,\varepsilon^{JK}\,\mathcal{R}^{-h}_{KL}}{\xi - m^2} \quad \text{[massive internal line]} \tag{3.5}$$

or along a massless line by averaging over the internal helicity states

$$\mathcal{M} \longrightarrow \frac{1}{2}\sum_{\pm h} \frac{\mathcal{L}^h_{IJ}\,\mathcal{R}^{-h}_{KL}}{\xi} \quad \text{[massless internal line]}. \tag{3.6}$$

In either case, ξ becomes a Mandelstam variable s, t, or u, depending on how the external momenta are added, and $\mathcal{M}(\xi)$ becomes singular as $\xi = P^2 \to m^2 \geq 0$ with residue

$$\mathrm{Res}\big(\mathcal{M}, m^2\big) = \lim_{\xi \to m^2} \big(\xi - m^2\big)\,\mathcal{M}(\xi) = \begin{cases} \mathcal{L}^h_{IJ}\,\varepsilon^{JK}\,\mathcal{R}^{-h}_{KL} & \text{for } m > 0, \\ \frac{1}{2}\sum_{\pm h} \mathcal{L}^h_{IJ}\,\mathcal{R}^{-h}_{KL} & \text{for } m = 0. \end{cases} \tag{3.7}$$

The cluster decomposition principle requires that all possible factorizations occur in this way [23]. Thinking of $\xi \in \mathbb{C}$ as a BCFW shift of the internal momentum $P^{\alpha\dot\alpha} = \xi \lambda^\alpha_{\mathcal{L}} \tilde\lambda^{\dot\alpha}_{\mathcal{R}}$, we can calculate any amplitude by finding all ξ values that factorize it along its channels. In other words, the full amplitude is encoded in terms of its residues. The analytic function

$$\frac{\mathcal{M}(\xi)}{\xi - m^2} \tag{3.8}$$

has a simple pole whenever ξ becomes a Mandelstam variable with internal momentum P^2. Note that the physical amplitude *is* the residue at the origin (i.e., no BCFW shift)

$$\mathrm{Res}\left(\frac{\mathcal{M}}{\xi}, 0\right) = \lim_{\xi \to 0} \xi \frac{\mathcal{M}(\xi)}{\xi} = \mathcal{M}(0), \tag{3.9}$$

and that a finite mass for any internal line implies $\mathcal{M}(\xi) \to 0$ as $\xi \to \infty$. Therefore, the closed contour integral of $\mathcal{M}(\xi)/(\xi - m^2)$ around a circle of infinite radius must vanish, and Cauchy's residue theorem yields

$$\oint \frac{\mathcal{M}(\xi)}{\xi - m^2}\,\mathrm{d}\xi = 2\pi\mathrm{i}\left(\mathcal{M}(0) + \frac{\mathrm{Res}(\mathcal{M}, s)}{s - m^2} + \frac{\mathrm{Res}(\mathcal{M}, t)}{t - m^2} + \frac{\mathrm{Res}(\mathcal{M}, u)}{u - m^2}\right) = 0 \quad \text{[4-particle]}. \tag{3.10}$$

Following [6], we can now see how the full amplitude indeed factorizes across all internal lines

$$\mathcal{M} = -\frac{R_s}{s - m^2} - \frac{R_t}{t - m^2} - \frac{R_u}{u - m^2} = \frac{\mathcal{N}(s, t, u)}{(s - m^2)(t - m^2)(u - m^2)}, \tag{3.11}$$

where $R_s \equiv \mathrm{Res}(\mathcal{M}, s)$ is the s-channel residue, and the numerator is

$$\mathcal{N}(s, t, u) = R_s(t - m^2)(u - m^2) + R_t(s - m^2)(u - m^2) + R_u(s - m^2)(t - m^2). \tag{3.12}$$

The above logic applies for higher N-particle amplitudes, where we would have to consider all possible partitions factorizing the amplitude along each internal line.

3.3. Analytical structure of couplings

Proceeding with eq. (3.11), we shall calculate amplitudes by factorizing them along internal lines according to eqs. (3.5) and (3.6). It is well known that the massless coupling is singular, and the residue for one factorization channel will have a pole from *another* channel. Its amplitude is a non-perturbative quantity, completely fixed by helicity constraints [24]

$$\mathcal{M}^{h_1 h_2 h_3} = \begin{cases} g\,\langle 12\rangle^{h_3 - h_1 - h_2}\,\langle 23\rangle^{h_1 - h_2 - h_3}\,\langle 31\rangle^{h_2 - h_3 - h_1} & \text{for } h_1 + h_2 + h_3 < 0, \\ \tilde{g}\,[12]^{h_1 + h_2 - h_3}\,[23]^{h_2 + h_3 - h_1}\,[31]^{h_3 + h_1 - h_2} & \text{for } h_1 + h_2 + h_3 > 0, \end{cases} \tag{3.13}$$

with dimensionless coupling constants g and $\tilde{g}$. Referring back to fig. (3.1), black vertices correspond to the coupling with mostly negative helicity in terms of $\langle\cdot\rangle$ brackets and white vertices to the mostly positive helicity coupling in terms of $[\cdot]$ brackets. To see the singularity structure of a massless scattering amplitude, let us calculate the s-channel residue of the massless spin 1 amplitude $1^-2^+3^-4^+$ according to eq. (3.13). We obtain

$$R_s = \mathcal{L}^{-+-}\mathcal{R}^{+-+} = \left(g\frac{\langle P1\rangle^3}{\langle 12\rangle\langle 2P\rangle}\right)\left(\tilde{g}\frac{[4P]^3}{[34][P3]}\right) = g\tilde{g}\frac{\langle 1P\rangle^3\,[P4]^3}{\langle 12\rangle[34]\langle 2P\rangle[P3]} = g\tilde{g}\frac{\langle 13\rangle^2\,[24]^2}{u}, \tag{3.14}$$

where we used $P^\mu = p_1^\mu + p_2^\mu = p_3^\mu + p_4^\mu$ in the last step. We find that the residue of the s-channel itself has a u-channel pole. Therefore, the amplitude factorized in this way has in fact *two* poles: su. This is a clear violation of the cluster decomposition principle, which guarantees that a *local* theory (i.e., a connected scattering diagram) cannot have more than a single pole or branch cut. Therefore, although spinor helicity amplitudes are manifestly unitary, they cannot always be formulated in a local way. In the above example, we saw that the u-channel pole arises because the massless couplings $\mathcal{L}^{-+-}$ and $\mathcal{R}^{+-+}$ are themselves singular when either of the brackets in the denominator vanish. For this reason, any scattering amplitude that can be factorized with a massless coupling will be non-local.

Despite its singularity structure, the massless coupling is remarkably simple. Recall section 2.3, where we noted that complex momenta transform covariantly under the product group $\mathrm{SL}(2,\mathbb{C})_{\mathcal{L}} \otimes \mathrm{SL}(2,\mathbb{C})_{\mathcal{R}}$, with a left subgroup $\mathcal{L}$ spanned by an undotted basis $\{\lambda_\alpha\}$ and a right subgroup $\mathcal{R}$ spanned by a dotted basis $\{\tilde{\lambda}_{\dot{\alpha}}\}$. Yet eq. (3.13) prescribes a single tensor structure for massless couplings that always transforms *either* entirely within the $\mathcal{L}$ subgroup if $\sum_i h_i < 0$ *or* entirely within the $\mathcal{R}$ subgroup if $\sum_i h_i > 0$. Massive couplings, on the other hand, are more complicated because they generically transform in *both* $\mathcal{L}$ and $\mathcal{R}$, and they always do so with multiple independent tensor structures. This fact will provide strong constraints on the structure of the massive couplings and thus on the configuration of scattering amplitudes constructed from them. And so, in contrast to QFT, we can already appreciate that the spinor helicity formalism becomes simpler at higher energies. When taken to high energy, a massive scattering amplitude breaks up into a simpler massless amplitude for each admissible *spin configuration* of the external particles' spin and helicity values. Coalescence describes the opposite procedure: reducing the energy of the process results in a merging of its ultrarelativistic configurations to form a single massive amplitude. The physics of mass acquisition and its manifestation in QFT via the Higgs mechanism and in twistor theory will be explored in sections 5 and 6, respectively.

Now we shall see that *massive* couplings are also singular in certain cases when couplings consist

of two massive particles, each with a set of little group indices $\{I_1, \ldots, I_{2s}\}$, and one massless particle with helicity variable h. Importantly, quantum electrodynamics (QED) is one such case with $s = \frac{1}{2}$. The issue is more delicate than the all massless case. There is no analogue of eq. (3.13) because helicity is not conserved for massive particles. Following a constructive approach [6], we can expose the crux of the matter—a degeneracy in spanning the Lorentz cover $\mathrm{SL}(2,\mathbb{C})$—by expressing any massive amplitude as a contraction of tensors: one transforming under the little group and the other transforming explicitly under the Lorentz group. For example, the QED coupling, having little group indices I and J, and helicity h, can be written as the contraction

$$\mathcal{M}^h_{IJ} = \frac{1}{\sqrt{2}m}\lambda^\alpha_{1I}\lambda^\beta_{2J}M^h_{\alpha\beta}, \tag{3.15}$$

with the $\sqrt{2}m$ appearing for dimensional consistency according to eqs. (2.13) and (2.14). We identify the first piece $W^{\alpha\beta}_{IJ} = \lambda^\alpha_{1I}\lambda^\beta_{2J}$ as a natural choice for a rank-2 tensor transforming under the SU(2) little group according to the *massive* helicity spinors from the two electrons. The remaining piece $M^h_{\alpha\beta}$ is the coupling with little group indices stripped off, thus transforming only under the Lorentz group with indices α and β. We can construct $M^h_{\alpha\beta}$ using two distinct tensors $(\,\cdot\,)_{\alpha\beta}$ owing to the fact that irreducible representations of the Lorentz group are determined by the direct sum of algebras $\mathfrak{so}(1,3) = \mathfrak{su}(2) \oplus \mathfrak{su}(2)$ for half-integer spins s_1 and s_2, and that there are exactly $N = s_1 + s_2 - |s_1 - s_2| + 1$ distinct such representations [15]. For example, QED has $s_1 = s_2 = \frac{1}{2}$ and thus $N = 2$ distinct couplings: a *minimal* one representing momentum and helicity constraints, and an *auxiliary* one between the electron's magnetic dipole and the electromagnetic field, as we shall soon see.

The aforementioned degeneracy of $M^h_{\alpha\beta}$ in spanning $\mathrm{SL}(2,\mathbb{C})$ occurs when the two massive particles have equal mass. This is clearly a prevalent issue, since fundamental interactions involving elementary particles are precisely of this nature, e.g., the electron-photon interaction in QED. To see the issue, let us find two basis spinors u_α and v_α to construct $M^h_{\alpha\beta}$. We can simply use the helicity spinor from the massless particle to define $u_\alpha \equiv \lambda_{3\alpha} = \langle 3 \,.$ The second basis spinor will

require the massive particles. Simply choosing $\boldsymbol{p}_1^\mu$, for now, we can write

$$v_\alpha \equiv \frac{1}{\sqrt{2}m}\tilde{\lambda}_3^{\dot{\alpha}}\boldsymbol{p}_{1\dot{\alpha}\alpha} = \frac{1}{\sqrt{2}m}[3\,\mathbf{1}\rangle\langle\mathbf{1}. \tag{3.16}$$

These basis spinors point in distinct directions provided that

$$v_\alpha u^\alpha = \frac{1}{\sqrt{2}m}[3\mathbf{1}]\langle\mathbf{1}3\rangle \tag{3.17}$$

does not vanish. In the case of equal masses $m_1 = m_2$, conservation of momentum $\boldsymbol{p}_1^\mu + p_3^\mu = \boldsymbol{p}_2^\mu$ implies that $2\boldsymbol{p}_1 \cdot p_3 = \langle\mathbf{1}3\rangle[3\mathbf{1}] = m_2 - m_1 = 0$. Therefore, the basis $\{u, v\}$ is degenerate for equal masses and no longer spans $\mathrm{SL}(2,\mathbb{C})$. This difficulty is an indication that something interesting is happening. A crucial observation of Arkani-Hamed, Huang, and Huang [6] is that u_α and v_α are parallel in Lorentz space but not in the little group space. According to eq. (2.1), u scales under the little group as $\lambda_3 \to z\lambda_3$, while v scales as $\tilde{\lambda}_3 \to \frac{1}{z}\tilde{\lambda}_3$. Therefore, we introduce the proportionality factor x, such that

$$v_\alpha = x u_\alpha. \tag{3.18}$$

Notice that x must scale like $\tilde{\lambda}$ under the little group as $x \to \frac{1}{z}x$ for consistency

$$v_\alpha = x u_\alpha \longrightarrow \frac{1}{z}\left(\frac{1}{z}x\right)(z u_\alpha) = \frac{1}{z}x u_\alpha = \frac{1}{z}v_\alpha. \tag{3.19}$$

Bringing everything together, the general stripped amplitude $M^h_{\{\alpha\}\{\beta\}}$ with indices $\{\alpha\} \equiv \alpha_1, \ldots, \alpha_{s_1}$ and $\{\beta\} \equiv \beta_1, \ldots, \beta_{s_2}$ can be constructed as the sum of N distinct tensors

$$M^h_{\{\alpha\}\{\beta\}} = \sum_{i=|s_1-s_2|}^{s_1+s_2} g\,(\sqrt{2}m)^{s_1+s_2-i} x^{h+i}\left(u^{2i}\varepsilon^{s_1+s_2-i}\right)_{\{\alpha\}\{\beta\}}, \tag{3.20}$$

where the x factor carries photon helicity h and all possible combinations of u_α, v_α, and $\varepsilon_{\alpha\beta}$ provide exactly $2s_1+2s_2$ Lorentz indices. It is clear the x factor plays a central role in this generative formula for interactions involving massive particles. In addition to its little-group scaling and its helicity weight, the x factor is also singular. This can be seen by contracting $v_\alpha = x u_\alpha$ in eq. (3.16) with a

generic reference spinor χ^α and then letting $\chi^\alpha \to \lambda_3^\alpha$:

$$x u_\alpha \chi^\alpha = v_\alpha \chi^\alpha \quad \Longrightarrow \quad x = \frac{v_\alpha \chi^\alpha}{u_\alpha \chi^\alpha} = \frac{1}{\sqrt{2}m} \frac{[3\mathbf{1}]\langle \mathbf{1}\chi\rangle}{\langle 3\chi\rangle} = \frac{1}{\sqrt{2}m} \frac{[3\,|\boldsymbol{p}_1|\,\chi\rangle}{\langle 3\chi\rangle}. \tag{3.21}$$

Similar to the case for all-massless couplings in eq. (3.14), we see that the factorization residue for massive couplings also possess an *additional* pole, thus revealing its non-local nature. Finally, notice that our choice of basis spinor v_α in eq. (3.16) could have been written instead using $\boldsymbol{p}_2$. Strictly, we need both momenta to avoid the trivial result of forward scattering, where $\boldsymbol{p}_1^\mu = \boldsymbol{p}_2^\mu$. Indeed, defining v_α as the average of incoming and outgoing momenta $\frac{1}{2}(\boldsymbol{p}_{1\dot\alpha\alpha} + \boldsymbol{p}_2^{\alpha\dot\alpha})$ or via eq. (2.5) as the difference $\frac{1}{2}(\boldsymbol{p}_{1\dot\alpha\alpha} - \boldsymbol{p}_{2\dot\alpha\alpha})$ leads to the formal (and non-trivial) definition of the x factor

$$x = \frac{1}{2\sqrt{2}m}\left(\frac{[3\mathbf{1}]\langle \mathbf{1}\chi\rangle}{\langle 3\chi\rangle} + \frac{\langle \phi \mathbf{2}\rangle[\mathbf{2}3]}{\langle \phi 3\rangle}\right) = \frac{1}{2\sqrt{2}m}\frac{[3\,|(\boldsymbol{p}_1 - \boldsymbol{p}_2)|\,\chi\rangle}{\langle 3\chi\rangle}. \tag{3.22}$$

In the last equality, we put $\phi = \chi$ for simplicity. The minus sign between the momenta of the fermions is crucial for spin statistics under $\mathbf{1} \leftrightarrow \mathbf{2}$ particle exchange.[6] The x factor will feature prominently in our work ahead as a tool to calculate an amplitude in terms of the massive external particles and to study its singularity structure.

Returning to eq. (3.20), note that the first term in the series is the minimal coupling with the lowest-dimensional operator $(\cdot)_{\{\alpha\}\{\beta\}}$ constructed from the smallest possible number of basis spinors. In the case of equal spin $s_1 = s_2$, the minimal coupling operator consists of $s_1 + s_2$ copies of the Levi–Civita symbol and is devoid of basis spinors. The remaining terms are the auxiliary couplings with higher-dimensional operators and thus coupling constants with mass dimension $g_i \equiv g\,(\sqrt{2}m)^{-i}$. The auxiliary couplings represent multipole moment interactions with copies of the basis spinors. For example, consider the QED interaction of electron lines $\mathbf{1}$ and $\mathbf{2}$ and a photon line 3 with positive helicity $h = +1$. Using eq. (3.20), the stripped amplitude is

$$M^{+1}_{\alpha\beta} = g\sqrt{2}mx\left(\varepsilon_{\alpha\beta} + \frac{x}{\sqrt{2}m}(uu)_{\alpha\beta}\right). \tag{3.23}$$

[6] Indeed, electron lines $\mathbf{1}$ and $\mathbf{2}$ are distinguishable, since one must be flowing into the vertex and the other one flowing out, hence the appearance of upstairs indices in one momentum and downstairs indices in the other: $\boldsymbol{p}_1^{\alpha\dot\alpha} + \boldsymbol{p}_{2\dot\alpha\alpha}$.

This formula prescribes how the external lines must contract in the minimal and auxiliary couplings. Notice that the x factor in the minimal coupling $x\varepsilon_{\alpha\beta}$ provides the correct $h = +1$ weight for the positive helicity photon, a point we shall return to in the next paragraph. Dressing the stripped amplitude with the massive external lines, according to eq. (3.15), yields the full amplitude

$$\mathcal{M}_{IJ}^{+1} = g\left(x\,\langle\mathbf{12}\rangle + x^2\frac{\langle\mathbf{13}\rangle\langle\mathbf{32}\rangle}{\sqrt{2}m}\right). \tag{3.24}$$

Here, we see that the minimal coupling simply contracts the external electron lines using the Levi–Civita symbol $\varepsilon_{\alpha\beta}$, while the auxiliary coupling represents the interaction between the electron magnetic dipole moment (lines **1** and **2**) and electromagnetic field (line 3). Indeed, the spinor matrix $(uu)_{\alpha\beta}$ corresponds to the familiar additional term $\frac{e}{2}F_{\mu\nu}\sigma^{\mu\nu}$ appearing in Dirac's equations of motion when an electron is coupled to a photon [15], as well as to the Bohr magneton term $\frac{e}{2m}\vec{B}\cdot\vec{\sigma}$ appearing in the non-relativistic Schrödinger–Pauli equation [25].

Our final point about the analytical structure of massive couplings has to do with their representation in the complexified momentum space $\mathrm{SL}(2,\mathbb{C})_{\mathcal{L}}\otimes\mathrm{SL}(2,\mathbb{C})_{\mathcal{R}}$. Note that the calculations in this section could have been performed using a right-handed spinor basis with *dotted* Lorentz indices $\{\tilde{u}_{\dot{\alpha}},\tilde{v}_{\dot{\beta}}\}$ instead of the undotted basis. The procedure is parallel to that above, where we first define right-handed basis spinors $\tilde{u}_{\dot{\alpha}}\equiv\tilde{\lambda}_{3\dot{\alpha}}$ and $\tilde{v}_{\dot{\alpha}}$ analogously to eq. (3.16) with the crucial difference being that the x factor must be negated and inverted in order to provide the correct little-group weight, a consequence of the conjugation rules that we shall explore next in section 3.4. Therefore, instead of eq. (3.18), we would have $\tilde{v}_{\dot{\alpha}} = -\frac{1}{x}\tilde{u}_{\dot{\alpha}}$. Ultimately, we would again arrive at an expansion of N coupling terms analogous to those in eq. (3.20) but now using $\tilde{\lambda}$. Indeed, we now see that massive couplings do generically transform in *both* $\mathcal{L}$ and $\mathcal{R}$ subgroups. However, these expansions must be redundant, since there can only be N independent tensor structures, not $2N$, determined entirely by the spin of the massive particles s_1 and s_2 as discussed earlier in this section (see the paragraph following eq. (3.15)). The two expansions are of course not independent, and we shall see in the following section that they are in fact conjugates of one another. As it often turns out in physics, one of the bases will be more practical than the others for solving a given

problem. Although we can make this determination by appealing to prior knowledge about the QED coupling,[7] we shall approach this here by examining how these couplings coalesce from the high-energy limit (HE). Consider the coupling for a positive helicity photon given by eq. (3.24). In the dotted basis, the expansion is

$$\mathcal{M}_{IJ}^{+1} = -\tilde{g}x\left([\mathbf{12}] - \frac{[\mathbf{13}][\mathbf{32}]}{\sqrt{2}mx}\right). \tag{3.25}$$

Although the minimal coupling $-\tilde{g}x\,[\mathbf{12}]$ seems fine, it actually coalesces from a coupling with a *negative* helicity photon, while $gx\,\langle\mathbf{12}\rangle$ coalesces from a positive helicity coupling. To see this, note that the electrons in either coupling must have opposite spin, as one enters the vertex and the other exits, so that angular momentum is conserved. Then in the high-energy limit, either coupling $\mathcal{M}_{IJ}^{h}$ has exactly two spin configurations $(\mathbf{1}^{1/2}, \mathbf{2}^{1/2}, 3^{h}) \xrightarrow{\text{HE}} (1^{\pm 1/2}, 2^{\mp 1/2}, 3^{h})$. The positive helicity coupling $\mathcal{M}_{IJ}^{+1}$ at high energy, thus, satisfies the mostly positive helicity case of the massless coupling in eq. (3.13), and $\mathcal{M}_{IJ}^{-1}$ satisfies the mostly negative helicity case. Averaging over both configurations for each coupling yields their high-energy limits:

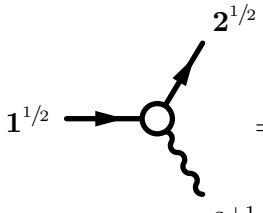

$$= gx\,\langle\mathbf{12}\rangle \xrightarrow{\text{HE}} \left\{\begin{array}{ll} \tilde{g}\dfrac{[31]^2}{[12]} & \text{for } (1^{+1/2}, 2^{-1/2}, 3^{+1}) \\[2ex] \tilde{g}\dfrac{[23]^2}{[12]} & \text{for } (1^{-1/2}, 2^{+1/2}, 3^{+1}) \end{array}\right\} \longrightarrow \tilde{g}\frac{[13]^2 + [23]^2}{2\,[12]}, \tag{3.26}$$

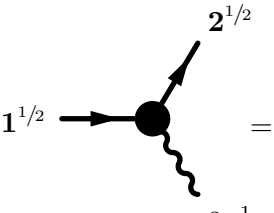

$$= -\frac{\tilde{g}}{x}\,[\mathbf{12}] \xrightarrow{\text{HE}} \left\{\begin{array}{ll} g\dfrac{\langle 23\rangle^2}{\langle 12\rangle} & \text{for } (1^{+1/2}, 2^{-1/2}, 3^{-1}) \\[2ex] g\dfrac{\langle 31\rangle^2}{\langle 12\rangle} & \text{for } (1^{-1/2}, 2^{+1/2}, 3^{-1}) \end{array}\right\} \longrightarrow g\frac{\langle 13\rangle^2 + \langle 23\rangle^2}{2\,\langle 12\rangle}. \tag{3.27}$$

[7] Arguments along these lines appear elsewhere [6, 11, 15, 26].

Thus, $gx\,\langle\mathbf{12}\rangle$ is the natural choice for the minimal coupling with a positive helicity photon, and by symmetry $-\tilde{g}x\,[\mathbf{12}]$ is natural for the negative helicity photon. A similar argument can be made for the auxiliary couplings. Therefore, we write the full QED couplings, manifestly transforming in both $\mathcal{L}$ and $\mathcal{R}$ subgroups each with exactly $N = 2$ independent terms, as follows:

$$\mathcal{M}^{+1}_{IJ} = gx\,\langle\mathbf{12}\rangle + gx^2\frac{\langle\mathbf{13}\rangle\langle\mathbf{32}\rangle}{\sqrt{2}m} \quad \text{and} \quad \mathcal{M}^{-1}_{IJ} = -\frac{\tilde{g}}{x}\,[\mathbf{12}] + \tilde{g}\frac{[\mathbf{13}][\mathbf{32}]}{\sqrt{2}m}. \tag{3.28}$$

These couplings will be the building blocks for scattering amplitudes. To calculate cross sections, we shall require their conjugation and crossing symmetry relations, which are the subject of the next section.

3.4. Conjugation and crossing symmetry

Scattering amplitudes constructed by gluing the spinor helicity couplings shown above will possess many of the same properties as those derived using QFT. We can still interpret $\mathcal{M}$ as an S-matrix element $\langle f|\mathcal{M}|i\rangle$ whose asymptotic states $|p_a, \sigma_a\rangle$ are encoded by the external helicity spinors with little group indices I_a and helicities h_a. It is unitary because we learned in section 2 that $\mathcal{M}$ is factorizable, that its poles correspond to on-shell particles, and that the bi-spinor representation of the phase space $\mathrm{SL}(2,\mathbb{C})_{\mathcal{L}} \otimes \mathrm{SL}(2,\mathbb{C})_{\mathcal{R}}$ is complete. And it is manifestly Lorentz invariant, since the Lorentz indices $\alpha, \dot{\alpha}, \beta, \dot{\beta}, \ldots$ do not appear in the full couplings presented in section 3.3 and thus cannot appear in any scattering amplitude constructed from them.

On the other hand, we have seen important differences with QFT. The spinor helicity formalism is fundamentally a particle theory not a field theory, and its phase space is the complex-valued bi-spinor representation of momentum, not the real-valued 4-vector representation. Consequently, Lagrangian densities, virtual particles, and gauge redundancies associated with 4-vector particle embedding are all absent.[8] In a unitary and Lorentz-invariant field theory, the celebrated CPT

[8] However, Lorentz invariance does impose the little group scaling z of eq. (2.1).

theorem guarantees the invariance of Lagrangian density terms. Furthermore, it implies that the scattering amplitude for any given process is the same as that for its inverse process, where particles are replaced with antiparticles with reversed spin [23]. Despite the lacking field theory, we shall expect our unitary and Lorentz-invariant spinor helicity amplitudes to inherit CPT invariance. In deriving the conjugation rules for helicity spinors below, it will be necessary to combine the Hermitian adjoint $(\cdot)^\dagger$ and the crossing relation $p^\mu \to -p^\mu$ in order to produce the net action of sending particles to antiparticles with spin (or helicity) and handedness reversed. These rules are succinctly referred to in the literature as *crossing symmetry* [16, 17], where all particles are taken to be incoming, and thus all outgoing particles are assigned the negative of their physical 4-momentum.[9]

Here, however, we shall continue using physical momenta (and watching our signs) in order to better appreciate how crossing symmetry works and also to compare our amplitudes and cross sections with standard results in the literature. With $\mathcal{M}$ being an S-matrix element, the Hermitian adjoint is required to calculate the cross section $|\mathcal{M}|^2 = \mathcal{M}^\dagger\mathcal{M}$. In quantum mechanics, this involves the replacement of kets $|\phi\rangle$ by bras $\langle\phi|$ and vice versa [25], but our bi-spinor representation has *two* ket types: a left-handed $|\boldsymbol{\lambda}\rangle$ and a right-handed $|\boldsymbol{\lambda}]$. Well, we have seen handedness (or chirality) before in Dirac 4-spinor fields $\psi(x)$, which transform in the reducible $\left(\frac{1}{2},0\right)\oplus\left(0,\frac{1}{2}\right)$ representation of $\mathrm{SL}(2,\mathbb{C})$. In that case, the appropriate conjugation $\bar{\psi}(x) \equiv \psi(x)^\dagger\gamma^0$ swaps the left- and right-handed components to account for the anti-Hermitian boost generators of the Lorentz group. Thus, Dirac conjugation replaces an incoming left-handed fermion $\psi(x)$ by an outgoing right-handed one $\bar{\psi}(x)$ with momentum and spin unchanged [15].

Proceeding accordingly for a massless helicity spinor, we might simply expect that $\overline{|\lambda\rangle} = |\lambda]$ and similarly that $\overline{|\lambda]} = |\lambda\rangle$, so handedness changes but momentum does not

$$\overline{|\lambda\rangle[\lambda|} = \overline{[\lambda\,\lambda\rangle} = |\lambda\rangle[\lambda|. \tag{3.29}$$

[9] Some authors instead adapt the all outgoing convention and negate the momentum of incoming particles.

This is indeed the adjoint operation on helicity (Weyl) spinors seen in the literature, which we shall refer to as Weyl conjugation. To understand this, consider the matrix representation of the basis spinors in appendix A. Notice that we can move from $\lambda\rangle \propto \zeta^{+\alpha}$ to $[\lambda \propto \tilde{\zeta}^{-\dot{\alpha}}$ using Hermitian conjugation and the ε symbol. However, an overall minus sign reverses the 4-momentum, but this can be prevented with the crossing relation $p^\mu \to -p^\mu$, yielding the correct result

$$\begin{aligned}
\overline{\lambda\rangle} = \overline{\lambda^\alpha} &= \frac{1}{\sqrt[4]{2}}\sqrt{-E-p_z}\,\varepsilon_{\alpha\beta}\left(\zeta^{+\beta}\right)^\dagger \\
&= \frac{1}{\sqrt[4]{2}}\sqrt{-E-p_z}\begin{pmatrix}-s^* & c\end{pmatrix} \\
&= \frac{1}{\sqrt[4]{2}}\sqrt{E+p_z}\begin{pmatrix}s^* & -c\end{pmatrix} \\
&= \frac{1}{\sqrt[4]{2}}\sqrt{E+p_z}\,\tilde{\zeta}^{-\dot{\alpha}} \\
&= \tilde{\lambda}^{\dot{\alpha}} = [\lambda\,. \qquad (3.30)
\end{aligned}$$

Weyl conjugation thus reverses the spin (by swapping the basis-spinor sign) as well as the handedness (by toggling the tilde/dot notation): $\zeta^{\pm\alpha} \leftrightarrow \tilde{\zeta}^{\mp\dot{\alpha}}$. The little group basis $\{\zeta_I^\pm\}$ has the same transformation properties as the spinor bases $\{\zeta^{\pm\alpha}\}$ and $\{\tilde{\zeta}^{\pm\dot{\alpha}}\}$, which means that Weyl conjugation reverses spin and raises/lowers the index: $\zeta_I^\pm \leftrightarrow \zeta^{\mp I}$. Taken together, we obtain the conjugation rules for massive helicity spinors

$$\overline{\boldsymbol{\lambda}\rangle} = \overline{\lambda_I^\alpha} = \overline{\lambda\rangle\,\zeta_I^-} + \overline{\eta\rangle\,\zeta_I^+} = [\lambda\,\zeta^{+I} + [\eta\,\zeta^{-I} = \tilde{\lambda}^{\dot{\alpha}I} = [\boldsymbol{\lambda}\,, \qquad (3.31)$$

$$\overline{\boldsymbol{\lambda}]} = \overline{\tilde{\lambda}_{\dot{\alpha}I}} = \overline{\lambda]\,\zeta_I^+} + \overline{\eta]\,\zeta_I^-} = \langle\lambda\,\zeta^{-I} + \langle\eta\,\zeta^{+I} = \lambda_\alpha^I = \langle\boldsymbol{\lambda}\,. \qquad (3.32)$$

These rules are a straightforward generalization of the massless ones in eq. (3.30). Indeed, the momentum for massive particles is also unchanged under conjugation, and we can now appreciate how the adjoint of $\langle\mathbf{12}\rangle[\mathbf{34}]$ will take the simple and suggestive form $\overline{\langle\mathbf{12}\rangle[\mathbf{34}]} = \langle\mathbf{43}\rangle[\mathbf{21}]$, where the particles have reversed roles in the scattering process.

The last ingredient of $\mathcal{M}$ to conjugate is the x factor. We can proceed by rearranging eq. (3.21)

$$x = \frac{1}{\sqrt{2}m}\frac{[3\,|\boldsymbol{p}_1|\,\chi\rangle}{\langle 3\chi\rangle} \Longrightarrow \sqrt{2}m\,\langle 3\chi\rangle\,x = [3\,|\boldsymbol{p}_1|\,\chi\rangle\,, \qquad (3.33)$$

and conjugating both sides of the equation to find

$$\begin{aligned}
&\overline{\sqrt{2}m\,\langle 3\chi\rangle\, x} = \overline{[3\,|\boldsymbol{p}_1|\,\chi\rangle} \\
&\Rightarrow \sqrt{2}m\,[\chi 3]\,\overline{x} = [\chi\,|\boldsymbol{p}_1|\,3\rangle \\
&\Rightarrow \overline{x} = \frac{1}{\sqrt{2}m}\frac{[\chi\,|\boldsymbol{p}_1|\,3\rangle}{[\chi 3]}.
\end{aligned} \tag{3.34}$$

This last quantity can be directly related to x by expanding the spinors and multiplying numerator and denominator by $-\sqrt{2}m$

$$\begin{aligned}
\overline{x} &= \frac{1}{\sqrt{2}m}\frac{\tilde{\chi}^{\dot{\alpha}}\boldsymbol{p}_{1\dot{\alpha}\alpha}\lambda_3^{\alpha}}{\tilde{\chi}^{\dot{\alpha}}\tilde{\lambda}_{3\dot{\alpha}}} = \frac{-\sqrt{2}m}{-2m^2}\frac{\boldsymbol{p}_{1\dot{\alpha}\alpha}\lambda_3^{\alpha}}{\tilde{\lambda}_{3\dot{\alpha}}} \\
&= -\frac{\sqrt{2}m}{\boldsymbol{p}_1^{\alpha\dot{\alpha}}}\frac{\lambda_3^{\alpha}}{\tilde{\lambda}_{3\dot{\alpha}}} = -\sqrt{2}m\frac{\chi_\alpha}{\chi_\alpha}\frac{\lambda_3^{\alpha}}{\boldsymbol{p}_1^{\alpha\dot{\alpha}}\tilde{\lambda}_{3\dot{\alpha}}} \\
&= -\sqrt{2}m\frac{\langle\chi 3\rangle}{\langle\chi\,|\boldsymbol{p}_1|\,3]} = -\sqrt{2}m\frac{\langle 3\chi\rangle}{[3\,|\boldsymbol{p}_1|\,\chi\rangle} \\
&= -\frac{1}{x}.
\end{aligned} \tag{3.35}$$

We see that the right-handed basis $\{\tilde{u}_{\dot{\alpha}}, \tilde{v}_{\dot{\alpha}}\}$ discussed in the paragraph following eq. (3.24) of section 3.3 is simply the adjoint of the left-handed basis, where $\overline{v_\alpha} = \overline{xu_\alpha} \Rightarrow \tilde{v}_{\dot{\alpha}} = -\frac{1}{x}\tilde{u}_{\dot{\alpha}}$. At this stage, we are able to express a scattering process as an on-shell diagram and to construct its amplitude by gluing together couplings, subject to momentum conservation and helicity constraints. We now do so for the most basic processes.

3.5. Primordial amplitudes

Our work ahead will focus on Bhabha scattering and Compton scattering. These processes provide a natural starting point as they are relatively simple yet embody the most prevalent motifs encountered in particle physics. We calculate their minimal coupling amplitudes in QED here using the spinor helicity formalism.

We begin with Bhabha annihilation $e^-e^+ \to \mu^+\mu^-$. This is the simplest scattering process in QED at leading order. Ironically, already at 1-loop in QFT, this particular amplitude reveals an

important theoretical issue in particle physics, that of infrared divergences. More will follow on this in section 5. For now, at leading order, the only Feynman diagram is the s channel, where a photon is exchanged. Therefore, the on-shell diagram should only factorize along a massless internal line. Consider the corresponding diagrams shown below.

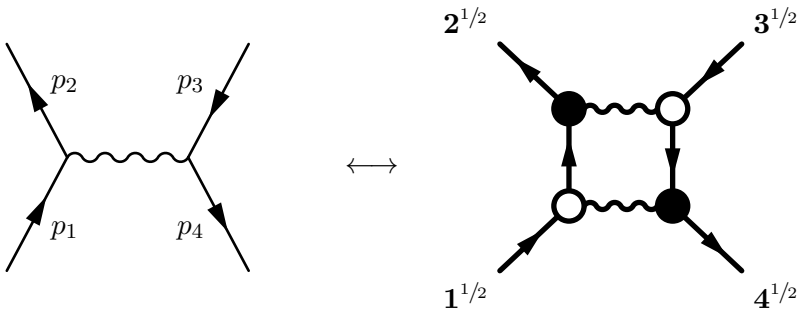

(3.36)

The on-shell diagram looks like that for Compton scattering in fig. (3.1), except that its lines **2** and **3** are now fermions (a positron and an anti-muon, respectively) and that the top edge of the box is now a photon. Yet, these differences completely change the behavior of the process. Like the Feynman diagram, we see a continuous fermionic path between lines **1** to **2** as well as between lines **3** to **4**, with both paths exchanging force carriers. Indeed, there are only two consistent factorizations here, obtained by the deletion of either the top or bottom edges in the box, where a single photon line is exchanged. Notice that the two other factorizations arising from the deletion of the left or right edges of the box must vanish because they allow two massless lines to escape, in conflict with the external all-massive data. The only difference between the two valid factorizations is the internal photon's helicity. Averaging over both cases according to eq. (3.6) thus yields the amplitude

$$\mathcal{M}(\mathbf{1}^{1/2},\mathbf{2}^{1/2},\mathbf{3}^{1/2},\mathbf{4}^{1/2}) = \frac{1}{2}\sum_{h=\pm 1}\frac{\mathcal{L}_{IJ}^{h}\,\mathcal{R}_{KL}^{-h}}{s} = \frac{\mathcal{L}_{IJ}^{+1}\,\mathcal{R}_{KL}^{-1}}{2s} + \frac{\mathcal{L}_{IJ}^{-1}\,\mathcal{R}_{KL}^{+1}}{2s}. \tag{3.37}$$

The minimal couplings in eq. (3.28) provide the leading order contribution

$$\begin{aligned}\mathcal{M}(\mathbf{1}^{1/2},\mathbf{2}^{1/2},\mathbf{3}^{1/2},\mathbf{4}^{1/2}) &= \left(gx_{12}\,\langle\mathbf{12}\rangle\right)\frac{1}{2s}\left(-\tilde{g}\frac{1}{x_{34}}\,[\mathbf{34}]\right)+\left(-\tilde{g}\frac{1}{x_{12}}\,[\mathbf{12}]\right)\frac{1}{2s}\left(gx_{34}\,\langle\mathbf{34}\rangle\right)\\ &= -\frac{g\tilde{g}}{2s}\left(\frac{x_{12}}{x_{34}}\,\langle\mathbf{12}\rangle[\mathbf{34}]+\frac{x_{34}}{x_{12}}\,\langle\mathbf{34}\rangle[\mathbf{12}]\right)\\ &= \frac{2e^2}{s}\left(\frac{x_{12}}{x_{34}}\,\langle\mathbf{12}\rangle[\mathbf{34}]+\frac{x_{34}}{x_{12}}\,\langle\mathbf{34}\rangle[\mathbf{12}]\right)\end{aligned} \tag{3.38}$$

after setting the coupling constants to $g \equiv -2e$ and $\tilde{g} \equiv -g$ for QED. This expression is the scattering amplitude for *all* possible asymptotic states of the four spin-$\frac{1}{2}$ particles. Let us pause to examine its remarkable features. First, its manifest symmetry, with one term being the conjugate of the other, justify the simplicity of this scattering process and its corresponding diagram. Nevertheless, the term $\langle\mathbf{12}\rangle[\mathbf{34}]$ is not *too* simple, as it prescribes how all the Lorentz and little group indices of these massive helicity spinors are being contracted. Thus are encoded the rich dynamics of the interaction. For example, only four of the 2^4 distinct spin configurations conserve angular momentum; the rest are inadmissible and must have vanishing amplitudes. The four configurations are those where the two external lines on both sides have opposite spin. In that case, each bracket leads to a generically non-zero factor like $[\mathbf{1}\,|\bar{\sigma}_\mu|\,\mathbf{2}\rangle$ and $\langle\mathbf{1}\,|\sigma_\mu|\,\mathbf{2}]$. All other configurations have at least one side with equal spins in both lines, and the amplitude vanishes due to the appearance of at least one factor like $\langle\mathbf{1}\,|\sigma_\mu|\,\mathbf{2}\rangle = 0$ or $[\mathbf{1}\,|\bar{\sigma}_\mu|\,\mathbf{2}] = 0$. Finally, let us examine the quotient of x factors. We saw in section 3.3 that x can encode the presence of additional poles and thus indicate the non-locality of the amplitude. Well, for Bhabha *annihilation*, there cannot be any other singularities because the incoming electron *must* annihilate the incoming positron to produce an outgoing muon–antimuon pair. The amplitude can only have one pole; therefore, the process must be local. Using eqs. (3.21), (3.34) and (3.35) with the internal massless line k^μ playing the role of basis spinor for *both* couplings, we have

$$x_{12} = \frac{1}{\sqrt{2}m}\frac{[k\,|\boldsymbol{p}_1|\,\chi\rangle}{\langle k\chi\rangle} \quad\text{and}\quad \frac{1}{x_{34}} = \frac{-1}{\sqrt{2}m}\frac{[\phi\,|\boldsymbol{p}_3|\,k\rangle}{[\phi k]}, \tag{3.39}$$

where χ and ϕ are the reference spinors. The quotient is then

$$\frac{x_{12}}{x_{34}} = -\frac{1}{2m^2}\frac{[\phi\,|\boldsymbol{p}_3|\,k\rangle[k\,|\boldsymbol{p}_1|\,\chi\rangle}{[\phi k]\langle k\chi\rangle} = -\frac{1}{2m^2}\frac{[\phi\,|\boldsymbol{p}_3\cdot k\cdot \boldsymbol{p}_1|\,\chi\rangle}{[\phi\,|k|\,\chi\rangle} = -\frac{\boldsymbol{p}_1\cdot\boldsymbol{p}_3}{2m^2}, \tag{3.40}$$

where, in the last step, we lowered the k indices and raised the $\boldsymbol{p}_1$ indices to make simplifying cancellations. But something is wrong here because the reciprocal x_{34}/x_{12} leads to the same result and thus implies $\boldsymbol{p}_1\cdot\boldsymbol{p}_3 = \pm 2m^2 = \text{const}$, which contradicts the effect of scattering angle. Indeed, by eschewing the formal x factor defined in eq. (3.22), we omitted the degree of freedom *between* $\boldsymbol{p}_1$ and $\boldsymbol{p}_2$, namely their scattering angle! Repeating the above calculation, this time including the relevant scattering information by formalizing, say, x_{12}, leads to the slightly more descriptive amplitude for Bhabha annihilation

$$\mathcal{M}(\mathbf{1}^{1/2},\mathbf{2}^{1/2},\mathbf{3}^{1/2},\mathbf{4}^{1/2}) = -\frac{e^2}{2}\frac{(\boldsymbol{p}_1-\boldsymbol{p}_2)\cdot\boldsymbol{p}_3}{sm^2}\Big(\langle\mathbf{12}\rangle[\mathbf{34}]+\langle\mathbf{34}\rangle[\mathbf{12}]\Big). \tag{3.41}$$

The amplitude is manifestly local with its only pole in the s channel. That no additional poles appear in the calculation hinges on the fact that for Bhabha annihilation both couplings share a common basis spinor. Finally, the amplitude vanishes at forward scattering $\boldsymbol{p}_1^\mu = \boldsymbol{p}_2^\mu$, when the incident particles have parallel trajectories and annihilation does not take place.

Next, let us consider Compton scattering $e^-\gamma \to \gamma e^-$, which has two Feynman diagrams corresponding to the s and u channels shown in fig. (3.1) of section 3.1. As above, we can again factorize along the s channel, but this time the internal line is the massive $\boldsymbol{k}^\mu$. Using eq. (3.5), at minimal coupling we have

$$\begin{aligned}\mathcal{M}(\mathbf{1}^{1/2},2^-,3^+,\mathbf{4}^{1/2}) &= \frac{\mathcal{L}^{-1}_{IJ}\varepsilon^{JK}\mathcal{R}^{+1}_{KL}}{s-m^2}\\ &= \Big(-\tilde{g}\frac{1}{x_{12}}[\boldsymbol{k}\mathbf{1}]\Big)\frac{1}{s-m^2}\Big(g x_{34}\langle\mathbf{4}\boldsymbol{k}\rangle\Big)\\ &= -\frac{g\tilde{g}}{s-m^2}\frac{x_{34}}{x_{12}}\langle\mathbf{4}\boldsymbol{k}\rangle[\boldsymbol{k}\mathbf{1}].\end{aligned} \tag{3.42}$$

Unlike Bhabha annihilation, we expect another pole to appear in the x factors of the residue. This time, crucially, the external photon lines 2 and 3 provide *distinct* basis spinors for the left and right

sides, respectively. Along with the external electron lines **1** and **4**, the quotient becomes

$$\frac{x_{34}}{x_{12}} = -\frac{1}{2m^2}\frac{[\phi\,|\boldsymbol{p}_1|\,2\rangle[3\,|\boldsymbol{p}_4|\,\chi\rangle}{[\phi 2]\langle 3\chi\rangle}. \tag{3.43}$$

Now, by choosing the reference spinor of each side to be the basis spinor of the other side, i.e., let $[\chi \to [3$ and $\langle\phi \to \langle 2$, the denominator reveals a second pole: $[32]\langle 32\rangle = -2p_2\cdot p_3 = t$. Although there is no t channel for Compton scattering, we did factorize along the s channel so that $s-m^2=0$, and thus $s+t+u=2m^2$ implies $t=-(u-m^2)$. Therefore, we can write $-[32]\langle 23\rangle = u-m^2$, and our residue is indeed singular along the u channel, as expected. Further simplification is possible by noting that conservation of momentum requires that $\sum_{j=1}^{4}\langle ij\rangle[jk]=0$ for any null momenta i and k. Therefore, $[\mathbf{31}]\langle\mathbf{12}\rangle+[\mathbf{34}]\langle\mathbf{42}\rangle=0$, which implies $[3\,|\boldsymbol{p}_1|\,2\rangle = -[3\,|\boldsymbol{p}_4|\,2\rangle$ and that each side of this last equation must also be equal to $\frac{1}{2}[3\,|(\boldsymbol{p}_1-\boldsymbol{p}_4)|\,2\rangle$. Substituting this last expression into eq. (3.43) leads to the more descriptive quotient

$$\frac{x_{34}}{x_{12}} = -\frac{1}{8m^2}\frac{[3\,|(\boldsymbol{p}_1-\boldsymbol{p}_4)|\,2\rangle^2}{u-m^2}, \tag{3.44}$$

which forces the amplitude to vanish at forward scattering $\boldsymbol{p}_1^\mu = \boldsymbol{p}_4^\mu$, and where the u channel is made manifest. Note that the square in the numerator acts on the entire bracket. Combining this with eq. (3.42) and writing the internal line as $\boldsymbol{k}^\mu = \boldsymbol{p}_1^\mu + p_2^\mu$ yields the amplitude at leading order

$$\begin{aligned}\mathcal{M}(\mathbf{1}^{1/2},2^-,3^+,\mathbf{4}^{1/2}) &= \frac{g\tilde{g}}{(s-m^2)}\frac{[3\,|(\boldsymbol{p}_1-\boldsymbol{p}_4)|\,2\rangle^2}{8m^2(u-m^2)}\,\langle\mathbf{4}\,|(\boldsymbol{p}_1+p_2)|\,\mathbf{1}]\\ &= g\tilde{g}\frac{[3\,|(\boldsymbol{p}_1-\boldsymbol{p}_4)|\,2\rangle}{(s-m^2)(u-m^2)}\frac{[3\,|(\boldsymbol{p}_1-\boldsymbol{p}_4)|\,2\rangle\langle\mathbf{4}\,|(\boldsymbol{p}_1+p_2)|\,\mathbf{1}]}{8m^2}\\ &= -e^2\frac{[3\,|(\boldsymbol{p}_1-\boldsymbol{p}_4)|\,2\rangle}{(s-m^2)(u-m^2)}\Big(\,\langle\mathbf{12}\rangle[\mathbf{43}]+\langle\mathbf{42}\rangle[\mathbf{13}]\,\Big)\end{aligned} \tag{3.45}$$

after replacing the coupling constants with $g=-2e$ and $\tilde{g}=-g$, and after simplifying the last factor using eqs. (2.13) and (2.14) as well as $\langle\mathbf{12}\rangle[\mathbf{21}]=\langle\mathbf{42}\rangle[\mathbf{24}]=0$ in the last step. Upon visual inspection, the structure of this amplitude says a great deal about the underlying scattering process. The external photons appear as $2\rangle$ and $3]$, indicating that line 2 has negative helicity and line 3

has positive helicity, as labeled in the diagram. Indeed, the amplitude with those helicities reversed $\mathcal{M}(\mathbf{1}^{1/2}, 2^+, 3^-, \mathbf{4}^{1/2})$ looks exactly like eq. (3.45) after exchanging the symbols $2 \leftrightarrow 3$. Analogously, the handedness of the scattered electron also changes from left $\langle\mathbf{1}$ to right $[\mathbf{4}$ in the first term and vice versa in the second. Moreover, the two terms transparently encode the factorization channels: the first term is the s channel, coupling lines $\mathbf{1}$ with 2 and lines 3 with $\mathbf{4}$, while the second term is the u channel, coupling lines $\mathbf{1}$ with 3 and lines 2 with $\mathbf{4}$.

Remarkably, thus does the spinor helicity formalism allow us to calculate scattering amplitudes. We obtain a single object that manifestly transforms within a representation of the Poincaré group determined by the helicity and little group indices of its asymptotic states according to eqs. (3.3) and (3.4), respectively. That its analytical structure inherently prioritizes mass and spin over 4-momentum, and that it encodes multiple factorization channels all at once, suggests that the primacy of locality and even spacetime ought to be re-evaluated. Lest we get ahead of ourselves, it is appropriate to first compare these results with their well-established QFT counterparts. We thus turn to the task of calculating their associated cross sections, whence a direct comparison may be made. Proceeding accordingly, we shall restrict our work in this paper to the leading-order contributions obtained from minimal coupling. Future studies of the contributions from the auxiliary couplings could directly apply the methods developed here.

4. Cross sections

In this section, we lay out the challenges, methods, and results for calculating cross sections in the spinor helicity formalism. First, we show that massive spinor helicity amplitudes are tensor objects and represent the spin configurations of the scattering process all at once. Second, in order to calculate unpolarized cross sections, two complementary methods are developed to expand the scattering amplitude over its spin configurations. Finally, we calculate cross sections for Bhabha annihilation and Compton scattering amplitudes from the previous section. On one hand, we aim to demonstrate how to use massive spinors effectively. On the other, we provide non-trivial checks

by comparing our results with well-known theoretical data from QFT.

4.1. Square of the amplitude and unpolarized scattering

Equipped with the methods and results laid out in sections 2 and 3, we can now tackle the problem of calculating the rate of any scattering process from its unpolarized cross section

$$\sigma = \frac{1}{N}\sum_{\text{spin}} |\mathcal{M}|^2. \tag{4.1}$$

We must average over all N distinct spin configurations in order to compare with experiment. Given $\mathcal{M}$, we can easily calculate its conjugate $\mathcal{M}^\dagger$, but the task of expanding the square of the (modulus of the) amplitude $|\mathcal{M}|^2 = \mathcal{M}\mathcal{M}^\dagger$ is delicate because $\mathcal{M}$ in the spinor helicity formalism is an explicit function of the external helicity states but *not* of the external spin states. As was shown in the preceding section, all possible configurations are implicitly represented in the tensor structure of the scattering amplitude. Therefore, to calculate the unpolarized cross section, we must essentially extract the configurations, square them separately, and add them up. We shall learn how to do this in two ways in the following sections, but first it is instructive to review how it is done in QFT using Dirac algebra [15].

Let us take for example the Bhabha annihilation process shown in fig. (3.36). Focusing only on the left hand side of the process, we have the QED interaction $-\mathrm{i}e\bar{v}(p_2)\gamma^\mu u(p_1)$. Its contribution to the cross section is proportional to

$$\sum_{s'}\sum_{s}\left[\bar{u}_b^{s'}(p_1)\gamma^\mu_{bc}v_c^s(p_2)\,\bar{v}_d^s(p_2)\gamma^\nu_{da}u_a^{s'}(p_1)\right], \tag{4.2}$$

where Latin letters a, b, c, d are the Dirac 4-spinor indices, and we sum over all spin states s and s'. As Dirac taught us, we sum over spins using the spinor outer products

$$\sum_s u_a^s(p)\bar{u}_b^s(p) = \left(\not{p} + m\mathbb{1}\right)_{ab} \quad \text{and} \quad \sum_s v_a^s(p)\bar{v}_b^s(p) = \left(\not{p} - m\mathbb{1}\right)_{ab}, \tag{4.3}$$

and trace over the Dirac indices, reducing eq. (4.2) to an expression that is covariant only with the

Lorentz group

$$\begin{aligned}(\not{p}_1 + m\mathbb{1})_{ab}\gamma^\mu_{bc}(\not{p}_2 - m\mathbb{1})_{cd}\gamma^\nu_{da} &= \mathrm{Tr}\left[(\not{p}_1 + m)\gamma^\mu(\not{p}_2 - m)\gamma^\nu\right] \\ &= 4\left(p_1^\mu p_2^\nu + p_2^\mu p_1^\nu - p_1^\rho p_2^\rho g^{\mu\nu}\right) - 4m^2 g^{\mu\nu}. \end{aligned} \tag{4.4}$$

Thus are the non-trivial rules for coupling fermions beautifully encoded in QFT: as the Dirac algebra[10] over spinors equipped with multiplication defined by the gamma matrix γ^μ_{ab}. The incoming momenta p_1^μ and p_2^μ on the left side of the process get paired-up in eq. (4.4) in such a way that, when contracted with the outgoing momenta on the right side of the process, we obtain a Lorentz invariant quantity where the left- and right-handed chiralities do not mix.[11] Namely, the $(p_1 \cdot p_2)(p_3 \cdot p_4)$ term cancels out to yield the unpolarized Bhabha cross section at leading order

$$\sigma_{\text{Bhabha}} = \frac{8e^4}{s^2}\Big[(p_1 \cdot p_3)(p_2 \cdot p_4) + (p_1 \cdot p_4)(p_2 \cdot p_3) + m^2(p_1 \cdot p_2 + p_3 \cdot p_4) + 2m^4\Big]. \tag{4.5}$$

Although this is by now a familiar calculation, thus easily taken for granted, the expansion of $|\mathcal{M}|^2$ is clearly a rather delicate process in QFT. What, then, are the massive spinor helicity analogues to Dirac's γ-matrix and its consequent spinor outer product and trace operations? The short answer is coalescence. Massive spinor helicity amplitudes and cross sections find their analogous coupling rules in the high-energy limit, which is fully determined by the massless coupling eq. (3.13). In the following section 4.2, we shall formulate a method using the high-energy limit to calculate massless cross sections and then a related *quasi*-limit to calculate massive cross sections like eq. (4.5). The constructive method that was presented in section 3 for calculating scattering amplitudes will then be extended to cross sections, whence the analogue to eq. (4.4) will be obtained and will serve as a building block for directly calculating massive cross sections.

[10] Incidentally, the Dirac algebra is a special case of a *Clifford algebra* that also underlies the algebra of twistors appearing in section 6 to synthesize the spinor helicity formalism.

[11] Recall the discussion in section 2.1 about how the left- and right-handed chiralities transform in separate irreducible representations $\left(\frac{1}{2}, 0\right)$ and $\left(0, \frac{1}{2}\right)$, respectively.

Before moving on, we seize the opportunity to make contact with QFT and show explicitly how the Dirac algebra manifests itself in the spinor helicity formalism. Consider the QED interaction between two electrons and a positive helicity photon. Summing over both spin configurations, we have

$$\begin{aligned}\sum_s \bar{u}(p_2)^{-s}\not{\epsilon}_3^+ u(p_1)^s &= \bar{u}(p_2)^{-\frac{1}{2}}\not{\epsilon}_3^+ u(p_1)^{\frac{1}{2}} + \bar{u}(p_2)^{\frac{1}{2}}\not{\epsilon}_3^+ u(p_1)^{-\frac{1}{2}} \\ &= \left\langle \boldsymbol{u}_2 \left| \epsilon_{3\mu}^+ \gamma^\mu \right| \boldsymbol{u}_1 \right] + \left[\boldsymbol{u}_2 \left| \epsilon_{3\mu}^+ \gamma^\mu \right| \boldsymbol{u}_1 \right\rangle = \left\langle \mathbf{2} \left| \epsilon_{3\mu}^+ \sigma^\mu \right| \mathbf{1} \right] + \left[\mathbf{2} \left| \epsilon_{3\mu}^+ \bar{\sigma}^\mu \right| \mathbf{1} \right\rangle ,\end{aligned} \tag{4.6}$$

where in the last step, we contracted all the Dirac indices using

$$\begin{aligned}\gamma^\mu_{ab} \equiv \begin{pmatrix} 0 & \sigma^{\mu\alpha\dot{\alpha}} \\ \bar{\sigma}^\mu_{\dot{\alpha}\alpha} & 0 \end{pmatrix}, \qquad u(p)^{-\frac{1}{2}} \equiv \boldsymbol{u}_p\rangle = \begin{pmatrix} \lambda_I^\alpha \\ 0 \end{pmatrix}, \qquad u(p)^{\frac{1}{2}} \equiv \boldsymbol{u}_p] = \begin{pmatrix} 0 \\ \tilde{\lambda}_{\dot{\alpha}I} \end{pmatrix}, \\ \bar{u}(p)^{-\frac{1}{2}} \equiv \langle \boldsymbol{u}_p = \begin{pmatrix} \lambda_\alpha^I & 0 \end{pmatrix}, \qquad \bar{u}(p)^{\frac{1}{2}} \equiv [\boldsymbol{u}_p = \begin{pmatrix} 0 & \tilde{\lambda}^{\dot{\alpha}I} \end{pmatrix}.\end{aligned} \tag{4.7}$$

Converting from a Lorentz 4-vector index μ to bi-spinor indices $\alpha\dot{\alpha}$ with the identities

$$\epsilon_p^{+\nu} = \frac{1}{2}\bar{\sigma}^\nu_{\dot{\alpha}\alpha}\epsilon_p^{+\alpha\dot{\alpha}}, \quad \bar{\sigma}^\nu_{\dot{\alpha}\alpha} = \varepsilon_{\alpha\beta}\varepsilon_{\dot{\alpha}\dot{\beta}}\sigma^{\nu\beta\dot{\beta}}, \quad g_{\mu\nu}\sigma^{\mu\alpha\dot{\alpha}}\sigma^{\nu\beta\dot{\beta}} = 2\varepsilon^{\alpha\beta}\varepsilon^{\dot{\alpha}\dot{\beta}}, \tag{4.8}$$

and writing out the polarizations using the spinor helicity notation [15]

$$\left[\epsilon_p^+(\chi)\right]^{\alpha\dot{\alpha}} = \sqrt{2}\frac{\chi\rangle[p}{\langle\chi p\rangle} \quad \text{and} \quad \left[\epsilon_p^+(\chi)\right]_{\dot{\alpha}\alpha} = \sqrt{2}\frac{p]\langle\chi}{\langle\chi p\rangle} \tag{4.9}$$

leads us back to the positive helicity minimal coupling

$$\begin{aligned}\left\langle \mathbf{2} \left| \epsilon_{3\mu}^+ \sigma^\mu \right| \mathbf{1} \right] + \left[\mathbf{2} \left| \epsilon_{3\mu}^+ \bar{\sigma}^\mu \right| \mathbf{1} \right\rangle &= \langle \mathbf{2} \left| \epsilon_3^+ \right| \mathbf{1}] + [\mathbf{2} \left| \epsilon_3^+ \right| \mathbf{1} \rangle \\ &= \lambda_{2\alpha}^I \epsilon_3^{+\alpha\dot{\alpha}} \tilde{\lambda}_{1\dot{\alpha}I} + \tilde{\lambda}_2^{\dot{\alpha}I} \epsilon_{3\dot{\alpha}\alpha}^+ \lambda_{1I}^\alpha \\ &= \sqrt{2}\frac{\langle \mathbf{2}\chi\rangle[\mathbf{31}]}{\langle\chi 3\rangle} + \sqrt{2}\frac{[\mathbf{23}]\langle\chi\mathbf{1}\rangle}{\langle\chi 3\rangle} \\ &= \sqrt{2}\frac{\langle\chi\mathbf{1}\rangle[\mathbf{13}] - \langle\chi\mathbf{2}\rangle[\mathbf{23}]}{\sqrt{2}m\,\langle\chi 3\rangle}\langle\mathbf{12}\rangle \\ &= -2\sqrt{2}\,x\,\langle\mathbf{12}\rangle\,.\end{aligned} \tag{4.10}$$

Taken together, we see that the Dirac algebra in QFT is encoded in the massive couplings of eq. (3.28). Direct links from Dirac to Weyl ($\gamma^{\mu}_{ab} \to \sigma^{\mu\alpha\dot{\alpha}}$) and from Lorentz 4-vectors to bi-spinors ($g_{\mu\nu} \to \varepsilon^{\alpha\beta}\varepsilon^{\dot{\alpha}\dot{\beta}}$) are evident in this calculation and, furthermore, suggest that the physics described by the QED interaction $\sum_s \bar{u}(p_2)^{-s} \not{\epsilon}_3^{+} u(p_1)^s$ has a simpler formulation in $x\,\langle\mathbf{12}\rangle$.

4.2. High-energy limit and quasi-limit expansions

We showed in fig. (3.26) how $x\,\langle\mathbf{12}\rangle$ coalesces from couplings at high energy with a positive helicity photon, i.e., where only $3]$ appears and not $3\rangle$. Our approach was to use conservation of angular momentum to determine the admissible spin configurations and use them to calculate the high-energy limit directly from the massless coupling in eq. (3.13). Here, we discuss how to formally take such limits by returning to our definition of massive helicity spinors in eqs. (2.6) to (2.8), where each spin state is represented by a massless helicity spinor paired with a little group basis spinor $\zeta_I^{\pm}$. We can determine the high-energy limit of any *particular* spin state of a massive helicity spinor by keeping the term with the correct basis spinor and by taking the mass to zero via $p_z \to E$. For example, consider $\langle\boldsymbol{\lambda} = \lambda^I_\alpha = \lambda_\alpha\zeta^{-I} + \eta_\alpha\zeta^{+I}$ and $[\boldsymbol{\lambda} = \tilde{\lambda}^{\dot{\alpha}I} = \tilde{\lambda}^{\dot{\alpha}}\zeta^{+I} + \tilde{\eta}^{\dot{\alpha}}\zeta^{-I}$. The negative spin state $s = -\frac{1}{2}$ of $\langle\boldsymbol{\lambda}$ is $\lambda_\alpha\zeta^{-I}$, and there are no issues letting $p_z \to E$ for λ_α. Therefore, the high-energy limit of $\langle\boldsymbol{\lambda}$, when insisting on spin state $-\frac{1}{2}$ is simply $\langle\lambda$, and we write

$$\lim_{-\mathrm{HE}} \langle\boldsymbol{\lambda} = \langle\lambda \quad \text{or equivalently} \quad \langle\boldsymbol{\lambda} \xrightarrow{-\mathrm{HE}} \langle\lambda\,. \tag{4.11}$$

On the other hand, the positive spin state of $\langle\boldsymbol{\lambda}$ is $\eta_\alpha\zeta^{+I}$, but $\langle\eta$ will vanish as $p_z \to E$. It is $[\boldsymbol{\lambda}$ that has the non-vanishing positive spin $\tilde{\lambda}^{\dot{\alpha}}\zeta^{+I}$ component at high energy, so we will exchange angle and square brackets using $\boldsymbol{p}_{\dot{\alpha}\alpha}\boldsymbol{p}^{\alpha\dot{\alpha}} = [\boldsymbol{\lambda}\boldsymbol{\lambda}]\langle\boldsymbol{\lambda}\boldsymbol{\lambda}\rangle = -2m^2$ as follows:

$$\lim_{+\mathrm{HE}} \langle\boldsymbol{\lambda} = \lim_{+\mathrm{HE}} \frac{[\boldsymbol{\lambda}\boldsymbol{\lambda}]}{-\sqrt{2}m}\langle\boldsymbol{\lambda} = \lim_{+\mathrm{HE}} [\boldsymbol{\lambda}\,\frac{\boldsymbol{p}_{\dot{\alpha}\alpha}}{-\sqrt{2}m}\frac{\boldsymbol{p}^{\alpha\dot{\alpha}}}{\sqrt{2}m} = \lim_{+\mathrm{HE}} [\boldsymbol{\lambda}\,\frac{\boldsymbol{p}_{\dot{\alpha}\alpha}\boldsymbol{p}^{\alpha\dot{\alpha}}}{-2m^2} = [\lambda \quad \text{thus} \quad \langle\boldsymbol{\lambda} \xrightarrow{+\mathrm{HE}} [\lambda. \tag{4.12}$$

Therefore, the high-energy limit for a single massive helicity spinor is very simple: replace its boldface type with λ for $s = -\frac{1}{2}$ or $\tilde{\lambda}$ for $s = +\frac{1}{2}$ as follows

$$\langle \boldsymbol{\lambda} \, , \, [\boldsymbol{\lambda} \xrightarrow{\text{HE}} \begin{cases} \langle \lambda & \text{for } s = -\frac{1}{2}, \\ [\lambda & \text{for } s = +\frac{1}{2}, \end{cases} \quad \text{and} \quad \boldsymbol{\lambda}\rangle \, , \, \boldsymbol{\lambda}] \xrightarrow{\text{HE}} \begin{cases} \lambda\rangle & \text{for } s = -\frac{1}{2}, \\ \lambda] & \text{for } s = +\frac{1}{2}. \end{cases} \tag{4.13}$$

The rules for calculating the high-energy limit for a scattering amplitude are based on this. For a given spin configuration, each massive particle will be assigned a particular spin state s. In the case of a spin-$\frac{1}{2}$ particle, the amplitude can only have one spinor appear for that particle in each term of the amplitude to indicate its spin as either $s = -\frac{1}{2}$ with an angle bracket (λ) or $+\frac{1}{2}$ with a square bracket ($\tilde{\lambda}$). For higher-spin particles, each term of the amplitude will have exactly $2s$ spinors to collectively represent the particular spin state s as products of spinors. For example, a spin-1 particle must have two spinors to collectively represent $s = -1$ as $\lambda\lambda$, $s = 0$ as $\frac{1}{2}(\lambda\tilde{\lambda} + \tilde{\lambda}\lambda)$, and $s = +1$ as $\tilde{\lambda}\tilde{\lambda}$. Again, as in section 2.2, we see that a particle's spin determines exactly how many spinors for that particle must appear in each term of any scattering amplitude. The admissible spin configurations are thus determined by the amplitude and by its relation to the massless coupling in the high-energy limit. We shall see that the high-energy limit is an effective tool for calculating cross sections because it allows us to naturally expand the sum in eq. (4.1) by breaking up the scattering amplitude into its spin configurations.

Finally, let us relax the notion of "high-energy limit" in order to apply this method to both massive and massless spinor helicity amplitudes. Admitting non-zero masses gives us more flexibility in manipulating our expressions and will, of course, be crucial for calculating massive cross sections. The idea is to take one small step *backward* from the high-energy limit in order to restore mass yet retain the expansion over configurations. We define the high-energy *quasi*-limit (qHE) as the result of the following procedure: first, take the high-energy limit to expand the amplitude into its spin configurations, and then restore the boldface type of the corresponding helicity spinors. The quasi-limit enables us to work with the massive amplitude just before it breaks up into its massless components.

We close by using these methods to reproduce the result of fig. (3.26). Expanding the x factor using eq. (3.22) leads to

$$\mathcal{M}_{IJ}^{+1} = gx\,\langle \mathbf{12}\rangle = g\frac{[3\,|(\boldsymbol{p}_1-\boldsymbol{p}_2)|\,\chi\rangle}{2\sqrt{2}m\,\langle 3\chi\rangle}\,\langle \mathbf{12}\rangle = -\frac{g}{2}\frac{[\mathbf{31}]\langle \mathbf{2}\chi\rangle + [\mathbf{32}]\langle \mathbf{1}\chi\rangle}{\langle 3\chi\rangle}. \tag{4.14}$$

Taking the high-energy limit reads

$$\mathcal{M}_{IJ}^{+1} \xrightarrow{\text{HE}} \begin{cases} -\dfrac{g}{2}\dfrac{[31]\langle 2\chi\rangle - [3\eta_2]\langle \eta_1\chi\rangle}{\langle 3\chi\rangle} = -g\dfrac{[31]\langle 2\chi\rangle}{\langle 3\chi\rangle} & \text{for } (1^{+1/2},2^{-1/2},3^{+1}), \\ \\ -\dfrac{g}{2}\dfrac{[3\eta_1]\langle \eta_2\phi\rangle - [32]\langle 1\phi\rangle}{\langle 3\phi\rangle} = +g\dfrac{[32]\langle 1\phi\rangle}{\langle 3\phi\rangle} & \text{for } (1^{-1/2},2^{+1/2},3^{+1}). \end{cases} \tag{4.15}$$

The average of these two configurations should give the high-energy limit from fig. (3.26), but we cannot make progress with massless spinors. Thus, let us take the quasi-limit of each configuration, choose references $\chi = \mathbf{1}$, $\phi = \mathbf{2}$, and average over configurations

$$\mathcal{M}_{IJ}^{+1} \xrightarrow{\text{qHE}} \left\{ \begin{array}{ll} -g\dfrac{[\mathbf{31}]\langle \mathbf{21}\rangle}{\langle \mathbf{31}\rangle} & \text{for } (1^{+1/2},2^{-1/2},3^{+1}) \\ \\ +g\dfrac{[\mathbf{32}]\langle \mathbf{12}\rangle}{\langle \mathbf{32}\rangle} & \text{for } (1^{-1/2},2^{+1/2},3^{+1}) \end{array} \right\} \longrightarrow -\frac{g}{2}\left(\frac{[\mathbf{31}]\langle \mathbf{21}\rangle}{\langle \mathbf{31}\rangle} - \frac{[\mathbf{32}]\langle \mathbf{12}\rangle}{\langle \mathbf{32}\rangle}\right). \tag{4.16}$$

Now we can manipulate the brackets using $\langle \mathbf{12}\rangle[\mathbf{21}] = 2m^2$ as well as $\langle \mathbf{13}\rangle[\mathbf{31}] = 2\boldsymbol{p}_1\cdot p_3 = -2m^2$ and $\langle \mathbf{23}\rangle[\mathbf{32}] = 2\boldsymbol{p}_2\cdot p_3 = 2m^2$, where the crucial minus sign between $\boldsymbol{p}_1\cdot p_3$ and $\boldsymbol{p}_2\cdot p_3$ is again due to incoming line **1** and outgoing line **2**. We indeed recover the high-energy limit with $\tilde{g} = -g$:

$$\mathcal{M}_{IJ}^{+1} \xrightarrow{\text{qHE}} -\frac{g}{2}\left(\frac{[\mathbf{31}]\langle \mathbf{21}\rangle}{\langle \mathbf{31}\rangle} - \frac{[\mathbf{32}]\langle \mathbf{12}\rangle}{\langle \mathbf{32}\rangle}\right) = -\frac{g}{2}\left(\frac{[\mathbf{31}]^2}{[\mathbf{12}]}\frac{2m^2}{2\boldsymbol{p}_1\cdot p_3} + \frac{[\mathbf{32}]^2}{[\mathbf{12}]}\frac{2m^2}{2\boldsymbol{p}_2\cdot p_3}\right) \xrightarrow{\text{HE}} \tilde{g}\frac{[13]^2+[23]^2}{2\,[12]}. \tag{4.17}$$

In the following sections, we shall see how these limits can be used to calculate massive cross sections with relative ease compared to the standard field theoretic approach.

4.3. Gluing partial cross sections

The constructive character of spinor helicity amplitudes suggests an alternative method for calculating cross sections by gluing together smaller pieces, obtained from couplings, that we shall call *partial cross sections*. It should be analogous to eq. (4.4), possessing bi-spinor Lorentz indices and nothing else. We shall require a generalized form of the square of the couplings in eq. (3.15), where the Lorentz indices are symmetrized and where the little group indices of the massive spinors are fully contracted, such that only external momenta $\boldsymbol{p}_{\dot{\alpha}\alpha}$ remain. The stripped coupling and its conjugate will provide the "glue" for adhesion

$$\left|M^h_{\alpha\beta}\right|^2 = \left(M^h_{\alpha\beta}\right)\left(M^h_{\alpha\beta}\right)^\dagger = \left(M^h_{\alpha\beta}\right)\left(M^{-h\dot{\alpha}\dot{\beta}}\right). \tag{4.18}$$

Minimal coupling in QED leads to a single term: $2m^2g^2\varepsilon_{\alpha\beta}\varepsilon^{\dot{\alpha}\dot{\beta}}$. If we include the auxiliary coupling from eq. (3.28), then we obtain additional terms that couple the electrons with the photon helicity spinors λ^α and $\tilde{\lambda}_{\dot{\alpha}}$

$$\left|M^h_{\alpha\beta}\right|^2 = g^2\left[2m^2\varepsilon_{\alpha\beta}\varepsilon^{\dot{\alpha}\dot{\beta}} - \frac{\sqrt{2}m}{x}\varepsilon_{\alpha\beta}\big(\tilde{\lambda}\tilde{\lambda}\big)^{\dot{\alpha}\dot{\beta}} + \sqrt{2}mx\big(\lambda\lambda\big)_{\alpha\beta}\varepsilon^{\dot{\alpha}\dot{\beta}} - \big(\lambda\lambda\big)_{\alpha\beta}\big(\tilde{\lambda}\tilde{\lambda}\big)^{\dot{\alpha}\dot{\beta}}\right]. \tag{4.19}$$

The electromagnetic field strength $F^{\mu\nu}$ in the spinor helicity formalism is $F^{\dot{\alpha}\dot{\beta}}_{\alpha\beta} = \varepsilon_{\alpha\beta}\tilde{\lambda}^{\dot{\alpha}}\tilde{\lambda}^{\dot{\beta}} + \lambda_\alpha\lambda_\beta\varepsilon^{\dot{\alpha}\dot{\beta}}$, and we can see its direct role in the auxiliary terms. Now, let us define the partial cross section as the square of the coupling

$$\sigma^{\dot{\alpha}\dot{\beta}}_{\alpha\beta} \equiv \left|\frac{\lambda_1\lambda_2}{\sqrt{2}m}M^h_{(\alpha\beta)}\right|^2 = \frac{\lambda_1\lambda_2}{\sqrt{2}m}\left[M^2\right]^{(\dot{\alpha}\dot{\beta})}_{(\alpha\beta)}\frac{\tilde{\lambda}_2\tilde{\lambda}_1}{\sqrt{2}m}. \tag{4.20}$$

Here, the Lorentz indices from the stripped amplitude are symmetrized

$$\left[M^2\right]^{(\dot{\alpha}\dot{\beta})}_{(\alpha\beta)} = 2m^2g^2\varepsilon_{(\alpha\beta)}\varepsilon^{(\dot{\alpha}\dot{\beta})} = m^2g^2\left[\varepsilon_{\alpha\beta}\varepsilon^{\dot{\alpha}\dot{\beta}} + \varepsilon_{\beta\alpha}\varepsilon^{\dot{\beta}\dot{\alpha}}\right]. \tag{4.21}$$

Also, the spinor indices for massive particles a and b are suppressed and will be contracted in all three possible ways: intra-particle to yield the original momenta $\tilde{\lambda}_{a\dot{\alpha}I}\lambda^I_{a\alpha} = \boldsymbol{p}_{a\dot{\alpha}\alpha}$, inter-particle to yield the inner products $\boldsymbol{p}_{a\dot{\delta}\delta}\boldsymbol{p}_b^{\delta\dot{\delta}} = \boldsymbol{p}_a \cdot \boldsymbol{p}_b$, and to yield mass terms $\frac{1}{\sqrt{2}m}\tilde{\lambda}^{\dot{\delta}I}_a\boldsymbol{p}_{a\dot{\delta}\delta}\lambda^\delta_{aI} = 2m^2$. Putting

everything together and averaging over these $2 \times 3 = 6$ possibilities yields the QED partial cross section at minimal coupling

$$\begin{aligned}\sigma_{\alpha\beta}^{\dot\alpha\dot\beta} &= \frac{g^2}{6}\left[\boldsymbol{p}_{1\dot\alpha\alpha}\boldsymbol{p}_{2\dot\beta\beta} + \boldsymbol{p}_{2\dot\alpha\alpha}\boldsymbol{p}_{1\dot\beta\beta} - \left(\varepsilon_{\alpha\beta}\varepsilon^{\dot\alpha\dot\beta} + \varepsilon_{\beta\alpha}\varepsilon^{\dot\beta\dot\alpha}\right)\left(\boldsymbol{p}_1\cdot\boldsymbol{p}_2 + 2m^2\right)\right] \\ &= \frac{g^2}{3}\left[\boldsymbol{p}_{1(\alpha}^{(\dot\alpha}\boldsymbol{p}_{2\beta)}^{\dot\beta)} - \varepsilon_{\alpha\beta}\varepsilon^{\dot\alpha\dot\beta}\left(\boldsymbol{p}_1\cdot\boldsymbol{p}_2 + 2m^2\right)\right]. \end{aligned} \tag{4.22}$$

With the relations $\boldsymbol{p}_{a\dot\alpha\alpha} \leftrightarrow p_a^\mu$ and $\varepsilon_{\alpha\beta}\varepsilon^{\dot\alpha\dot\beta} \leftrightarrow g^{\mu\nu}$, we see that the partial cross section is analogous to the left-hand side of the cross section $p_1^{(\mu}p_2^{\nu)} - g^{\mu\nu}\left(p_1^\rho p_2^\rho + 4m^2\right)$ that was calculated in eq. (4.4). Consequently, the cross section for Bhabha annihilation at minimal coupling is the gluing of two copies of eq. (4.22)

$$\sigma_{\text{Bhabha}} = \sigma_{12\alpha\beta}^{\dot\alpha\dot\beta}\frac{1}{s^2}\sigma_{34\dot\alpha\dot\beta}^{\alpha\beta}. \tag{4.23}$$

The partial cross section for particles of general spin s is derived in appendix B using the above combinatorial arguments. In the general case, there are $4s+1$ ways to distribute the massive spinor indices, and we find

$$\sigma_{\alpha_i\beta_i}^{\dot\alpha_i\dot\beta_i} = \frac{g^2}{4s+1}\sum_{n=0}^{2s}\frac{(-1)^{n+1}}{2}\left(\boldsymbol{p}_1\boldsymbol{p}_2\right)^{2s-n}{}_{(\alpha_i\beta_i}^{(\dot\alpha_i\dot\beta_i}\left(\varepsilon\tilde\varepsilon\right)^{n}{}_{\alpha_j\beta_j)}^{\dot\alpha_j\dot\beta_j)}\left[\left(\boldsymbol{p}_1\cdot\boldsymbol{p}_2\right)^n + m^{2n}\right]. \tag{4.24}$$

In order to contract everything, here, we have symmetrized indices with labels $1 \leq i < j \leq s$, as well as $2s-n$ copies of the momenta $\boldsymbol{p}_1$ and $\boldsymbol{p}_2$, and finally n copies of the Levi–Civita symbols. This approach for calculating cross sections bypasses scattering amplitudes altogether and may be suitable for computational methods. We shall not pursue this method further here, however, and will instead return to our study of scattering amplitudes and their high-energy behavior.

4.4. Bhabha cross section

Let us now calculate the cross section for Bhabha annihilation of fig. (3.36). The scattering amplitude in eq. (3.38) written in terms of the quotient x_{12}/x_{34} has a simple conjugate due to the property $\overline{x} = -1/x$. Applying the rules of section 3.4, we obtain

$$\mathcal{M}^\dagger = \frac{2e^2}{s}\left(\frac{\overline{x}_{12}}{\overline{x}_{34}}\overline{\langle\mathbf{12}\rangle[\mathbf{34}]} + \frac{\overline{x}_{34}}{\overline{x}_{12}}\overline{\langle\mathbf{34}\rangle[\mathbf{12}]}\right) = \frac{2e^2}{s}\left(\frac{x_{34}}{x_{12}}\langle\mathbf{43}\rangle[\mathbf{21}] + \frac{x_{12}}{x_{34}}\langle\mathbf{21}\rangle[\mathbf{43}]\right). \tag{4.25}$$

Naïvely expanding the square of the amplitude $|\mathcal{M}|^2 = \mathcal{M}\mathcal{M}^\dagger$ reduces to

$$|\mathcal{M}|^2 = \frac{4e^4}{s^2}\left\{2s^2 + \langle\mathbf{12}\rangle^2\,[\mathbf{34}]^2\left[\left(\frac{x_{12}}{x_{34}}\right)^2 + \left(\frac{x_{34}}{x_{12}}\right)^2\right]\right\}, \tag{4.26}$$

interesting, perhaps, in its own right but bearing little resemblance to the known formula in eq. (4.5), which is written entirely in terms of the external momenta of the process. The problem is that the naïve approach bypasses the expansion over spin configurations and subsequent contractions with the conjugate amplitude that was worked out in sections 4.2 and 4.3. Let us instead consider the high-energy limit of $\mathcal{M}$ in eq. (3.38). The massive spinors in the first term represent four possible spin configurations

$$\frac{x_{12}}{x_{34}}\,\langle\mathbf{12}\rangle[\mathbf{34}] \xrightarrow{\text{HE}} \begin{cases} \langle\eta_1 2\rangle[3\eta_4] \to [13]\langle 24\rangle & \text{for } (1^+, 2^-, 3^+, 4^-), \\ \langle\eta_1 2\rangle[\eta_3 4] \to [14]\langle 32\rangle & \text{for } (1^+, 2^-, 3^-, 4^+), \\ \langle 1\eta_2\rangle[3\eta_4] \to \langle 14\rangle[32] & \text{for } (1^-, 2^+, 3^+, 4^-), \\ \langle 1\eta_2\rangle[\eta_3 4] \to \langle 13\rangle[24] & \text{for } (1^-, 2^+, 3^-, 4^+). \end{cases} \tag{4.27}$$

noting that $x \xrightarrow{\text{HE}} 1$ because its numerator and denominator are both proportional to m, as seen in eq. (3.40).[12] Averaging over these configurations as well as those corresponding to the second term in eq. (3.38) yields the high-energy limit of the full amplitude

$$\mathcal{M} \xrightarrow{\text{HE}} \frac{e^2}{s}\Big(\underset{a}{\langle 14\rangle[32]} + \underset{b}{\langle 13\rangle[24]} + \underset{\bar{b}}{\langle 24\rangle[13]} + \underset{\bar{a}}{\langle 32\rangle[14]}\Big), \tag{4.28}$$

labeling the terms a, b, $\bar{b}$, and $\bar{a}$. The high-energy limit of $\mathcal{M}^\dagger$ is simply $\frac{e^2}{s}(\bar{a} + \bar{b} + b + a)$. Sixteen terms are obtained by squaring the amplitude, but $a^2 = b^2 = \bar{a}^2 = \bar{b}^2 = 0$, since $\langle ii\rangle = [ii] = 0$ for lightlike p_i^μ, $i \in \{1, 2, 3, 4\}$. Furthermore, $ab = \bar{a}b = a\bar{b} = \overline{ab} = 0$, since $\langle ij\rangle^2 = [ij]^2 = 0$ for all $i \neq j$. What remains is $2(a\bar{a} + b\bar{b})$ leading to the correct result at high energy

$$\sigma_{\text{Bhabha}} \xrightarrow{\text{HE}} \frac{2e^4}{s^2}\Big(\langle 14\rangle[41]\langle 23\rangle[32] + \langle 13\rangle[31]\langle 24\rangle[42]\Big) = \frac{2e^4}{s^2}\Big(t^2 + u^2\Big). \tag{4.29}$$

[12] Indeed, the x factor carries little group weight and can only appear in massive amplitudes.

Following the above expansion, we take the quasi-limit, restoring mass to all spinors. Now all 16 terms survive

$$\sigma_{\text{Bhabha}} \xrightarrow{\text{qHE}} \frac{2e^4}{s^2}\Big(\boldsymbol{a}^2+\bar{\boldsymbol{a}}^2+\boldsymbol{b}^2+\bar{\boldsymbol{b}}^2+2\big(\boldsymbol{ab}+\boldsymbol{a\bar{b}}+\bar{\boldsymbol{a}}\boldsymbol{b}+\overline{\boldsymbol{ab}}+\boldsymbol{a\bar{a}}+\boldsymbol{b\bar{b}}\big)\Big), \tag{4.30}$$

where boldfaced labels refer to the massive spinors they represent. Each of the four square-terms contributes $4m^4$. For example, $\boldsymbol{a}^2 = \langle\mathbf{14}\rangle^2\,[\mathbf{32}]^2 = \langle\mathbf{11}\rangle\langle\mathbf{44}\rangle[\mathbf{33}][\mathbf{22}] = 4m^2$. The $\boldsymbol{a\bar{a}}$ and $\boldsymbol{b\bar{b}}$ terms lead to the t- and u-channel invariants, namely,

$$\boldsymbol{a\bar{a}} = \langle\mathbf{14}\rangle[\mathbf{41}]\langle\mathbf{23}\rangle[\mathbf{32}] = \big(t-2m^2\big)^2, \tag{4.31}$$

$$\boldsymbol{b\bar{b}} = \langle\mathbf{13}\rangle[\mathbf{31}]\langle\mathbf{24}\rangle[\mathbf{42}] = \big(u-2m^2\big)^2. \tag{4.32}$$

The cross terms provide the s invariant

$$\begin{aligned}\boldsymbol{ab} &= \langle\mathbf{14}\rangle[\mathbf{32}]\langle\mathbf{31}\rangle[\mathbf{42}] = -\langle\mathbf{13}\rangle[\mathbf{32}]\langle\mathbf{14}\rangle[\mathbf{42}] = -\langle\mathbf{1}\,|\boldsymbol{p}_3|\,\mathbf{2}]\langle\mathbf{1}\,|\boldsymbol{p}_4|\,\mathbf{2}] = -\frac{1}{2}\langle\mathbf{11}\rangle[\mathbf{22}]\,\boldsymbol{p}_3\cdot\boldsymbol{p}_4\\ &= m^2\big(s-2m^2\big),\end{aligned} \tag{4.33}$$

and similarly for $\boldsymbol{a\bar{b}}$, $\bar{\boldsymbol{a}}\boldsymbol{b}$, and $\overline{\boldsymbol{ab}}$. Taken together, we find

$$\begin{aligned}\sigma_{\text{Bhabha}} &\xrightarrow{\text{qHE}} \frac{e^4}{s^2}\Big[16m^4+8m^2\big(s-2m^2\big)+2\big(t-2m^2\big)^2+2\big(u-2m^2\big)^2\Big]\\ &= \frac{e^4}{s^2}\Big[16m^4+16m^2s-8m^2\big(s+t+u\big)+2t^2+2u^2\Big]\\ &= \frac{e^4}{2s^2}\Big[t^2+u^2+8m^2s-8m^4\Big],\end{aligned} \tag{4.34}$$

which is the correct result with the Mandelstam invariants $s+t+u=4m^2$.

4.5. Compton cross section

Now we calculate the cross section for Compton scattering shown in fig. (3.1). The scattering amplitude in eq. (3.45) was obtained by contracting left and right minimal couplings given by eq. (3.42)

$$\mathcal{L}^{-1} = -\frac{\tilde{g}}{x_{12}}\,[\boldsymbol{k}\mathbf{1}] \quad \text{and} \quad \mathcal{R}^{+1} = g x_{34}\,\langle\mathbf{4}\boldsymbol{k}\rangle\,. \tag{4.35}$$

Recall eq. (4.10), where we showed the relationship between $x\,\langle \mathbf{12}\rangle$ and the QED interaction involving a positive helicity photon. Applying this result here, as well as its negative helicity counterpart, we have

$$x_{34}\,\langle \mathbf{4}\boldsymbol{k}\rangle = \frac{1}{2}\left(\left\langle \mathbf{4}\left|\epsilon^{+}_{3\mu}\sigma^{\mu}\right|\boldsymbol{k}\right] + \left[\mathbf{4}\left|\epsilon^{+}_{3\mu}\sigma^{\mu}\right|\boldsymbol{k}\right\rangle\right), \tag{4.36}$$

$$\frac{1}{x_{12}}\,[\mathbf{1}\boldsymbol{k}] = \frac{1}{2}\left(\left[\mathbf{1}\left|\epsilon^{-*}_{2\nu}\sigma^{\nu}\right|\boldsymbol{k}\right\rangle + \left\langle \mathbf{1}\left|\epsilon^{-*}_{2\nu}\sigma^{\nu}\right|\boldsymbol{k}\right]\right). \tag{4.37}$$

Combining both pieces, summing over polarizations $\mathrm{i}g_{\mu\nu} = \sum_{i=\pm 1}\epsilon^{i}_{\mu}\epsilon^{i*}_{\nu}$, and taking the high-energy limit yields

$$\begin{aligned}\frac{x_{34}}{x_{12}}\,\langle \mathbf{4}\boldsymbol{k}\rangle[\mathbf{1}\boldsymbol{k}] &= \frac{1}{2}\Big(\,\langle \mathbf{4}\,|\sigma^{\mu}|\,\boldsymbol{k}]\;g_{\mu\nu}\,[\mathbf{1}\,|\sigma^{\nu}|\,\boldsymbol{k}\rangle + [\mathbf{4}\,|\sigma^{\mu}|\,\boldsymbol{k}\rangle\;g_{\mu\nu}\,\langle \mathbf{1}\,|\sigma^{\nu}|\,\boldsymbol{k}]\,\Big)\\ &\xrightarrow{\text{HE}} \langle 4k\rangle[1k] + [4k]\langle 1k\rangle,\end{aligned} \tag{4.38}$$

where the identity in eq. (4.9) for $g_{\mu\nu}\sigma^{\mu}\sigma^{\nu}$ was used in the last step.

It is interesting that the high energy electrons have opposite spin in both configurations. Since the photons are external with fixed helicities 2^{-} and 3^{+}, the first term corresponds to the s channel, thus coupling lines 1 with 2 and 3 with 4. The second term corresponds to the u channel, swapping lines $2 \leftrightarrow 3$. Writing the scattering amplitude at high energy as

$$\mathcal{M} = \mathcal{M}_s + \mathcal{M}_u \xrightarrow{\text{HE}} g\tilde{g}\left(\frac{\langle 4k\rangle[1k]}{s} + \frac{\langle 1k\rangle[4k]}{u}\right), \tag{4.39}$$

we immediately see that $\mathcal{M}_s\mathcal{M}_u^{\dagger} \xrightarrow{\text{HE}} 0$ and $\mathcal{M}_s^{\dagger}\mathcal{M}_u \xrightarrow{\text{HE}} 0$ due to the contraction of identical massless spinors. Therefore, the high-energy limit does not have cross terms with $1/su$, and the *unpolarized* cross section reduces to the simple form known in the literature

$$\begin{aligned}\sigma_{\text{Compton}} &\xrightarrow{\text{HE}} \frac{1}{8}\sum_{h=\pm 1}\left(\left|\mathcal{M}_s^{h}\right|^2 + \left|\mathcal{M}_u^{h}\right|^2\right)\\ &= \frac{g^2\tilde{g}^2}{8}\left(\frac{1}{s^2}+\frac{1}{u^2}\right)\langle 4k\rangle[1k]\langle 1k\rangle[4k]\\ &= 2e^4\left(\frac{1}{s^2}+\frac{1}{u^2}\right)\langle 4\,|(p_1+p_2)|\,1]\langle 1\,|(p_2+p_4)|\,4]\end{aligned}$$

$$
\begin{aligned}
&= 2e^4 \left(\frac{1}{s^2} + \frac{1}{u^2}\right) \langle 42\rangle[21]\langle 12\rangle[24] \\
&= 2e^4 \left(\frac{u}{s} + \frac{s}{u}\right)
\end{aligned} \tag{4.40}
$$

with eight spin configurations in total, four per external photon helicity $2^{\mp}$ and $3^{\pm}$.

To get the massive cross section, we instead take the quasi-limit, where now the cross terms do survive

$$
|\mathcal{M}|^2 \xrightarrow{\text{qHE}} |\mathcal{M}_s|^2 + |\mathcal{M}_u|^2 + \mathcal{M}_s\mathcal{M}_u^\dagger + \mathcal{M}_s^\dagger\mathcal{M}_u. \tag{4.41}
$$

Starting with the first term, we have

$$
|\mathcal{M}_s|^2 = -g\tilde{g}\frac{\langle \boldsymbol{4k}\rangle[\boldsymbol{1k}]\langle \boldsymbol{k1}\rangle[\boldsymbol{k4}]}{\left(s-m^2\right)^2}, \tag{4.42}
$$

and the s channel momentum $\boldsymbol{k}^\mu = \boldsymbol{p}_1^\mu + p_2^\mu$ leads to the numerator

$$
\begin{aligned}
\langle \boldsymbol{4k}\rangle[\boldsymbol{1k}]\langle \boldsymbol{k1}\rangle[\boldsymbol{k4}] &= \Big(\langle \boldsymbol{44}\rangle[\boldsymbol{41}] + \langle \boldsymbol{42}\rangle[\boldsymbol{21}]\Big)\Big(\langle \boldsymbol{12}\rangle[\boldsymbol{24}] + \langle \boldsymbol{14}\rangle[\boldsymbol{44}]\Big) \\
&= (s-m^2)(u-m^2) - 2m^2(t-2m^2) + 4m^2\boldsymbol{p}_1\cdot p_2 \\
&= (s-m^2)(u-m^2) - 4m^2(s-m^2) + 4m^4
\end{aligned} \tag{4.43}
$$

using $t=0$ and $\boldsymbol{p}_1\cdot p_2 = s-m^2$. Similarly, the second term with u channel momentum $\boldsymbol{k}^\mu = p_2^\mu + \boldsymbol{p}_4^\mu$ has the same numerator after swapping $\boldsymbol{p}_1 \leftrightarrow \boldsymbol{p}_4$ and $s \leftrightarrow u$:

$$
\langle \boldsymbol{1k}\rangle[\boldsymbol{4k}]\langle \boldsymbol{k4}\rangle[\boldsymbol{k1}] = (s-m^2)(u-m^2) - 4m^2(u-m^2) + 4m^4. \tag{4.44}
$$

The cross terms use both s- and u-channel momenta and have the form

$$
\mathcal{M}_s\mathcal{M}_u^\dagger = g^2\tilde{g}^2\frac{\langle \boldsymbol{4}\,|(\boldsymbol{p}_1+p_2)|\,\boldsymbol{1}]}{s-m^2}\left(\frac{[\boldsymbol{4}\,|(p_2+\boldsymbol{p}_4)|\,\boldsymbol{1}\rangle}{u-m^2}\right)^\dagger \tag{4.45}
$$

with numerator

$$
\begin{aligned}
\langle \boldsymbol{4}\,|(\boldsymbol{p}_1+p_2)|\,\boldsymbol{1}]\langle \boldsymbol{1}\,|(p_2+\boldsymbol{p}_4)|\,\boldsymbol{4}] &= \big(\boldsymbol{p}_1^2 + \boldsymbol{p}_1\cdot p_2\big)\big(\boldsymbol{p}_4^2 + p_2\cdot\boldsymbol{p}_4\big) \\
&= 4m^4 - 2m^2\big(\boldsymbol{p}_1\cdot p_2 + p_2\cdot\boldsymbol{p}_4\big) + \boldsymbol{p}_1\cdot p_2^2\cdot\boldsymbol{p}_4 \\
&= 4m^4 - 2m^2\big(s+u-2m^2\big) \\
&= 4m^4.
\end{aligned} \tag{4.46}
$$

Note that lightlike $p_2^2 = 0$ and that the second term in the penultimate line vanishes due to the Mandelstam invariants $s + t + u = 2m^2$. This result implies $\mathcal{M}_s^\dagger \mathcal{M}_u = \left(\mathcal{M}_s \mathcal{M}_u^\dagger\right)^\dagger = 4m^4$.

Gathering everything leads to

$$\begin{aligned}\sigma_{\text{Compton}} &\xrightarrow{\text{qHE}} \frac{g^2\tilde{g}^2}{8}\left[\frac{(s-m^2)(u-m^2)-4m^2(u-m^2)+4m^4}{\left(s-m^2\right)^2}\right.\\ &\qquad\left.+\frac{(s-m^2)(u-m^2)-4m^2(s-m^2)+4m^4}{\left(u-m^2\right)^2}+\frac{8m^4}{(s-m^2)(u-m^2)}\right]\\ &\xrightarrow{\text{HE}} 2e^4\left(\frac{u}{s}+\frac{s}{u}\right),\end{aligned} \tag{4.47}$$

consistent with eq. (4.40) when $m \to 0$. The quasi-limit simplifies further, to the well-known form in the literature, upon using the Mandelstam invariants $u - m^2 = -(s - m^2)$

$$\begin{aligned}\sigma_{\text{Compton}} &\xrightarrow{\text{qHE}} 2e^4\left[\frac{u-m^2}{s-m^2}+\frac{s-m^2}{u-m^2}-4m^2\left(\frac{u-m^2}{\left(s-m^2\right)^2}+\frac{s-m^2}{\left(u-m^2\right)^2}\right)\right.\\ &\qquad\left.+4m^4\left(\frac{1}{\left(s-m^2\right)^2}+\frac{1}{\left(u-m^2\right)^2}\right)+\frac{8m^4}{(s-m^2)(u-m^2)}\right]\\ &= 2e^4\left[\frac{u-m^2}{s-m^2}+\frac{s-m^2}{u-m^2}+4m^2\left(\frac{1}{s-m^2}+\frac{1}{u-m^2}\right)+4m^4\left(\frac{1}{s-m^2}+\frac{1}{u-m^2}\right)^2\right].\end{aligned} \tag{4.48}$$

Performing this calculation in QFT is, of course, lengthier and more convoluted due to the redundancy built into the Dirac spinor embeddings in 4-vector fields. This typical "challenge problem" assigned to students now has a simpler solution. Now that we have performed several non-trivial checks of the massive spinor helicity formalism and have observed the computational benefits it offers, we shall turn to the examination of the potential insights it may reveal about fundamental interactions and the nature of spacetime.

5. Mass acquisition

We have thus extended the spinor helicity formalism toward the infrared region of the energy spectrum by including representations for massive particles, and we have calculated the scattering

amplitude and cross section of well known processes. It seems clear at this point that although the formulation and methods used here differ in significant ways from QFT, the standard results in the literature can nevertheless be reproduced with relative ease. Our departure from a manifestly local theory is, perhaps, the most important difference with QFT, since locality is a cornerstone of the Standard Model—upon which the central ideas of spontaneous symmetry breaking and effective field theory rest. Consequently, we shall begin by discussing the recent developments that have revealed an on-shell avatar of the Higgs mechanism, which essentially seems to be a manifestation of the coalescence of ultraviolet amplitudes when being reduced to low energies. Secondly, in order to investigate how locality and its absence might underlie this phenomenon, we shall put aside interactions to consider how the worldline of a particle is encoded by helicity spinors.

5.1. Coalescence and the Higgs mechanism

The idea about the existence of an on-shell avatar for the Higgs mechanism in the massive spinor helicity formalism traces back to Conde and Marzolla, who suggested that the helicity spinors representing the reference null vector for a massive particle change roles in the high-energy limit and effectively become the polarization vectors associated with a massless particle [7]. Arkani-Hamed *et al.* took this further by showing that the massive amplitude is the common low-energy limit of all possible external spin configurations of the corresponding massless amplitude [6]. Indeed, this merging of high-energy amplitudes is what we have been calling coalescence and is what was crucial for the calculation of unpolarized cross sections performed earlier in this paper. Their introductory Abelian example shows the essence of the mechanism: a spin-1 particle with mass m interacting with a massive Higgs scalar particle (which should have mass $\sqrt{2}m$) is the coalescence of spin configurations for coupling a massless spin 1 with two massless scalars. The process is therefore $(\mathbf{1}^1,\, \mathbf{2}^1, \mathbf{3}^0) \xrightarrow{\text{HE}} (1^h,\, 2^0, 3^0)$ with corresponding diagrams:

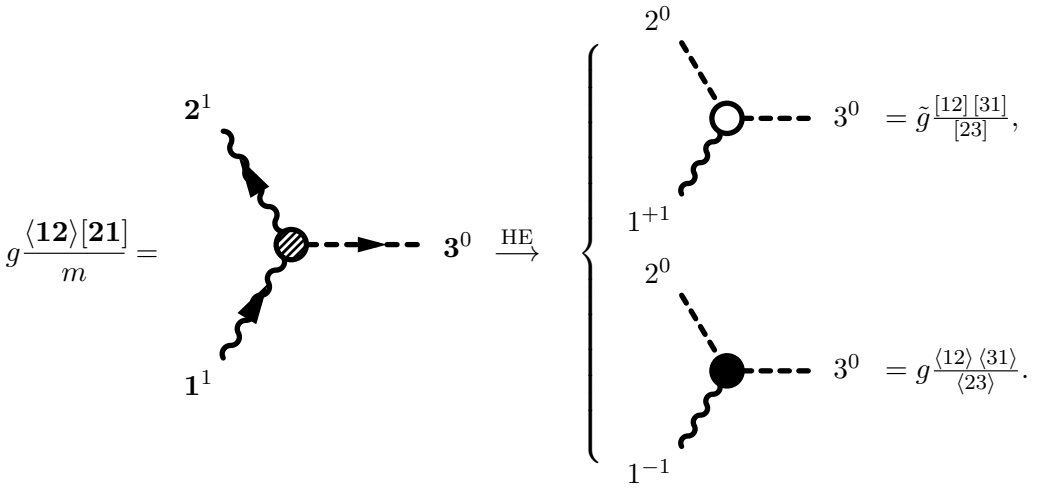

(5.1)

The general idea is that the two high-energy spin configurations of line 1^h and line 2^0 with a total of $2+1$ spin degrees of freedom coalesce at low-energy to represent a single massive spin 1 particle on lines $\mathbf{1}^1$ and $\mathbf{2}^1$ with three spin degrees of freedom. Thus, one can interpret the massless scalar line 2^0 as the Goldstone boson π. The remaining massive scalar line $\mathbf{3}^0$ plays a similar role to the Higgs boson σ that gets decoupled from the massive spin 1 particle A_μ in the nonlinear sigma model [15]. This interesting reformulation of mass acquisition presents new opportunities and raises important questions. The full particle spectrum after spontaneous symmetry breaking in QFT is tricky to interpret at best in the Abelian case and intractable at worst in non-Abelian and beyond-Standard-Model cases. This is due to the variety of kinetic mixing terms that can arise when expanding the Lagrangian density around the different vacua associated with the broken symmetry. For this reason, the decoupling limit that yields the nonlinear sigma model is a reasonable simplification which trades off information about σ in order to better understand the relationship between A_μ and π. Indeed, the CCWZ method (named after Callan, Coleman, Wess, and Zumino) of deducing π couplings in effective field theory from unbroken symmetry constraints in the full theory are accompanied by nonlinear transformations of π that complicate the nature between phenomena at the effective and the fundamental energy scales [27, 28]. In stark contrast, without any Lagrangian formulation to deal with, these issues seem to be absent in the spinor helicity formalism, whose

interactions are always accessible and in principle reducible to a conjunction of known couplings. Therefore, perhaps by analyzing mass acquisition via processes like fig. (5.1) more can be learned about effective field theory in general and Higgs physics in particular. Efforts along these lines are already underway within the Standard Model where important benchmarks have been achieved for tree-level calculations of the electroweak sector [29, 30] and quantum chromodynamics [31]. Beyond the Standard Model, the on-shell counterpart of the supersymmetrized Higgs mechanism appears to be a straightforward extension of the coalescence of superamplitudes, yet constraints on the Higgs supermultiplet and its interactions at low energy will require further analysis before new observables can be identified [12]. Regardless of the particular model, the advent of massive helicity spinors makes possible new on-shell analyses of effective field theory [32], Yang–Mills and Yukawa theories [33], and the deeper connection between spontaneously broken gauge theory and the unitary scattering of massive vector bosons [34]. On this last point, the spinor helicity formalism's departure from a manifestly local framework also raises important questions about what mass acquisition means for non-local representations of particles and their interactions.

5.2. Worldline representation

The bi-spinor representation of complexified momentum provides us with a more general setting to formulate scattering amplitudes by gluing together couplings. We learned that couplings and amplitudes constructed in this way are generally simpler than their QFT counterparts, especially when massless particles are involved, but this simplicity comes at the price of giving up locality. Let us dig deeper, before any interactions take place, by thinking about the worldline of a free particle moving through complexified Minkowski space $\mathbb{CM}$.

For a massless spin s particle, we expect its linear momentum to be null; thus, the matrix $p^{\alpha\dot{\alpha}}$ will be singular with vanishing determinant $\det p^{\alpha\dot{\alpha}} = \det p_{\dot{\alpha}\alpha} = 0$ and zero mass $p^2 = m^2 = 0$. The particle's worldline, therefore, is confined to lie on the null surface of the lightcone with null momentum given by the outer product $p^{\alpha\dot{\alpha}} = \lambda^\alpha \tilde{\lambda}^{\dot{\alpha}}$ and little group U(1) parameterized by the

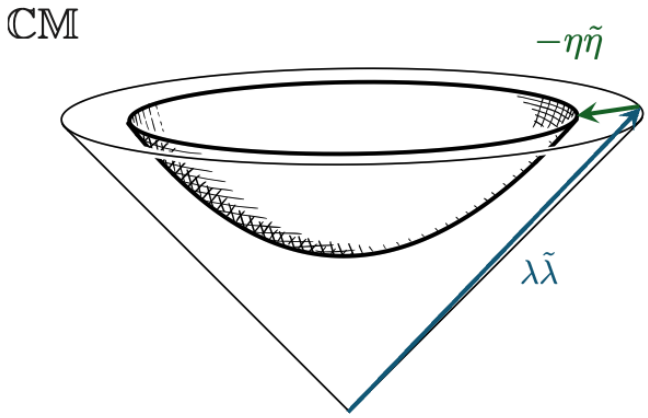

Figure 1: Future lightcone in complexified Minkowski space $\mathbb{CM}$. The null surface of the cone is parameterized by helicity spinors λ and $\tilde{\lambda}$. Its corresponding hyperbolic surface (shaded) in the interior of the cone is mapped with two additional helicity spinors η and $\tilde{\eta}$.

number $z \in \mathbb{C}$ in eq. (2.1). Thinking of this lightcone surface at future time $t > 0$ as the celestial complex 2-sphere, the required two complex degrees of freedom are provided by the Weyl spinors $\lambda^\alpha = \binom{a}{b}$ and $\tilde{\lambda}_{\dot{\alpha}} = \binom{\tilde{a}}{\tilde{b}}$ constrained by $\det p^{\alpha\dot{\alpha}} = 0$. A horizontal section of the future lightcone appears as a circle in fig. (1) instead of a sphere due to the suppression of one spatial dimension. Thus, any point on the celestial sphere is identified by the helicity spinors λ^α and $\tilde{\lambda}_{\dot{\alpha}}$, illustrated as a 4-vector pointing to this circle. Generally, we shall interpret lines in this and similar figures as 2-surfaces of spacetime, and surfaces in such figures as volumes of spacetime.

The massive spin s particle with a timelike momentum $p^2 = m^2 > 0$ and full-rank matrix $\det \boldsymbol{p}^{\alpha\dot{\alpha}} = m^2$ is defined by introducing two additional Weyl spinors η^α and $\tilde{\eta}_{\dot{\alpha}}$ according to eq. (2.6), which scale with mass m, so that $\boldsymbol{p}^{\alpha\dot{\alpha}} = \lambda^\alpha\tilde{\lambda}^{\dot{\alpha}} - \eta^\alpha\tilde{\eta}^{\dot{\alpha}} \xrightarrow{\text{HE}} p^{\alpha\dot{\alpha}} = \lambda^\alpha\tilde{\lambda}^{\dot{\alpha}}$. In line with Conde and Marzolla's suggestion [7] mentioned above in section 5.1, we can think of $\lambda^\alpha\tilde{\lambda}^{\dot{\alpha}}$ as the reference null vector directed toward a point on the celestial sphere that is parallel to $\boldsymbol{p}^{\alpha\dot{\alpha}}$. In the high-energy limit $\eta^\alpha\tilde{\eta}^{\dot{\alpha}}$ vanishes with $m \to 0$, and $\lambda^\alpha\tilde{\lambda}^{\dot{\alpha}}$ corresponds to null momentum p^μ, which is perpendicular to the massless particle's polarization vectors ϵ_1^μ and ϵ_2^μ. At low energies, the survival

of $\eta^\alpha\tilde{\eta}^{\dot{\alpha}}$ categorically increases the particle's degrees of freedom such that p^μ becomes timelike with $p^2 = m^2 > 0$, and the little group becomes SU(2) with $2s+1$ degrees of freedom. The massive particle's worldline has thus been peeled off from the null surface of the lightcone. At each moment in time $t > 0$, it will intersect the corresponding hyperbolic 3-surface inside the lightcone, as illustrated in fig. (1).

From this kinematical perspective, the acquisition of mass therefore indicates the excursion of the worldline inside the lightcone; a worldline whose depth beneath the null surface is parameterized by the bi-spinor $\eta^\alpha\tilde{\eta}^{\dot{\alpha}}$, which scales with m and is orthogonal to $\lambda^\alpha\tilde{\lambda}^{\dot{\alpha}}$ as can be seen from eqs. (2.7) and (2.8). In other words, a massive particle is *localized* within the lightcone's interior. This point of view complements the dynamical aspects of the scattering amplitudes we studied earlier, which showed that amplitudes constructed entirely from massless couplings are manifestly non-local, those involving massive particles as well as residual x factors still possess some non-local features, and only when all external particles become massive and all x factors cancel does locality manifest itself. This relationship between locality and mass is intriguing because it has always been obfuscated in QFT, where we imposed the locality of our quantum fields so that the breaking of their gauge symmetries could underlie the Higgs mechanism. Further exploration of the interplay between mass and locality might therefore enrich our understanding about particle physics and spacetime. We pursue this in the next and final section by subsuming the spinor helicity formalism within twistor theory, whose intrinsically non-local projective geometry can account for both mass acquisition and the emergence of spacetime.

6. Massive helicity spinors in twistor theory

The spinor helicity formalism suggests that locality is not a fundamental property of the universe but one that emerges from the coalescence of particle interactions at low energy. Despite their efficiency, helicity spinors lack a clear geometrical picture of the particles they represent. Indeed, these complex-valued objects do not exist in our real spacetime, yet they do encode 4-momentum,

and they do transform correctly under the Poincaré group. Sixty years ago, Roger Penrose proposed a new kind of algebra with an incidentally similar character, one which describes Minkowski space and its covariant Poincaré operations based on an abstract and by definition non-local geometry called projective twistor space [20]. Accordingly, we briefly review twistor theory and demonstrate how the ideas discussed in the previous sections—helicity spinors, complexified momentum, mass acquisition, and the emergence of a local spacetime—can all be encapsulated within Penrose's theory.

6.1. Twistors and the null rays of spacetime

In this section, we demonstrate how null rays forming the lightcones of Minkowski space $\mathbb{M}$ emerge from twistor theory. To do this, we first provide a brief introduction to twistors by adapting the notation set by Penrose and Rindler [35] with slight modifications to suit our purpose. A general introduction to the theory and its motivations is also given by Penrose [36].

The twistor Z^a is an object whose four components indexed by $a = 0, 1, 2, 3$ are coordinates into a complex-valued vector space called twistor space $\mathbb{T}$. By considering the three ratios of these coordinates, we obtain new (homogeneous) coordinates for a three-dimensional projection of $\mathbb{T}$ called *projective twistor space* $\mathbb{PT}$. The significance of this is that each *point* in $\mathbb{PT}$ can be made to correspond to a *ray* in spacetime; thus, a twistor variable in this projective space can represent the entire worldline of a particle or even a null ray of spacetime itself. This is achieved in a remarkable way for our Lorentzian 4-real-dimensional spacetime because in this particular case the celestial sphere is a conformal manifold whose homogeneous coordinates have the topology of the complex-valued Riemann sphere. In this sense, Minkowski space $\mathbb{M}$ is naturally generalized by twistor theory to a complex Minkowski space $\mathbb{CM}$, whose null rays and worldlines—and anything built from them—are analytic functions with a direct physical interpretation.[13]

[13]The compactification of $\mathbb{M}$ and $\mathbb{CM}$, including rays at infinity, is crucial for leveraging the complex geometry and analysis of this construction. Assume this done in what follows.

Now, the key distinction between twistors representing worldlines and those representing null rays is that the former should encode spin (by "twisting") while the latter should not. As we have seen throughout this paper, both the linear and angular momentum of a particle can be efficiently encoded as spinor helicity variables. This fact is leveraged in twistor theory by recasting the four components of Z^a as two spinors ω^α and $\tilde{\lambda}_{\dot{\alpha}}$ respectively called the *primary* and *projection* parts of the twistor

$$\mathsf{Z}^a = \begin{pmatrix} \omega^\alpha \\ \tilde{\lambda}_{\dot{\alpha}} \end{pmatrix}. \tag{6.1}$$

We shall treat these parts exactly like helicity spinors, where $\tilde{\lambda}_{\dot{\alpha}}$ is associated with linear momentum and ω^α with angular momentum. It is important to keep in mind that all twistors in $\mathbb{PT}$ must correspond to *some* direction and, therefore, $\tilde{\lambda}_{\dot{\alpha}} \neq 0$. To establish a correspondence between a twistor in $\mathbb{PT}$ and a line in Minkowski space, the spinor parts are constrained by the *incidence relation*

$$\omega^\alpha = \mathrm{i} r^{\alpha\dot{\alpha}} \tilde{\lambda}_{\dot{\alpha}}, \tag{6.2}$$

which can be thought of as the locus of points $r^{\alpha\dot{\alpha}} \in \mathbb{CM}$ that satisfies this equation for *fixed* ω^α and $\tilde{\lambda}_{\dot{\alpha}}$.[14] The particular locus of points where ω^α vanishes is called the α-plane, shifted from the origin by $\mathring{r}^{\alpha\dot{\alpha}}$ and given by

$$r^{\alpha\dot{\alpha}} = \mathring{r}^{\alpha\dot{\alpha}} + \kappa^\alpha \tilde{\lambda}^{\dot{\alpha}} \quad \text{for all } \kappa^\alpha. \tag{6.3}$$

That κ^α is arbitrary makes this a 2-complex-dimensional surface in $\mathbb{CM}$. In $\mathbb{PT}$, the α-plane corresponds to the 2-complex-parameter "star of lines" passing through the point Z^a, as shown in part A of fig. (2). We shall also require the complementary picture of this correspondence given by the *dual* twistor W_a with downstairs index a and dual incidence relation

$$\mathsf{W}_a = \begin{pmatrix} \xi_\alpha & \tilde{\pi}^{\dot{\alpha}} \end{pmatrix} \quad \text{such that} \quad \tilde{\pi}^{\dot{\alpha}} = -\mathrm{i}\xi_\alpha r^{\alpha\dot{\alpha}}. \tag{6.4}$$

[14] The bi-spinor $r^{\alpha\dot{\alpha}}$ is related to r^μ in the same way that $p^{\alpha\dot{\alpha}}$ is related to p^μ in eq. (2.2).

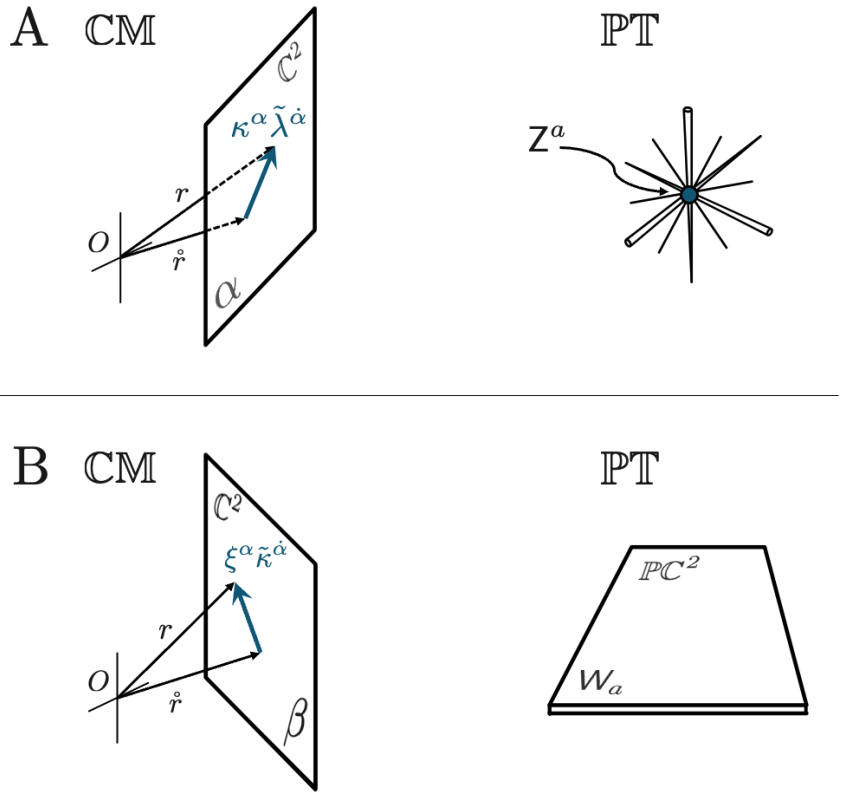

Figure 2: Twistor α-plane in $\mathbb{CM}$ and corresponding star of lines in $\mathbb{PT}$ (A). Dual twistor β-plane in $\mathbb{CM}$ and corresponding projective plane in $\mathbb{PT}$ (B).

The locus of points where the spinor part $\tilde{\pi}^{\dot\alpha}$ of W_a vanishes is called the β-plane, given by

$$r^{\alpha\dot\alpha} = \mathring{r}^{\alpha\dot\alpha} + \xi^\alpha\tilde{\kappa}^{\dot\alpha} \quad \text{for all } \tilde{\kappa}^{\dot\alpha}. \tag{6.5}$$

The β-plane in $\mathbb{CM}$ corresponds to a 2-complex-parameter "projective plane" in $\mathbb{PT}$, as shown in part B of fig. (2). Thus, we obtain the full correspondence between twistor Z^a and dual twistor W_a: in $\mathbb{CM}$ the α-plane is dual to the β-plane, and in $\mathbb{PT}$ the star of lines is dual to the projective plane. It is from the *incidence* of W and Z, given by $\mathsf{W}_a\mathsf{Z}^a = 0$, which is surprisingly rich in structure, whence the geometry of spacetime and the worldline of elementary particles can emerge. There is no privileged scale in projective geometry; instead, the vanishing contraction $\mathsf{W}_a\mathsf{Z}^a = 0$ answers the

question, 'Where in $\mathbb{PT}$ do Z and W intersect?' Whether we are dealing with null rays or worldlines is determined by the spin s associated with the twistors, which we can now define as follows

$$s = \frac{1}{2}\mathsf{Z}^a\bar{\mathsf{Z}}_a = \frac{1}{2}\begin{pmatrix}\omega^\alpha \\ \tilde{\lambda}_{\dot{\alpha}}\end{pmatrix}\begin{pmatrix}\lambda_\alpha & \tilde{\omega}^{\dot{\alpha}}\end{pmatrix} = \frac{1}{2}\left(\omega^\alpha\lambda_\alpha + \tilde{\lambda}_{\dot{\alpha}}\tilde{\omega}^{\dot{\alpha}}\right), \tag{6.6}$$

where $\bar{\mathsf{Z}}_a$ is the dual twistor of Z^a.

The projective twistor space is divided into three subsets based on s. In this section, we focus only on twistors without spin ($s = 0$) called *null twistors*, which sit in the null projective twistor space $\mathbb{PN} \subset \mathbb{PT}$. The incidence of a null twistor Z^a with another null dual twistor W_a corresponds to the intersection of the α_{Z}- and β_{W}-planes and thus traces out a generally complex-valued *null geodesic* L through $\mathbb{CM}$, given by

$$r^{\alpha\dot{\alpha}}(u) = \mathring{r}^{\alpha\dot{\alpha}} + u\xi^\alpha\tilde{\lambda}^{\dot{\alpha}} \quad \text{for } u \in \mathbb{C}. \tag{6.7}$$

In $\mathbb{PT}$, this corresponds to the intersection of the star of lines of Z^a and projective plane of W_a, which is a "plane pencil of lines" in $\mathbb{PN}$, as shown in fig. (3). Since L is parameterized by complex-valued u, it has the topology of the Riemann sphere S^2. The null geodesic gets its name from the great circle on the Riemann sphere, where u takes on real numbers. However, L must also contain some complex-valued points $r^{\alpha\dot{\alpha}}$ corresponding to values u off of the great circle. Only for the special case $\mathsf{W}_a = \bar{\mathsf{Z}}_a = \begin{pmatrix}\lambda_\alpha & \tilde{\omega}^{\dot{\alpha}}\end{pmatrix}$ does the locus $r^{\alpha\dot{\alpha}}$ only take on real values, thus describing the real null ray Z

$$r^{\alpha\dot{\alpha}}(h) = \mathring{r}^{\alpha\dot{\alpha}} + h\lambda^\alpha\tilde{\lambda}^{\dot{\alpha}} \quad \text{for } h \in \mathbb{R}. \tag{6.8}$$

And so we see that the set of null twistors in $\mathbb{PN}$ gives rise to all real null rays for all lightcones in real Minkowski space $\mathbb{M}$. It is in this way that spacetime emerges from twistor theory.

Before moving on to the non-null subsets of $\mathbb{PT}$, we now show that eq. (6.8) is the locus in $\mathbb{M}$ of Z^a where $\omega^\alpha = 0$. This calculation will be useful in the following sections. Still assuming that $\tilde{\lambda}_{\dot{\alpha}} \neq 0$, consider the incidence relation

$$\mathrm{i}r^{\alpha\dot{\alpha}}\tilde{\lambda}_{\dot{\alpha}} = \mathring{\omega}^\alpha, \tag{6.9}$$

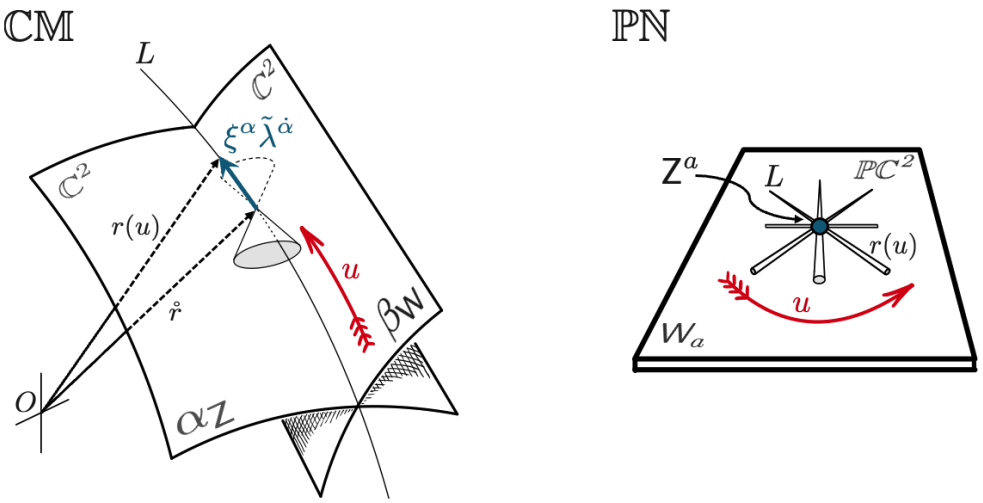

Figure 3: A null geodesic is traced out by the incidence $\mathsf{W}_a\mathsf{Z}^a = 0$, corresponding to a complex-valued null ray L through $\mathbb{CM}$ and a plane pencil of lines (also L) in $\mathbb{PN}$ parameterized by $u \in \mathbb{C}$.

where we consider the angular momentum spinor at the origin $\mathring{\omega}^\alpha$, which is non-zero and orthogonal to λ^α so that $\mathring{\omega}^\alpha\lambda_\alpha = 0$. By contracting the incidence relation with $\mathring{\tilde{\omega}}^{\dot{\alpha}}$, the solution of points can be obtained

$$r^{\alpha\dot{\alpha}} = \left(\mathrm{i}\tilde{\lambda}_{\dot{\beta}}\mathring{\tilde{\omega}}^{\dot{\beta}}\right)^{-1}\mathring{\omega}^\alpha\mathring{\tilde{\omega}}^{\dot{\alpha}}. \tag{6.10}$$

Note that the elements of the factor $\mathring{\omega}^\alpha\mathring{\tilde{\omega}}^{\dot{\alpha}}$ are real because

$$\mathring{\omega}^\alpha\mathring{\tilde{\omega}}^{\dot{\alpha}} = \mathring{\omega}^\alpha\left(\mathring{\omega}^\alpha\right)^* = \left|\mathring{\omega}^\alpha\right|^2 \in \mathbb{R}. \tag{6.11}$$

Also, since Z^a is a null twistor, eq. (6.6) implies that

$$\begin{aligned}\mathsf{Z}^a\bar{\mathsf{Z}}_a = 0 &\Rightarrow \mathring{\omega}^\alpha\lambda_\alpha + \mathring{\tilde{\omega}}^{\dot{\alpha}}\tilde{\lambda}_{\dot{\alpha}} = 0\\ &\Rightarrow \mathring{\omega}^\alpha\lambda_\alpha = -\left(\mathring{\omega}^\alpha\lambda_\alpha\right)^*\\ &\Rightarrow \mathring{\omega}^\alpha\lambda_\alpha \text{ is purely imaginary,}\end{aligned} \tag{6.12}$$

and thus $\mathrm{i}\mathring{\omega}^{\alpha}\lambda_{\alpha}$ is real. Therefore, we can conclude that all points $r^{\alpha\dot{\alpha}}$ satisfying eq. (6.10) form a real locus in $\mathbb{M}$. Finally, to recover the parameterization of this locus in eq. (6.8), note that one of these points must be the displacement of the ray from the origin $\mathring{r}^{\alpha\dot{\alpha}}$. Consider the difference

$$\begin{aligned} \mathrm{i}r^{\alpha\dot{\alpha}}\tilde{\lambda}_{\dot{\alpha}} &= \mathring{\omega}^{\alpha} \\ -\mathrm{i}\mathring{r}^{\alpha\dot{\alpha}}\tilde{\lambda}_{\dot{\alpha}} &= \mathring{\omega}^{\alpha} \\ \hline \left(r^{\alpha\dot{\alpha}} - \mathring{r}^{\alpha\dot{\alpha}}\right)\tilde{\lambda}_{\dot{\alpha}} &= 0. \end{aligned}$$

This means that the displacement along the null ray $r^{\alpha\dot{\alpha}} - \mathring{r}^{\alpha\dot{\alpha}}$ is real and also annihilates $\tilde{\lambda}_{\dot{\alpha}}$. We can, therefore, identify it with a real-scaled version of λ^{α}, and that is exactly what the term $h\lambda^{\alpha}\tilde{\lambda}^{\dot{\alpha}}$ in eq. (6.8) represents. Here, we considered the spinor part representing angular momentum evaluated at the origin $\mathring{\omega}^{\alpha}$. It will be useful in the next section to note that the origin in $\mathbb{CM}$ is arbitrary, and $\omega^{\alpha} \to \omega^{\alpha} - \mathrm{i}r^{\alpha\dot{\alpha}}\tilde{\lambda}_{\dot{\alpha}}$, while $\tilde{\lambda}_{\dot{\alpha}}$ remains fixed under a change in origin. The opposite is true for dual twistors $\mathsf{W}_a = \begin{pmatrix} \xi_{\alpha} & \tilde{\pi}^{\dot{\alpha}} \end{pmatrix}$, where ξ_{α} is constant and $\tilde{\pi}^{\dot{\alpha}} \to \tilde{\pi}^{\dot{\alpha}} + \mathrm{i}\xi_{\alpha}r^{\alpha\dot{\alpha}}$ [35].

6.2. Lightlike null hyperplane

The previous section showed that null twistors, i.e., those with $s = 0$, give rise to the real null rays of spacetime, upon which ω^{α} vanishes and no angular momentum is associated with the ray. We also saw that null twistors only correspond to the null projective subspace $\mathbb{PN} \subset \mathbb{PT}$. Now we consider the case where Z^a has spin $s \neq 0$. From eq. (6.6), we have $\omega^{\alpha}\lambda_{\alpha} = s$, since $\overline{\tilde{\lambda}_{\dot{\alpha}}\tilde{\omega}^{\dot{\alpha}}} = \omega^{\alpha}\lambda_{\alpha}$. This implies that $\omega^{\alpha} \neq 0$ for all real points in $\mathbb{CM}$. Recall that ω^{α} is the spinor field associated with angular momentum, and we shall now see that Z^a with $s \neq 0$ indeed represents a massless particle in $\mathbb{M}$ with helicity. For this reason, it is called a *lightlike twistor*.

Twistors with $s > 0$ are said to have positive helicity and live in the subspace $\mathbb{PT}^{+}$, while those with $s < 0$ are their negative counterparts sitting in $\mathbb{PT}^{-}$. Unlike the case of null twistors, the incidence relation in eq. (6.2) for lightlike twistors can only be satisfied by a locus of complex points $r^{\alpha\dot{\alpha}} \in \mathbb{CM}$. In other words, the α-plane, upon which ω^{α} vanishes, contains no real points. The lightlike dual twistor $\mathsf{W}_a = \begin{pmatrix} \xi_{\alpha} & \tilde{\pi}^{\dot{\alpha}} \end{pmatrix}$ also has $s \neq 0$, and thus $\xi_{\alpha}\pi^{\alpha} = s$. The dual incidence

relation $\tilde{\pi}^{\dot{\alpha}} = -\mathrm{i}\xi_\alpha r^{\alpha\dot{\alpha}}$ is satisfied for complex $r^{\alpha\dot{\alpha}} \in \mathbb{CM}$; its β-plane, upon which $\tilde{\pi}^{\dot{\alpha}}$ vanishes, also contains no real points. Therefore, when considering the incidence of lightlike twistors $\mathsf{W}_a\mathsf{Z}^a = 0$, the null geodesic $r^{\alpha\dot{\alpha}}(u)$ will be entirely complex valued. The lightlike α_Z and β_W planes do still meet where $\omega^\alpha = \tilde{\pi}^{\dot{\alpha}} = 0$; however, this occurs on a locus of points forming a complex null geodesic. These twistors nevertheless have a reality structure, which possesses angular momentum, is null, and is remarkably non-local. This offers an explanation for the non-local properties we previously encountered for massless helicity spinors, and it also justifies why we qualify these non-null twistors as being lightlike. The structure in $\mathbb{M}$ is not localized as a single ray, as it was for null twistors, but instead consists of a special family of null rays called a *Robinson congruence* [20] that forms a null hyperplane Π and fills $\mathbb{R}^3$ entirely. Snapshots of this congruence in $\mathbb{M}$ are strikingly beautiful and can be described mathematically as a stereographic projection of *Clifford parallels* on the three-sphere S^3. Renditions shown elsewhere illustrate a system of oriented circles twisting around each other and filling all space, thus encoding the angular momentum of the system [35, 36].

To visualize this in $\mathbb{M}$, note that the spinor part ω^α of the lightlike twistor is non-zero and takes the null direction that intersects the single ray of the corresponding null twistor Z^a whose constant, linear momentum $p^{\alpha\dot{\alpha}} = \lambda^\alpha\tilde{\lambda}^{\dot{\alpha}}$ matches that of the lightlike twistor fig. (4). Therefore, we can visualize the null hyperplane Π of a lightlike twistor as *the family of null directions for all lightcones* whose vertices lie on Z^a. It is in this sense that the lightlike twistor does not have a worldline and is therefore not localized.

Taken together, a lightlike particle is described by a twistor $\mathsf{Z}^a = \begin{pmatrix} \omega^\alpha \\ \tilde{\lambda}_{\dot{\alpha}} \end{pmatrix}$ up to a phase $e^{\mathrm{i}\theta}$ for θ real. Although not important for our purposes here, this phase arises from differences between the orientated plane elements defined by bi-spinors $\omega^\alpha\omega^\beta$ and $\tilde{\lambda}^{\dot{\alpha}}\tilde{\lambda}^{\dot{\beta}}$, as illustrated by the "flags" in fig. (4). Whether it has a role to play in the physical theory, e.g., by describing quantum interference or polarization effects, remains unclear. Its 4-momentum $p^\mu \mapsto p^{\alpha\dot{\alpha}} \equiv \lambda^\alpha\tilde{\lambda}^{\dot{\alpha}}$ and 6-angular momentum relative to the origin are [35]

$$M^{\mu\nu} \mapsto M^{\alpha\dot{\alpha}\beta\dot{\beta}} \equiv \mathrm{i}\omega^{(\alpha}\lambda^{\beta)}\varepsilon^{\dot{\alpha}\dot{\beta}} - \mathrm{i}\varepsilon^{\alpha\beta}\tilde{\omega}^{(\dot{\alpha}}\tilde{\lambda}^{\dot{\beta})}. \tag{6.13}$$

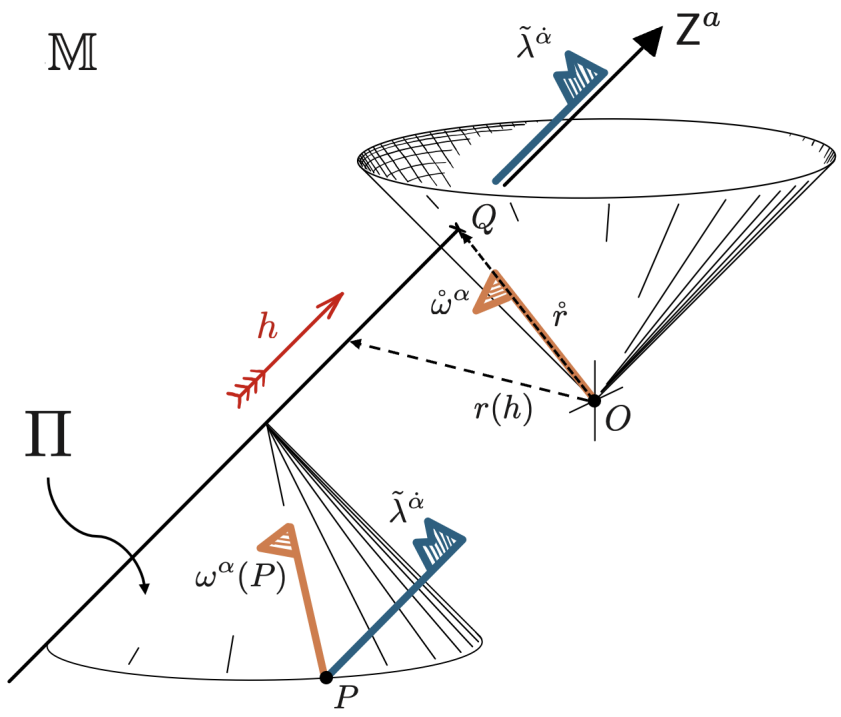

Figure 4: Null hyperplane Π of a lightlike twistor Z^a in Minkowski space $\mathbb{M}$. Both spinor parts ω^{α} and $\tilde{\lambda}_{\dot{\alpha}}$ are non-zero everywhere in $\mathbb{M}$. At any point P, ω^{α} points along the lightcone whose vertex lies on the null ray given by Z^a, thus encoding the non-zero angular momentum. Point Q on the null ray Z^a is closest to the origin O. Adapted from fig. 6-2 of Penrose & Rindler [35].

Under a displacement $r^{\alpha\dot{\alpha}}$ of the origin, the linear momentum remains constant $p^{\alpha\dot{\alpha}} \to p^{\alpha\dot{\alpha}}$, and the angular momentum transforms according to

$$M^{\alpha\dot{\alpha}\beta\dot{\beta}} \to M^{\alpha\dot{\alpha}\beta\dot{\beta}} - 2r^{[\alpha\dot{\alpha}}p^{\beta\dot{\beta}]} \tag{6.14}$$

with square brackets representing antisymmetrization of the Lorentz indices. We can derive a formula for Π by attempting to find the locus $r^{\alpha\dot{\alpha}}$ satisfying the relativistic center-of-mass given by $p_\mu M^{\mu\nu} = 0$ [37]. Without loss of generality, choose $\mathring{r}^{\mu}$ such that $p_\mu \mathring{r}^{\mu} = 0$ and $r^{\mu}(h) = \mathring{r}^{\mu} + hp^{\mu}$,

for $h \in \mathbb{R}$, as shown in fig. (4). Now consider,

$$M^{\mu\nu}(\mathring{r}^{\mu})p_{\nu} = \mathring{M}^{\mu\nu}p_{\nu} - 2\mathring{r}^{[\mu}p^{\nu]}p_{\nu} = \mathring{M}^{\mu\nu}p_{\nu} - \mathring{r}^{\mu}p^2 = 0. \tag{6.15}$$

Solving for $\mathring{r}^{\mu}$ in the last equation, we obtain the real parameterization for the locus forming Π

$$r^{\mu}(h) = \frac{\mathring{M}^{\mu\nu}p_{\nu}}{p_{\sigma}p^{\sigma}} + hp^{\mu} \quad \text{for } h \in \mathbb{R}. \tag{6.16}$$

If p^{μ} is lightlike, then $p^2 = 0$ and the relativistic center-of-mass $p_{\mu}M^{\mu\nu} = 0$ has no solution unless $\mathring{M}^{\mu\nu} = r^{\mu}p^{\nu} - p^{\mu}r^{\nu}$, which implies

$$\mathring{M}^{\mu\nu}p_{\nu} = r^{\mu}p^2 - p^{\mu}\left(r_{\nu}p^{\nu}\right) = -p^{\mu}\left(r_{\nu}p^{\nu}\right). \tag{6.17}$$

Therefore, the relativistic center-of-mass exists only if $\mathring{M}^{\mu\nu}p_{\nu}$ is proportional to the linear momentum p^{μ} and $r_{\nu}p^{\nu} = k$ for constant k. This last result follows from the fact that lightlike particles must have exactly two spin degrees of freedom, thus $s \neq 0$, and a constant spin vector

$$S_{\mu} = \star M_{\mu\nu}p^{\nu} = \star\mathring{M}_{\mu\nu}p^{\nu} = \mathring{S}_{\mu}, \tag{6.18}$$

where $\star$ indicates the Hodge dual $\star M_{\mu\nu} = \frac{1}{2}e_{\mu\nu\rho\sigma}M^{\rho\sigma}$ [35]. This in turn implies

$$S_{\mu} = \star M_{\mu\nu}p^{\nu} = sp_{\mu}, \tag{6.19}$$

where the spin s is, of course, also constant and non-zero. Therefore, we can conclude that the relativistic center-of-mass is satisfied on the locus of points r^{μ} where $r_{\mu}p^{\mu} = k$ is constant, which is indeed a 3-real-dimensional hyperplane Π in $\mathbb{CM}$ corresponding to the Robinson congruence that fills $\mathbb{R}^3$ in $\mathbb{M}$. It is not hard to see that Π is the locus of points where $\omega^{\alpha}(r^{\alpha\dot{\alpha}})$ satisfies $\omega^{\alpha}\lambda_{\alpha} = s$, as was claimed at the beginning of this subsection, since the relativistic center-of-mass according to eq. (6.13) implies

$$\begin{aligned} p_{\mu}M^{\mu\nu} = 0 &\rightarrow p_{\dot{\alpha}\alpha}M^{\alpha\dot{\alpha}\beta\dot{\beta}} = 0 \\ &\Rightarrow \mathrm{i}\lambda^{\beta}\tilde{\lambda}^{\dot{\beta}}\left(-\omega^{\alpha}\tilde{\lambda}_{\alpha} + \tilde{\lambda}_{\dot{\alpha}}\tilde{\omega}^{\dot{\alpha}}\right) = 0 \\ &\Rightarrow \omega^{\alpha}\lambda_{\alpha} = \tilde{\lambda}_{\dot{\alpha}}\tilde{\omega}^{\dot{\alpha}}. \end{aligned} \tag{6.20}$$

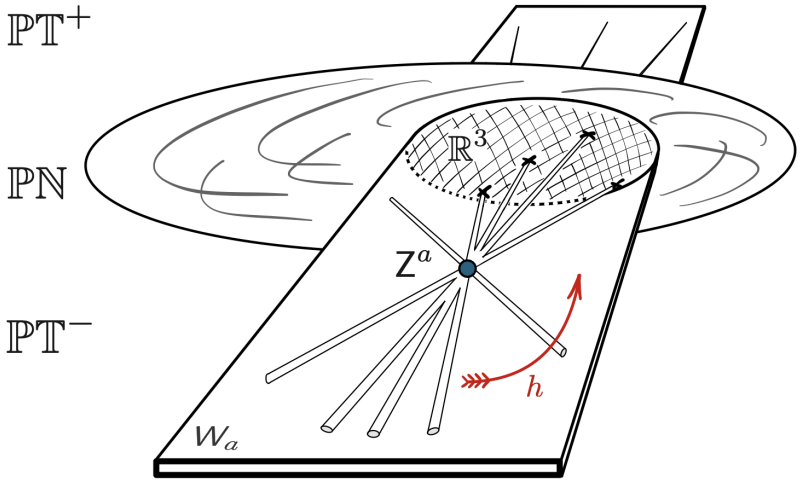

Figure 5: Incidence of lightlike twistor Z^a and dual twistor W_a in projective twistor space $\mathbb{PT}$. The Robinson congruence is generated by those plane pencil lines intersecting $\mathbb{PN}$. Adapted from fig. 33.14 of Penrose [36].

Note that this is same constraint we found upon expanding $s = \frac{1}{2}Z^a\bar{Z}_a$ in eq. (6.6).

In projective twistor space, we can consider the corresponding incidence $W_aZ^a = 0$, whose geometry is similar to that for null twistors, shown on the right hand side of fig. (3). The main difference is that both Z^a and W_a now extend beyond $\mathbb{PN}$. For example, if Z^a has negative helicity, it will be located in $\mathbb{PT}^-$. Some subset within its star of lines will, however, pass through $\mathbb{PN}$. Since W_a is dual to some lightlike twistor, its projective plane $\mathbb{PC}^2$ will also intersect with $\mathbb{PN}$. Thus, the plane pencil of lines satisfying their incidence parameterizes a 3-real-dimensional region in $\mathbb{PN}$ whose points correspond to the Robinson congruence of rays in $\mathbb{M}$, as shown in fig. (5).

6.3. Massive timelike worldline

Earlier in this paper, we constructed massive helicity spinors and their scattering amplitudes by considering the linear combination of massless spinors λ^α and η^α and their duals, as in eq. (2.6).

This led to the description of a particle with timelike momentum $\boldsymbol{p}^{\alpha\dot{\alpha}} = \lambda^{\alpha}\tilde{\lambda}^{\dot{\alpha}} - \eta^{\alpha}\tilde{\eta}^{\dot{\alpha}}$ and mass $\boldsymbol{p}^2 = m^2$. We learned that massive helicity spinor couplings are non-local (sort of) due to their x factor, but their amplitudes can become local if all x factors cancel out.

In a similar fashion, we shall now see that a massive particle can be represented by the linear combination of lightlike twistors X^a and Z^a

$$\mathsf{Y}^a = \begin{pmatrix} \psi^{\alpha} \\ \tilde{\kappa}_{\dot{\alpha}} \end{pmatrix} \equiv \beta \mathsf{X}^a + \gamma \mathsf{Z}^a \quad \text{for } \beta,\, \gamma \in \mathbb{C}, \tag{6.21}$$

where

$$\mathsf{X}^a = \begin{pmatrix} \chi^{\alpha} \\ \tilde{\eta}_{\dot{\alpha}} \end{pmatrix} \quad \text{and} \quad \mathsf{Z}^a = \begin{pmatrix} \omega^{\alpha} \\ \tilde{\lambda}_{\dot{\alpha}} \end{pmatrix} \tag{6.22}$$

have helicity

$$s = \frac{1}{2}\mathsf{X}^a\bar{\mathsf{X}}_a = \frac{1}{2}\mathsf{Z}^a\bar{\mathsf{Z}}_a. \tag{6.23}$$

Interestingly, since Y^a represents a massive particle with non-zero spin s, its worldline must also be non-local in $\mathbb{M}$, since $\psi^{\alpha} \neq 0$ for all real points. In $\mathbb{CM}$, however, it turns out that Y^a *does* have unique timelike worldline that runs along the incidence of the null hyperplanes Π_{X} and Π_{Z}. By definition, these hyperplanes intersect if and only if $\mathsf{X}^a\bar{\mathsf{Z}}_a = \mathsf{Z}^a\bar{\mathsf{X}}_a = 0$. Being two 3-real-dimensional hyperplanes in $\mathbb{CM}$, their intersection is a 2-real-dimensional surface or, equivalently, a 1-complex-dimensional worldline. Each point on the worldline must satisfy both incidence relations

$$\mathrm{i}r^{\alpha\dot{\alpha}}\tilde{\lambda}_{\dot{\alpha}} = \omega^a, \tag{6.24}$$

$$\mathrm{i}r^{\alpha\dot{\alpha}}\tilde{\eta}_{\dot{\alpha}} = \chi^a. \tag{6.25}$$

Indeed, note that neither relation is satisfied on real points. For example,

$$\mathsf{Z}^a\bar{\mathsf{Z}}_a = \omega^{\alpha}\lambda_{\alpha} + \tilde{\lambda}_{\dot{\alpha}}\tilde{\omega}^{\dot{\alpha}} = 2s \Rightarrow \tilde{\lambda}_{\dot{\alpha}}\tilde{\omega}^{\dot{\alpha}} = 2s - \omega^{\alpha}\lambda_{\alpha}, \tag{6.26}$$

and also

$$\omega^{\alpha}\lambda_{\alpha} = \mathrm{i}r^{\alpha\dot{\alpha}}\tilde{\lambda}_{\dot{\alpha}}\lambda_{\alpha} \Rightarrow \tilde{\lambda}_{\dot{\alpha}}\tilde{\omega}^{\dot{\alpha}} = -\mathrm{i}r^{\alpha\dot{\alpha}}\tilde{\lambda}_{\dot{\alpha}}\lambda_a = 2s - \omega^{\alpha}\lambda_{\alpha}. \tag{6.27}$$

Therefore,

$$\overline{\omega^\alpha \lambda_\alpha} = 2s - \omega^\alpha \lambda_\alpha \notin \mathbb{R} \quad \text{for } s \neq 0, \tag{6.28}$$

and furthermore

$$\overline{\mathrm{i} r^{\alpha\dot{\alpha}} \tilde{\lambda}_{\dot{\alpha}} \lambda_\alpha} = \overline{\omega^\alpha \lambda_\alpha} = \tilde{\lambda}_{\dot{\alpha}} \tilde{\omega}^{\dot{\alpha}} = 2s - \mathrm{i} r^{\alpha\dot{\alpha}} \tilde{\lambda}_{\dot{\alpha}} \lambda_\alpha. \tag{6.29}$$

This implies that the matrix $r^{\alpha\dot{\alpha}}$ is not Hermitian; therefore, $\Pi_{\mathsf{X}} \cap \Pi_{\mathsf{Z}}$ must occur on a locus of complex points where $\chi^\alpha = \omega^\alpha = 0$. Consequently, following eq. (6.21), the primary part of Y^a also vanishes $\psi^\alpha = \beta\chi^\alpha + \gamma\omega^\alpha = 0$, and the above locus also defines the complex worldline of Y^a. Indeed, one can check by direct substitution using the incidence relations in eqs. (6.24) and (6.25) that the complex locus is

$$r^{\alpha\dot{\alpha}} = \frac{\omega^\alpha \tilde{\eta}^{\dot{\alpha}} - \chi^\alpha \tilde{\lambda}^{\dot{\alpha}}}{\mathrm{i} \tilde{\lambda}_{\dot{\beta}} \tilde{\eta}^{\dot{\beta}}}, \quad \text{where } \tilde{\lambda}_{\dot{\alpha}} \not\propto \tilde{\eta}_{\dot{\alpha}}. \tag{6.30}$$

So much for the worldline. The massive particle will also have non-zero spin

$$s_{\mathsf{Y}} = \frac{1}{2} \mathsf{Y}^a \bar{\mathsf{Y}}_a = \frac{|\beta|^2}{2} \mathsf{X}^a \bar{\mathsf{X}}_a + \frac{|\gamma|^2}{2} \mathsf{Z}^a \bar{\mathsf{Z}}_a = \frac{|\beta|^2 + |\gamma|^2}{2} s \tag{6.31}$$

and momentum

$$\tilde{\kappa}_{\dot{\alpha}} \kappa_\alpha = |\beta|^2 \tilde{\eta}_{\dot{\alpha}} \eta_\alpha + |\gamma|^2 \tilde{\lambda}_{\dot{\alpha}} \lambda_\alpha + \beta\gamma^* \tilde{\eta}_{\dot{\alpha}} \lambda_\alpha + \beta^* \gamma \tilde{\lambda}_{\dot{\alpha}} \eta_\alpha \tag{6.32}$$

for general $\beta, \gamma \in \mathbb{C}$. In the special case where $\gamma = \mathrm{i}\beta$, we find a familiar result where the momenta simply add up

$$\begin{aligned} p_{\mathsf{Y}\,\dot{\alpha}\alpha} \equiv \tilde{\kappa}_{\dot{\alpha}} \kappa_\alpha &= |\beta|^2 \left(\tilde{\eta}_{\dot{\alpha}} \eta_\alpha + \tilde{\lambda}_{\dot{\alpha}} \lambda_\alpha - \mathrm{i} \tilde{\eta}_{\dot{\alpha}} \lambda_\alpha + \mathrm{i} \tilde{\lambda}_{\dot{\alpha}} \eta_\alpha \right) \\ &= |\beta|^2 \left(p_{\mathsf{X}\,\dot{\alpha}\alpha} + p_{\mathsf{Z}\,\dot{\alpha}\alpha} \right) \quad \text{if } \tilde{\eta}_{\dot{\alpha}} \lambda_\alpha \text{ is Hermitian.} \end{aligned} \tag{6.33}$$

This equation is identical to $\boldsymbol{p}_{\dot{\alpha}\alpha} = \tilde{\lambda}_{\dot{\alpha}} \lambda_\alpha - \tilde{\eta}_{\dot{\alpha}} \eta_\alpha$ when $|\beta|^2 = 1$, with the exception of a minus sign indicating the opposite direction of $p_{\mathsf{X}\,\dot{\alpha}\alpha} = \tilde{\eta}_{\dot{\alpha}} \eta_\alpha$, which could be absorbed into the definition of X_a

in eq. (6.21). We thus recognize the massive helicity spinor as the projection part of what we shall call the *timelike twistor*

$$\mathsf{Y}^a = \mathsf{X}^a + \mathrm{i}\mathsf{Z}^a = \begin{pmatrix} \chi^\alpha + \mathrm{i}\omega^\alpha \\ \tilde{\eta}_{\dot{\alpha}} + \mathrm{i}\tilde{\lambda}_{\dot{\alpha}} \end{pmatrix}. \tag{6.34}$$

The spin of Y^a is encoded by the *total angular momentum twistor*, a bi-twistor with symmetrized indices

$$\mathsf{A}_{ab} = 2\bar{\mathsf{X}}_{(a}\mathsf{I}_{b)c}\mathsf{X}^c + 2\bar{\mathsf{Z}}_{(a}\mathsf{I}_{b)c}\mathsf{Z}^c, \quad \text{with } \mathsf{I}_{ab} \equiv \begin{pmatrix} 0 & 0 \\ 0 & \varepsilon^{\dot{\alpha}\dot{\beta}} \end{pmatrix}. \tag{6.35}$$

This is the sum of the angular momenta from X^a and Z^a. For example,

$$\mathsf{A}_{\mathsf{Z}ab} = 2\bar{\mathsf{Z}}_{(a}\mathsf{I}_{b)c}\mathsf{Z}^c = \begin{pmatrix} 0 & \lambda_\alpha\tilde{\lambda}^{\dot{\beta}} \\ \tilde{\lambda}^{\dot{\alpha}}\lambda_\beta & -2\tilde{\omega}^{(\dot{\alpha}}\tilde{\lambda}^{\dot{\beta})} \end{pmatrix}. \tag{6.36}$$

The mass follows from the "square" of the angular momentum [35, 38]

$$\begin{aligned} -\frac{1}{2}\mathsf{A}_{ab}\bar{\mathsf{A}}^{ab} &= 2\Big(\bar{\mathsf{X}}_{(a}\mathsf{I}_{b)c}\mathsf{X}^c + \bar{\mathsf{Z}}_{(a}\mathsf{I}_{b)c}\mathsf{Z}^c\Big)\Big(\mathsf{X}^{(a}\mathsf{I}^{b)c}\bar{\mathsf{X}}_c + \mathsf{Z}^{(a}\mathsf{I}^{b)c}\bar{\mathsf{Z}}_c\Big) \\ &= 2\left|\mathsf{X}^a\mathsf{Z}^b\mathsf{I}_{ab}\right|^2 \\ &= 2\left|\begin{pmatrix}\chi^\alpha \\ \tilde{\eta}_{\dot{\alpha}}\end{pmatrix}\begin{pmatrix}\omega^\beta \\ \tilde{\lambda}_{\dot{\beta}}\end{pmatrix}\begin{pmatrix}0 & 0 \\ 0 & \varepsilon^{\dot{\alpha}\dot{\beta}}\end{pmatrix}\right|^2 \\ &= 2\left|\tilde{\eta}_{\dot{\alpha}}\tilde{\lambda}^{\dot{\alpha}}\right|^2. \end{aligned} \tag{6.37}$$

Note the product of like-terms in the first line will vanish due to the fact that $\tilde{\eta}_{\dot{\alpha}}\tilde{\eta}^{\dot{\alpha}} = \tilde{\lambda}_{\dot{\alpha}}\tilde{\lambda}^{\dot{\alpha}} = 0$; therefore, only the cross-terms appear in the second line. We recognize this last expression as $p_{\mathsf{Y}}^2 = p_{\mathsf{Y}\dot{\alpha}\alpha}\, p_{\mathsf{Y}}^{\alpha\dot{\alpha}} = m^2$, since only cross-terms in $\big(\tilde{\kappa}_{\dot{\alpha}}\kappa_\alpha\big)\big(\kappa^\alpha\tilde{\kappa}^{\dot{\alpha}}\big)$ will be non-zero:

$$\begin{aligned} p_{\mathsf{Y}}^2 &= |\beta|^2|\gamma|^2\left(\tilde{\eta}_{\dot{\alpha}}\lambda_\alpha\tilde{\lambda}^{\dot{\alpha}}\eta^\alpha + \tilde{\lambda}_{\dot{\alpha}}\eta_\alpha\tilde{\eta}^{\dot{\alpha}}\lambda^\alpha\right) \\ &= 2|\beta|^2|\gamma|^2\left|\tilde{\eta}_{\dot{\alpha}}\tilde{\lambda}^{\dot{\alpha}}\right|^2 \\ &= m^2. \end{aligned} \tag{6.38}$$

Therefore, linear combinations of lightlike twistors can give rise to mass $m^2 = p_{\mathsf{Y}}^2 = -\frac{1}{2}\mathsf{A}_{ab}\bar{\mathsf{A}}^{ab}$. The resemblance of this last equation to the spinor helicity version $m^2 = \boldsymbol{p}^2 = -\frac{1}{2}\boldsymbol{p}_{\dot{\alpha}\alpha}\boldsymbol{p}^{\alpha\dot{\alpha}}$ from section 2.2 is clear and suggests, once again, that $\boldsymbol{p}_{\dot{\alpha}\alpha}$ is just a fragment of the more informative A_{ab} in eq. (6.36).

Finally, knowing that the linear and angular momenta of X^a and Z^a simply add up, as in eqs. (6.33) and (6.35), we recover two more familiar relations in Lorentz indices

$$p_{\mathsf{Y}}^{\mu} = p_{\mathsf{X}}^{\mu} + p_{\mathsf{Z}}^{\mu} \tag{6.39}$$

$$M_{\mathsf{Y}}^{\mu\nu}(r^{\mu}) = M_{\mathsf{X}}^{\mu\nu}(r^{\mu}) + M_{\mathsf{Z}}^{\mu\nu}(r^{\mu}). \tag{6.40}$$

It thus follows that the relativistic center-of-mass of Y^a, being the locus of points r^{μ} satisfying $p_{\mathsf{Y}\mu}M_{\mathsf{Y}}^{\mu\nu} = 0$, takes up the unique complex timelike worldline

$$r_{\mathsf{Y}}^{\mu}(h) = \frac{\mathring{M}_{\mathsf{Y}}^{\mu\nu}p_{\mathsf{Y}\nu}}{p_{\mathsf{Y}}^2} + hp_{\mathsf{Y}}^{\mu} \quad \text{for } h \in \mathbb{R}, \tag{6.41}$$

since the first term is now a well defined constant with $p_{\mathsf{Y}}^2 > 0$.

7. Outlook

The on-shell formulation of scattering amplitudes has been growing quickly in the recent years since it became possible to represent massive particles with helicity spinors. Initially limited to gluonic scattering, this development has dramatically extended the reach of the spinor helicity formalism, in principle, to any process being studied in a collider experiment. In addition to providing efficient tools to calculate amplitudes and cross sections, this formalism also offers a rare glimpse of an underlying particle theory, one that is distinct from the quantum field theory of the Standard Model. For what we can see, Parke and Taylor's seminal and "educated guess" about helicity amplitudes made forty years ago is indeed the correct answer to a question that we still cannot pose for lack of a theory.

Our contributions in this paper advance the field in three ways. First, in light of the rapidly progressing literature, we filled in much technical detail on the notation and formulation of massive helicity spinors (section 2) in order to further examine the diagrammatic and analytical structure of scattering amplitudes constructed from them (section 3). We chose a pedagogical tack to invite new students to the on-shell program by frequently comparing the spinor helicity formalism to quantum electrodynamics. Second, these details enabled us to develop new cross sectional methods, which we utilized to calculate Bhabha and Compton cross sections, comparing our results to known ones and confirmed their agreement at both high and low energies (section 4). Third, the frequent appearance of coalescence and non-locality during our study of massive scattering amplitudes prompted us to examine their relationship with mass acquisition. In addition to the dynamical aspect presenting itself as a coalescence of interactions, referred to in the literature as a Higgs avatar, we explored the kinematical aspect, which is closely related to the locality of particle worldlines (section 5). This last point led us to consider how helicity spinors might be naturally incorporated into twistor theory, where we found some correspondence to further pursue a deeper physical interpretation of the formalism as well as a satisfying explanation for its efficiency (section 6).

Several practical avenues as well as fundamental questions have come to our attention during the course of this work. We close by mentioning the most noteworthy ones from each category. On the practical side, much work remains in order to establish a comprehensive toolkit for calculating the rates of processes in collider experiments. The auxiliary couplings will play an important role in precision physics, and their contributions to the cross section will surely be complicated by high-spin interactions. Methodology for computing these efficiency, perhaps, via limits or partial cross sections, would be the first step in categorizing their contributions order-by-order so to better understand how they relate to Feynman's loop diagrams and how they may account for infrared divergences. With such a refined on-shell toolkit, bereft of limitations inherent to nonlinear sigma models, perhaps the finer details of the Higgs boson can be mapped out and tested. On the fundamental side, twistor theory seems like a natural host for helicity spinors according to the

observations presented here, but a broad analysis of the relationship between *massive* helicity spinors and twistors is needed to confirm this. Some preliminary questions are, 'How are higher-spin massive particles encoded by twistors?', 'How does a massive helicity spinor relate to the twistor's primary part, associated to angular momentum?', and 'How can a given massive spinor helicity amplitude be represented with twistor variables?' The paucity of answers to simple questions like these suggests indeed that massive helicity spinors are still primarily a computational tool. The earlier foundational works by Arkani-Hamed and collaborators that had only considered massless spinors for the amplituhedron and positive Grassmannian frameworks are surely a guide [39, 21]. Notably, the recent work by Albonico, Geyer, and Mason, has made inroads by utilizing massive helicity spinors to incorporate mass in a particular twistorial framework of string theory known as ambitwistor-strings [14]. These works, in addition to the already large corpus of literature presenting applications of massive spinors both within and beyond the Standard Model are a resource for new theoretical data to help narrow down the general theoretical framework we have outlined.

Acknowledgments

First arXiv posting. Acknowledgments will appear after discussions and revisions.

A. Spinor helicity conventions and bases

Massless helicity spinors and Levi–Civita symbols:

$$\lambda^\alpha = \lambda\rangle = \begin{pmatrix} a \\ b \end{pmatrix}, \quad \tilde{\lambda}^{\dot{\alpha}} = \lambda] = \begin{pmatrix} \tilde{a} \\ \tilde{b} \end{pmatrix}, \quad \varepsilon_{\alpha\beta} = \begin{pmatrix} 0 & -1 \\ 1 & 0 \end{pmatrix}, \quad \varepsilon_{\alpha\beta} = -\varepsilon^{\alpha\beta} = -\varepsilon^{\beta\alpha} = \varepsilon_{\dot{\alpha}\dot{\beta}} = \varepsilon_{IJ}.$$

Raising and lowering indices:

$$\lambda_\alpha = \langle\lambda = \varepsilon_{\alpha\beta}\lambda^\beta, \qquad \lambda_\alpha = \lambda^\beta\varepsilon_{\alpha\beta} = \lambda^\beta(-\varepsilon_{\beta\alpha}) = -\lambda^\beta\varepsilon_{\beta\alpha}.$$

$$\tilde{\lambda}^{\dot{\alpha}} = [\lambda = \varepsilon^{\dot{\alpha}\dot{\beta}}\tilde{\lambda}_{\dot{\beta}}, \qquad \tilde{\lambda}^{\dot{\alpha}} = \tilde{\lambda}_{\dot{\beta}}\varepsilon^{\dot{\alpha}\dot{\beta}} = \tilde{\lambda}_{\dot{\beta}}(-\varepsilon^{\dot{\beta}\dot{\alpha}}) = -\tilde{\lambda}_{\dot{\beta}}\varepsilon^{\dot{\beta}\dot{\alpha}}.$$

Inner products are antisymmetric because of $\varepsilon_{\alpha\beta}$ contraction:

$$\langle 12\rangle = \lambda_{1\alpha}\lambda_2^{\alpha} = \varepsilon_{\alpha\beta}\lambda_1^{\beta}\lambda_2^{\alpha} = \lambda_1^{\beta}\lambda_2^{\alpha}\varepsilon_{\alpha\beta} = -\lambda_1^{\beta}\lambda_{2\beta} = -\lambda_{2\beta}\lambda_1^{\beta} = -\langle 21\rangle,$$
$$[12] = \tilde{\lambda}_1^{\dot{\alpha}}\tilde{\lambda}_{2\dot{\alpha}} = \varepsilon^{\dot{\alpha}\dot{\beta}}\tilde{\lambda}_{1\dot{\beta}}\tilde{\lambda}_{2\dot{\alpha}} = \tilde{\lambda}_{1\dot{\beta}}\tilde{\lambda}_{2\dot{\alpha}}\varepsilon^{\dot{\alpha}\dot{\beta}} = -\tilde{\lambda}_{1\dot{\beta}}\tilde{\lambda}_2^{\dot{\beta}} = -\tilde{\lambda}_2^{\dot{\beta}}\tilde{\lambda}_{1\dot{\beta}} = -[21].$$

Note above that, unlike spinor *fields*, the spinor helicity variables must commute: $\lambda_1\lambda_2 = \lambda_2\lambda_1$.

$$\langle\lambda\chi\rangle = -\langle\chi\lambda\rangle \quad \text{and} \quad [\lambda\chi] = -[\chi\lambda] \quad \Leftrightarrow \quad \langle\lambda\lambda\rangle = [\lambda\lambda] = 0.$$

Thus, outer products like $\lambda^{\alpha}\chi_{\alpha}$ and $\tilde{\lambda}_{\dot{\alpha}}\tilde{\chi}^{\dot{\alpha}}$ are superfluous since $1\rangle\langle 2 = \langle 12\rangle$ and $1][2 = [12]$. Only the "mixed" outer product is used as it defines momentum:

$$p^{\alpha\dot{\alpha}} = \lambda^{\alpha}\tilde{\lambda}^{\dot{\alpha}} = \lambda\rangle[\lambda = \begin{pmatrix} a \\ b \end{pmatrix}\begin{pmatrix} \tilde{a} & \tilde{b} \end{pmatrix} = \begin{pmatrix} a\tilde{a} & a\tilde{b} \\ b\tilde{a} & b\tilde{b} \end{pmatrix}.$$

Spinor bases for general frame p^{μ}, rotated away from reference frame k^{μ} by angles θ and ϕ:

$$\zeta^{+\alpha} \equiv \begin{pmatrix} c \\ s \end{pmatrix} \quad \text{and} \quad \zeta^{-\alpha} \equiv \begin{pmatrix} -s^* \\ c \end{pmatrix} \quad \text{for} \quad c \equiv \cos\tfrac{\theta}{2} \quad \text{and} \quad s \equiv e^{\mathrm{i}\phi}\sin\tfrac{\theta}{2}$$

are diametrically opposed on S^2. Remaining spinor bases are derived using contraction rules:

$$\zeta_{\alpha}^{+} = \varepsilon_{\alpha\beta}\zeta^{+\beta} = \begin{pmatrix} -s & c \end{pmatrix}, \qquad \zeta_{\alpha}^{-} = \varepsilon_{\alpha\beta}\zeta^{-\beta} = \begin{pmatrix} -c - s^* \end{pmatrix},$$
$$\tilde{\zeta}_{\dot{\alpha}}^{-} \equiv \left(\zeta^{+\alpha}\right)^* = \begin{pmatrix} c \\ s^* \end{pmatrix}, \qquad \tilde{\zeta}_{\dot{\alpha}}^{+} \equiv \left(\zeta^{-\alpha}\right)^* = \begin{pmatrix} -s \\ c \end{pmatrix},$$
$$\tilde{\zeta}^{-\dot{\alpha}} = \varepsilon^{\dot{\alpha}\dot{\beta}}\tilde{\zeta}_{\dot{\beta}}^{-} = \begin{pmatrix} s^* & -c \end{pmatrix}, \qquad \tilde{\zeta}^{+\dot{\alpha}} = \varepsilon^{\dot{\alpha}\dot{\beta}}\tilde{\zeta}_{\dot{\beta}}^{+} = \begin{pmatrix} c & s \end{pmatrix}.$$

Little group basis is identified with $\zeta^{+\alpha}$ and $\zeta^{-\alpha}$ for reference $k^{\mu} \Rightarrow \theta = \phi = 0 \Rightarrow c = 1, s = 0$:

$$\zeta^{+I} = \begin{pmatrix} 1 \\ 0 \end{pmatrix} \leftrightarrow \zeta^{(k)+\alpha}, \qquad \zeta^{-I} = \begin{pmatrix} 0 \\ 1 \end{pmatrix} \leftrightarrow \zeta^{(k)-\alpha},$$
$$\zeta_I^{+} = \begin{pmatrix} 0 & 1 \end{pmatrix} \leftrightarrow \zeta^{(k)+}_{\alpha}, \qquad \zeta_I^{-} = \begin{pmatrix} -1 & 0 \end{pmatrix} \leftrightarrow \zeta^{(k)-}_{\alpha}.$$

The standard incoming/outgoing momenta convention is used with 4-point Mandelstam variables:

$$s = (p_1^\mu + p_2^\mu)^2 = (p_3^\mu + p_4^\mu)^2,$$
$$t = (p_2^\mu - p_3^\mu)^2 = (p_1^\mu - p_4^\mu)^2,$$
$$u = (p_1^\mu - p_3^\mu)^2 = (p_2^\mu - p_4^\mu)^2.$$

B. Partial cross section for general spin

For minimal coupling $(\mathbf{1}^s, \mathbf{2}^s, 3^0)$ with spin s, the partial cross section is the $\left[\begin{smallmatrix}4s\\4s\end{smallmatrix}\right]$-rank tensor

$$\sigma^{\{\dot\alpha_1\cdots\dot\alpha_{2s}\}\{\dot\beta_1\cdots\dot\beta_{2s}\}}_{\{\alpha_1\cdots\alpha_{2s}\}\{\beta_1\cdots\beta_{2s}\}} \quad \text{or concisely} \quad \sigma^{\dot\alpha_i\dot\beta_i}_{\alpha_i\beta_i} \quad \text{with } i \in \{1, 2, \ldots, 2s\}.$$

The case for $s = \frac{1}{2}$ is shown in eq. (4.22) of section 4.3. Consider now the case $s = 1$. There are 4 undotted and 4 dotted indices that will distribute over the 4 spinor helicity variables $\lambda_1\lambda_1\lambda_2\lambda_2$:

$$\sigma^{\dot\alpha_1\dot\alpha_2\dot\beta_1\dot\beta_2}_{\alpha_1\alpha_2\beta_1\beta_2} = \left|\frac{\lambda_{1I_1}\lambda_{1I_2}\lambda_{2J_1}\lambda_{2J_2}}{m^2} M^{+1}_{\alpha_1\alpha_2\beta_1\beta_2}\right|^2 \quad \text{or concisely} \quad \sigma^{\dot\alpha_i\dot\beta_i}_{\alpha_i\beta_i} = \left|\frac{(\lambda_1)^2_{I_i}(\lambda_2)^2_{J_i}}{m^2} M^{+1}_{\alpha_i\beta_i}\right|^2$$

with symmetrized indices appearing below for

$$|M|^{2\,(\dot\alpha_1\dot\alpha_2\dot\beta_1\dot\beta_2)}_{(\alpha_1\alpha_2\beta_1\beta_2)} = g^2m^2\varepsilon_{(\alpha_1\alpha_2}\varepsilon^{(\dot\alpha_1\dot\alpha_2}\varepsilon_{\beta_1\beta_2)}\varepsilon^{\dot\beta_1\dot\beta_2)} = \frac{g^2m^2}{4!}\sum_{\pi\in S_4}\varepsilon_{\pi_1\pi_2}\varepsilon^{\dot\pi_1\dot\pi_2}\varepsilon_{\pi_3\pi_4}\varepsilon^{\dot\pi_3\dot\pi_4},$$

where S_4 is the symmetric group of 4 elements 1234, and π is a permutation of these elements. With still more conciseness, the pattern becomes more apparent

$$|M|^{2\,(\dot\alpha_i\dot\beta_i)}_{(\alpha_i\beta_i)} = g^2m^2\,(\varepsilon\tilde\varepsilon)^{(\dot\alpha_i\dot\beta_i)}_{(\alpha_i\beta_i)}.$$

Note that the round brackets $(\varepsilon\tilde\varepsilon)$ are *not* symmetrization indices. This leads to

$$\sigma^{\dot\alpha_i\dot\beta_i}_{\alpha_i\beta_i} = \frac{g^2}{5}\Bigg[\boldsymbol{p}_{1\,(\alpha_1}\boldsymbol{p}^{\dot\alpha_1}_{1\,\alpha_2}\boldsymbol{p}^{\dot\alpha_2}_{2\,\beta_1}\boldsymbol{p}^{\dot\beta_1}_{2\,\beta_2)} - \frac{1}{2}\boldsymbol{p}^{(\dot\alpha_1}_{1\,(\alpha_1}\boldsymbol{p}^{\dot\alpha_2}_{1\,\alpha_2}\varepsilon_{\beta_1\beta_2)}\varepsilon^{\dot\beta_1\dot\beta_2)}\left(\boldsymbol{p}_{12}+m^2\right)$$
$$+\frac{1}{2}\varepsilon_{(\alpha_1\alpha_2}\varepsilon^{(\dot\alpha_1\dot\alpha_2}\varepsilon_{\beta_1\beta_2)}\varepsilon^{\dot\beta_1\dot\beta_2)}\left(\boldsymbol{p}_{12}^2+m^4\right)\Bigg],$$

where $\boldsymbol{p}_{12} \equiv \boldsymbol{p}_1 \cdot \boldsymbol{p}_2$. We see that there are generally 5 ways to distribute the indices, yielding terms: $\boldsymbol{p}_a^{\alpha\dot{\alpha}}$, $\boldsymbol{p}_{ab}$, m^2, $\boldsymbol{p}_{ab}^2$, and m^4. Also, a minus sign appears for each $\boldsymbol{p}_{12} + m^2$ contraction.

Altogether, for arbitrary spin s, there are $4s + 1$ ways to distribute the indices, so the general formula is, as claimed in the main text, eq. (4.24) of section 4.3,

$$\sigma_{\alpha_i\beta_i}^{\dot{\alpha}_i\dot{\beta}_i} = \frac{g^2}{4s+1} \sum_{n=0}^{2s} \frac{(-1)^{n+1}}{2} \big(\boldsymbol{p}_1 \boldsymbol{p}_2\big)^{2s-n} {}^{(\dot{\alpha}_i\dot{\beta}_i}_{(\alpha_i\beta_i} \big(\varepsilon\tilde{\varepsilon}\big)^{n\,\dot{\alpha}_j\dot{\beta}_j)}_{\alpha_j\beta_j)} \left[\boldsymbol{p}_{12}^n + m^{2n}\right].$$

for fully symmetrized indices with labels $1 \leq i < j \leq s$, as well as $2s - n$ copies of the momenta $\boldsymbol{p}_1$ and $\boldsymbol{p}_2$, and finally n copies of the Levi–Civita symbols.

References

[1] P.A.M. Dirac, *Quantum Theory of Emission and Absorption of Radiation*, *Proc. Roy. Soc. Lond. A* **114** (1927) 243.

[2] S.J. Parke and T.R. Taylor, *Amplitude for n-Gluon Scattering*, *Phys. Rev. Lett.* **56** (1986) 2459.

[3] R. Britto, F. Cachazo, B. Feng and E. Witten, *Direct Proof of the Tree-Level Scattering Amplitude Recursion Relation in Yang-Mills Theory*, *Phys. Rev. Lett.* **94** (2005) 181602.

[4] F. Cachazo, P. Svrcek and E. Witten, *MHV vertices and tree amplitudes in gauge theory*, *JHEP* **09** (2004) 006.

[5] E. Witten, *Perturbative gauge theory as a string theory in twistor space*, *Commun. Math. Phys.* **252** (2004) 189.

[6] N. Arkani-Hamed, T.-C. Huang and Y.-t. Huang, *Scattering amplitudes for all masses and spins*, *JHEP* **11** (2021) 070.

[7] E. Conde and A. Marzolla, *Lorentz Constraints on Massive Three-Point Amplitudes*, *JHEP* **09** (2016) 041.

[8] S. Dittmaier, *Weyl-van der Waerden formalism for helicity amplitudes of massive particles*, *Phys. Rev. D* **59** (1998) 016007.

[9] A. Ochirov, *Helicity amplitudes for QCD with massive quarks*, *JHEP* **2018** (2018) 089.

[10] G.F.S. Alves, E. Bertuzzo and G.M. Salla, *On-shell approach to neutrino oscillations*, *Phys. Rev. D* **106** (2022) 036028.

[11] A. Guevara, A. Ochirov and J. Vines, *Scattering of Spinning Black Holes from Exponentiated Soft Factors*, *JHEP* **09** (2019) 056.

[12] A. Herderschee, S. Koren and T. Trott, *Massive On-Shell Supersymmetric Scattering Amplitudes*, *JHEP* **10** (2019) 092.

[13] M. Chiodaroli, M. Gunaydin, H. Johansson and R. Roiban, *Spinor-helicity formalism for massive and massless amplitudes in five dimensions*, *JHEP* **02** (2023) 040.

[14] G. Albonico, Y. Geyer and L. Mason, *Massive ambitwistor-strings; twistorial models*, *JHEP* **01** (2024) 127.

[15] M.D. Schwartz, *Quantum Field Theory and the Standard Model*, Cambridge University Press, Cambridge, U.K. (2013).

[16] L.J. Dixon, *A brief introduction to modern amplitude methods*, in *Theoretical Advanced Study Institute in Elementary Particle Physics: Particle Physics: The Higgs Boson and Beyond*, pp. 31–67, 2014.

[17] H. Elvang and Y.-t. Huang, *Scattering Amplitudes in Gauge Theory and Gravity*, Cambridge University Press, Cambridge, U.K. (2015).

[18] H. Georgi, *Lie algebras in particle physics*, Perseus Books, Reading, MA, 2nd ed. (1999).

[19] N. Christensen, B. Field, A. Moore and S. Pinto, *Two-, three-, and four-body decays in the constructive standard model*, *Phys. Rev. D* **101** (2020) 065019.

[20] R. Penrose, *Twistor algebra*, *J. Math. Phys.* **8** (1967) 345.

[21] N. Arkani-Hamed, J.L. Bourjaily, F. Cachazo, A.B. Goncharov, A. Postnikov and J. Trnka, *Grassmannian Geometry of Scattering Amplitudes*, Cambridge University Press (2016).

[22] C. Cohen-Tannoudji, B. Diu and F. Laloë, *Quantum Mechanics*, vol. 2, Wiley, Hoboken, NJ (1991).

[23] S. Weinberg, *The Quantum Theory of Fields. Vol. 1: Foundations*, Cambridge University Press, Cambridge, U.K. (2005).

[24] P. Benincasa and F. Cachazo, *Consistency Conditions on the S-Matrix of Massless Particles*, `[arXiv:hep-th/0705.4305]`.

[25] C. Cohen-Tannoudji, B. Diu and F. Laloë, *Quantum Mechanics*, vol. 1, Wiley, Hoboken, NJ, 1 ed. (1991).

[26] N. Arkani-Hamed, T.-C. Huang and Y.-t. Huang, *The EFT-Hedron*, *JHEP* **05** (2021) 259.

[27] S.R. Coleman, J. Wess and B. Zumino, *Structure of phenomenological Lagrangians. 1.*, *Phys. Rev.* **177** (1969) 2239.

[28] C.G. Callan, Jr., S.R. Coleman, J. Wess and B. Zumino, *Structure of phenomenological Lagrangians. 2.*, *Phys. Rev.* **177** (1969) 2247.

[29] B. Bachu and A. Yelleshpur, *On-Shell Electroweak Sector and the Higgs Mechanism*, *JHEP* **08** (2020) 039.

[30] G. Durieux, T. Kitahara, Y. Shadmi and Y. Weiss, *The electroweak effective field theory from on-shell amplitudes*, *JHEP* **01** (2020) 119.

[31] S. Ballav and A. Manna, *Recursion relations for scattering amplitudes with massive particles II: Massive vector bosons*, *Nucl. Phys. B* **983** (2022) 115935.

[32] R. Balkin, G. Durieux, T. Kitahara, Y. Shadmi and Y. Weiss, *On-shell Higgsing for EFTs*, *JHEP* **03** (2022) 129.

[33] B. Bachu, *Spontaneous symmetry breaking from an on-shell perspective*, *JHEP* **02** (2024) 098.

[34] D. Liu and Z. Yin, *Gauge invariance from on-shell massive amplitudes and tree-level unitarity*, *Phys. Rev. D* **106** (2022) 076003.

[35] R. Penrose and W. Rindler, *Spinors and Space-Time: Spinor and Twistor Methods in Space-Time Geometry*, vol. 2, Cambridge University Press, Cambridge, U.K. (1986).

[36] R. Penrose, *The Road to Reality: A Complete Guide to the Laws of the Universe*, Jonathan Cape (Random House), London, U.K. (2004).

[37] J.L. Synge, *Relativity: The Special Theory*, North-Holland Publishing Co., 2 ed. (1965).

[38] R. Penrose and M. MacCallum, *Twistor theory: an approach to the quantisation of fields and space-time*, *Phys. Rep.* **6** (1972) 241.

[39] N. Arkani-Hamed and J. Trnka, *The Amplituhedron*, *JHEP* **10** (2014) 030 [1312.2007].